Re-engineering root system architecture for steeper and deeper rooting in cereals

Fay Mari Arcadia Walsh

Submitted in accordance with the requirements for the degree of Doctor of Philosophy

The University of Leeds

School of Biology

Faculty of Biological Sciences

December 2023

The candidate confirms that the work submitted is their own and that appropriate credit has been given where reference has been made to the work of others.

-

The YoGI wheat landrace panel seeds were obtained from the Harper lab and details of the panel can be found in Barratt et al. (2023). Ryan Kaye from the Kepinski lab grew and imaged the YoGI wheat landrace panel, Fay Walsh the PhD candidate performed the image and data analysis.

NIAB (Cambridge) performed the DII-VENUS and mDII-VENUS wheat transformation and copy number analysis, Fay Walsh generated the constructs and carried out the plant phenotyping, imaging and auxin treatment experiments.

The *qSOR1-A:qSOR1-A*, *qSOR1-A:qsor1-A* (*R136K*) and *ZmUbi:qsor1-D* (*R135A*) wheat transformation and copy number analysis was performed by the Crop Transformation group at the John Innes Centre (Norwich). Fay Walsh generated the constructs for transformation and performed the phenotypic analysis.

The *lazy2D* (*lazy2 R143A*) and *LAZY2:LAZY2* Arabidopsis lines in Col-0 and *lazy2* backgrounds were generated by Adam Binns from the Kepinski lab (Binns, 2022). Fay Walsh grew the plants and performed the phenotypic analyses presented in this thesis.

-

Acknowledgements

I would like to thank my supervisor Stefan for the support and guidance during my PhD journey. Thank you to my co-supervisor Laura for feedback, help and advice on all things wheat-related! Thanks to everyone in the Kepinski lab especially Adam, Martina, Sibo and Suruchi, it's been great working with you. I am grateful to the Gosden Legacy for providing the funding and support for my PhD. Finally, a big thank you to all family and friends, especially friends within FBS, and to Andrew for supporting me throughout everything.

Abstract

Steeper and deeper plant root system architecture is predicted to increase uptake of water and nitrogen soil resources, in addition to improving drought avoidance and carbon sequestration. Soil resource uptake is a major root system function determined by the spatial arrangement of roots. Gravitropism describes plant growth in response to gravity and root gravitropic responses strongly influence root system architecture development. The goal of this work was to investigate mechanisms and genes underlying cereal root system architecture for achieving steeper and deeper rooting. This work investigated phenotyping methods and the variation in root system architecture in wheat varieties and landraces, and gravitropic setpoint angle maintenance in wheat and rice lateral roots. Auxin plays a central role in gravitropism and the absence of an auxin reporter in wheat initiated the development of a wheat DII-VENUS auxin reporter.

Root gravitropic mechanisms and genes have been extensively studied in many plant species but limited research has been translated into wheat. The *LAZY* gene family have important functions in regulating root and shoot growth angles. Nine wheat *LAZY* homoeologs have been discovered, now named the *LAZY1*, *DRO1* and *qSOR1* A, B and D homoeologs. Extended domain III (D3X) was characterised in wheat, as D3X is an important *LAZY* domain for Arabidopsis lateral root growth angle control, with D3X mutations inducing a steeper lateral root phenotype. Extended domain III mutations in D3X-containing wheat *LAZY* genes were introduced via transformation or in a TILLING background. These wheat mutants had steeper seminal roots, suggesting wheat lateral root growth angle may be controlled by a different mechanism. These findings have important implications for utilising the *LAZY* gene family in crop root system architecture modification. Overall, this work addressed gaps in the understanding of cereal root growth angle control and made new discoveries in the functions of the wheat *LAZY* gene family, contributing towards achieving steeper and deeper root system architecture for crop yield improvement in a changing climate.

Table of Contents

List of Figures

List of Tables

Abbreviations

2D – two-dimensional

3D – three-dimensional

AGO – antigravitropic offset

ANOVA – analysis of variance

ARF – Auxin Response Factor

ATS – *Arabidopsis thaliana* salts

Aux/IAA – Auxin/Indole-3-acetic acid

AuxRE – Auxin Response Element

cDNA – complementary DNA

D3X – extended domain III

DII – Domain II

DMSO – Dimethyl Sulfoxide

DNA – Deoxyribonucleic acid

dNTP – Deoxynucleotide triphosphate

DRO1 – Deeper Rooting 1

EAR-like motif - ethylene-responsive element binding factor-associated amphiphilic repression

EMS – ethyl methanesulfonate

GSA – gravitropic setpoint angle

GWAS – genome-wide association studies

IAA – indole-3-acetic acid

Indel – insertion and/or deletion mutation

KASP – kompetitive allele-specific PCR

LA1 – LAZY1

LB – Luria-Bertani

miRNA - microRNA

NGR – Negative Gravitropic Response of Roots

PCR – Polymerase Chain Reaction

PI – Propidium Iodide

PIN – PIN-FORMED

RNA – Ribonucleic acid

RPM – revolutions per minute

RSA – root system architecture

SEM – standard error of mean

SNP – Single Nucleotide Polymorphism

TAC1 – TILLER ANGLE CONTROL 1

TILLING – Targeting Induced Local Lesions In Genomes

TPL – TOPLESS repressor protein

QTL – Quantitative Trait Locus

qPCR – Quantitative Polymerase Chain Reaction

qSOR1 – quantitative trait locus for SOIL SURFACE ROOTING 1

WT – wild type

X-ray CT – X-ray computed tomography

Chapter 1

General Introduction

Chapter 1: General Introduction

1.1 Increasing crop yields

Increasing food production whilst reducing intensive fertiliser and pesticide inputs, and adapting to a changing climate is a major challenge facing arable farming globally. Cereals including wheat (*Triticum aestivum*), rice (*Oryza sativa*) and maize (*Zea mays*) make up almost half of the global calorific intake (Milani et al., 2022). A 25 – 70% increase on the 2017 global food production level is predicted to be required by 2050 to meet the demands of the growing global population (Hunter et al., 2017). Agricultural intensification including higher fertiliser and pesticide inputs, and the development of dwarf high-yielding varieties occurred during the 20th century Green Revolution. The effects of the introduction of dwarfing *REDUCED HEIGHT* (*Rht*) alleles in wheat included reduced stem height and a greater number of productive tillers which resulted in increased crop yields (Jobson et al., 2019). These developments and other factors caused a 40% increase in cereal production between 1960 and 1990 (Evans and Lawson, 2020). However, the current intensive agricultural practices which are linked to the Green Revolution are contributing to climate change by causing a fifth of global greenhouse gas emissions (Tubiello et al., 2021), and loss of soil fertility and biodiversity (Tsiafouli et al., 2015).

Climate change is predicted to hinder increases in crop productivity due to the effects of higher temperatures and increased CO_2 levels (Lobell and Gourdji, 2012). Droughts and extreme heat reduced cereal production by up to 10% in the second half of the 20th century (Lesk et al., 2016). These extreme weather events are expected to become more frequent in the future which will further impact crop production (Lesk et al., 2016). Management strategies including changing sowing times, or growing different crop species or varieties may help to alleviate some of the negative impacts (Lobell and Gourdji, 2012). A second Green Revolution is thought to now be needed to develop new more resilient crop cultivars with higher nutrient use efficiency, which will produce greater yields in lower input conditions (Lynch, 2007). The development of genome editing and precision breeding techniques has allowed advances in crop breeding to generate new crop varieties with desired traits (Gao, 2021).

Understanding the genetic variation and developmental pathways of crop plants will be crucial for producing new resilient crop varieties which can withstand biotic and abiotic stresses (Bailey-Serres et al., 2019). The root system architecture of crop plants is a key target for improving crop yields under environmental stress, particularly in water- or nutrient-limited conditions (de Dorlodot et al., 2007). Wheat is the third largest cereal crop harvested worldwide after maize and rice, and wheat is vulnerable to biotic and abiotic stresses particularly during the grain filling stage (Asseng et al., 2011). Elite cultivars are high-yielding cultivated varieties developed in modern crop breeding programs (Sanchez et al., 2023). In 2007, modern wheat cultivars were found to have a reduction in root biomass compared to pre-Green Revolution wheat landraces (Waines and Ehdaie, 2007). This may indicate that modern cultivars have smaller than optimum root systems for water and nutrient uptake and suggests that beneficial root traits have been neglected during the Green Revolution (Waines and Ehdaie, 2007).

1.2 Plant root system architecture

Root system architecture (RSA) describes the spatial distribution of plant root systems in the soil (de Dorlodot et al., 2007). Plant root systems provide structural support and determine the efficiency of nutrient and water uptake from the soil environment, as nutrients and water are heterogeneously distributed in soil layers (Li et al., 2016). Root system architecture formation has a considerable genetic basis but environmental factors including water availability, light, temperature and soil oxygen content have also been shown to influence root system development (Rich and Watt, 2013). Plant roots are divided into embryonic roots emerging from the embryo such as dicot taproots or monocot seminal roots (Fig. 1.1), and post-embryonic roots which form from existing roots or non-root tissues (adventitious roots) (Atkinson et al., 2014). Post-embryonic roots include lateral roots forming from embryonic roots, as well as crown or nodal roots which form the majority of fibrous root systems (Atkinson et al., 2014).

Monocot cereal species such as rice, wheat and maize have fibrous root systems, consisting of seminal, lateral and nodal or crown roots which have different developmental pathways. Root system development in wheat and other monocots starts with the emergence of up to seven embryonic seminal roots (Fig. 1.1a), followed by post-embryonic nodal crown roots which will form most of the

mature root system (Rich and Watt, 2013). In contrast, post-embryonic adventitious roots in dicots constitute a smaller proportion of the root system compared to cereal plant crown roots (Rich and Watt, 2013). Following seminal root development, lateral roots initiate from endodermis and pericycle cells in seminal and crown roots (Orman-Ligeza et al., 2013). Dicotyledonous species such as *Arabidopsis thaliana* have a taproot system consisting of lateral roots branching off from the primary taproot (Fig. 1.1b) (Atkinson et al., 2014).
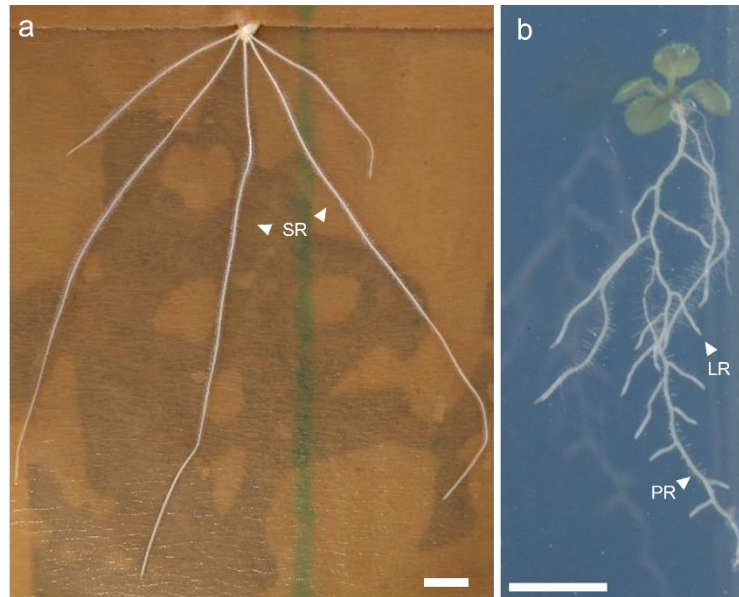
Figure 1.1: Differences between monocot and dicot root system architecture.
(a) 5-day old wheat plant (monocot) grown on germination paper, SR: seminal roots, scale bar = 10 mm. (b) 9-day old Arabidopsis seedling (dicot) grown on agar, PR: primary root, LR = lateral root, scale bar = 5 mm.

Root phenomics studies can be a challenge to perform due to the difficulty in imaging soil-grown root systems, which makes it important to have a lab-based method that closely matches field conditions. Root phenotyping within a two-dimensional (2D) controlled growth environment such as transparent agar or germination paper methods allows whole seedling root system visualisation but may not be representative of field conditions (Atkinson et al., 2019). Another 2D phenotyping method involves growing plants around the perimeter of soil-filled clear pots or thin soil-filled containers which allows visualisation of soil-grown seedling root phenotypes (Richard et al., 2015).

Root system phenotyping of plants grown in field conditions gives the best representation of root system architecture, however, these methods can be

destructive and time intensive. Invasive field methods include soil coring and 'shovelomics' where mature root crowns are excavated for root system data collection and analysis (York et al., 2019). Growing plants in mesh baskets or colanders in soil allows analysis of root growth angle by quantifying the angles of roots emerging from the mesh (Oyanagi et al., 1993b, Uga et al., 2013). A non-invasive root phenotyping method uses X-ray computed tomography (X-ray CT) scanning to image plant roots which are grown or transferred in soil columns for imaging (Urfan et al., 2022). The multiple factors influencing root development indicates that it is important to grow plant species in both controlled and field conditions to aid the understanding of the different root phenotypes found in both growth environments (Fiorani and Schurr, 2013).

1.3 Steeper and deeper root systems

Improving crop plant resistance to drought is a major aim in crop breeding due to the increased occurrence of drought events and water shortages (Luo et al., 2019). Optimisation of root architecture is a promising strategy for improving drought resistance (Luo et al., 2019). The "steep, cheap and deep" ideotype is proposed to optimise acquisition of water and nitrogen in the form of nitrate (Lynch, 2013). Water and nitrate are mobile in soil and can accumulate deeper underground. This steep, cheap deep ideotype consists of steep root growth angles, few but long lateral roots and seminal or initial crown roots capable of accessing shallow soil resources (Lynch, 2013). Modelling has been used to predict that a narrower root system architecture and a deeper root system can result in higher crop yields in water-deficit conditions (Manschadi et al., 2010).

A shallow root system phenotype (Fig. 1.2a) is hypothesised to be optimal for phosphorus uptake which is an important limiting resource and relatively immobile in soil in the form of phosphate (Lynch, 2013). Phosphate deficiency is a global issue in agricultural soils (López-Arredondo et al., 2014). However, there are negative consequences of phosphate fertiliser application including excess application leading to environmental issues such as eutrophication, and rock phosphate is also a non-renewable resource (van de Wiel et al., 2016). Root traits associated with increased phosphate uptake efficiency include shallow root growth angles, greater numbers of adventitious and lateral roots, and long root hairs for topsoil foraging (Lynch, 2013). Shallow, surface rooting has been

demonstrated in rice plants with a loss-of-function allele of *qSOR1* (*quantitative trait locus for SOIL SURFACE ROOTING 1*) (Kitomi et al., 2020). Another study found that overexpressing *PSTOL1* (*Phosphorus-starvation tolerance 1*) improves phosphorus uptake ability and increases early crown root growth (Gamuyao et al., 2012).
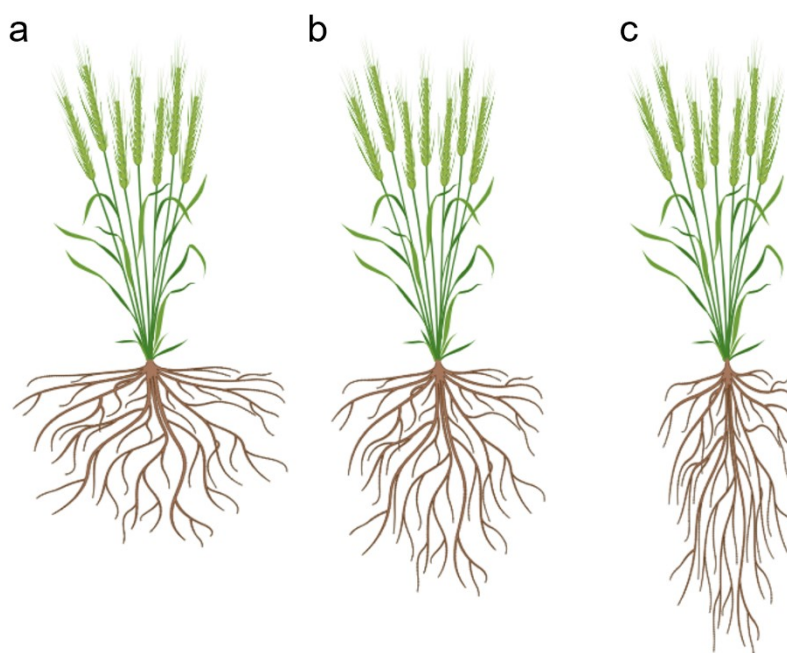
Figure 1.2: Plant root system architecture ideotypes.

Wheat plant diagrams representing different root system architecture ideotypes. (a) Shallow root system architecture hypothesised to be optimal for phosphorus uptake. (b) Standard root system architecture (c) Steep and deep root system architecture hypothesised to be optimal for water and nitrogen uptake. Diagram not to scale, created with BioRender.

Deeper plant root system architecture is hypothesised to increase carbon sequestration and uptake of water and nitrate (Fig. 1.2c) (Lynch, 2022). Increasing sequestration of carbon in soils is thought to be possible by increasing plant rooting depth so that higher levels of atmospheric CO_2 are sequestered underground (Kell, 2011). Photosynthesis and allocation of CO_2 to plant roots is the main method of carbon transfer to soil which means that increasing root growth can improve carbon sequestration in soils (Kell, 2011). Water and nutrient availability are major limiting factors on crop yields and deeper rooting has been shown to improve drought avoidance during water-limited growth conditions (Uga

et al., 2013, Lynch, 2022). Water accumulation in deeper soil layers is a water source less susceptible to evaporation and can be reached by deeper plant roots (Cao et al., 2018). Reliable water resources are crucial during the grain-filling stage of cereal development that occurs later in the growing season (Wasson et al., 2012).

Steeper root growth angles enable plant roots to reach further underground and access deep soil resources (Lynch, 2022). Root growth angle is one of the most important factors shaping plant root system architecture. In rice, overexpression of *DEEPER ROOTING 1* (*DRO1*) was discovered to increase vertical root growth and improve crop yield performance under drought conditions (Uga et al., 2013). Another gene named *ENHANCED GRAVITROPISM 2* (*EGT2*) was found to control seminal and lateral root growth angle in wheat and barley (*Hordeum vulgare*) (Kirschner et al., 2021). Seminal roots form only a small part of the eventual wheat root system, but early investigation of seminal root angle variation in Japanese wheat cultivars led to the hypothesis that seminal root angle can predict the root depth of field grown plants (Oyanagi, 1994, Oyanagi et al., 1993b). Seminal root angle has since been positively associated with crown root angle in mature wheat root systems (Manschadi et al., 2008).

1.4 Techniques and strategies for crop development

Modern elite crop cultivars are bred to be high yielding under intensive, high input conditions, so traits such as pathogen and disease resistance may not be present in elite germplasm (Newton et al., 2011). Modern cultivars may have reduced genetic diversity and have lost some potentially advantageous traits compared to landraces and wild relatives, due to intensive selection for final yield at the expense of other traits (Wingen et al., 2017). Different strategies can be used to reintroduce genetic diversity and beneficial crop traits into modern varieties including mutation breeding, traditional crop breeding programmes, and genome editing approaches (Gao, 2021). Favourable traits can be identified from mutagenized plant populations such as TILLING (Targeted Induced Local Lesions IN Genomes) lines (Kurowska et al., 2011). These TILLING populations have undergone mutagenesis such as ethyl methanesulfonate (EMS) mutagenesis followed by genome sequencing, and the resulting population can then be used to screen for traits or lines with mutations in genes of interest

(Kurowska et al., 2011, Krasileva et al., 2017). For example, lines with mutations in *EGT2* were identified in the wheat cv. Kronos TILLING population which led to the discovery that *EGT2* functions in wheat root growth angle control (Kirschner et al., 2021).

Landraces are useful sources of genetic variation for incorporation into elite varieties, such as the Watkins wheat landrace collection which contains unique Single Nucleotide Polymorphisms (SNPs) not present in modern wheat cultivars (Winfield et al., 2018). Breeding programmes can use introgression breeding to introduce a gene of interest from a wild variety or landrace into an elite modern cultivar (Palmgren et al., 2015). A submergence-tolerant rice landrace led to discovery that *SUBMERGENCE 1* (*SUB1*) improved yield under flood conditions when introgressed into modern rice cultivars (Bailey-Serres et al., 2010).

Traditional breeding methods are slow processes taking many crop generations with a review of root trait breeding programmes finding they can take up to 10 years (Palmgren et al., 2015, Tracy et al., 2020). The speed of crop development can be increased by marker-assisted selection (MAS) where DNA markers associated with target traits are selected to increase breeding efficiency. The detection of DNA markers and trait associations can be performed with quantitative trait loci (QTL) analysis and genome-wide association studies (GWAS) (Yang et al., 2016). A GWAS was performed with a population of elite durum wheat (*Triticum durum*) varieties to identify a QTL involved in root growth angle modulation (Alahmad et al., 2019). Orthology comparison between Arabidopsis and maize QTLs allowed discovery of 4 genes involved in root gravitropism (Yoshihara et al., 2022).

Reducing plant generation time can accelerate crop breeding programmes. The development of shuttle breeding during the Green Revolution allowed two growing seasons in one year as plant material was transferred between high and low altitudes during the year (Ortiz et al., 2007). The recent development of speed breeding involves growing plants in conditions of 22 hours light and 2 hours dark, which can shorten generation times. For example, average generation time in 5 wheat varieties was reduced from 102 – 105 days to 56 – 80 days under speed breeding conditions (Watson et al., 2018). This method works with multiple species with 4 to 6 generations per year achieved for wheat, barley (*Hordeum*

vulgare) and chickpea (*Cicer arientinum*) under speed breeding conditions, compared with only 2 to 3 generations per year under 12 hour day conditions (Watson et al., 2018).

Genome editing creates changes in the genome in the form of insertions, deletions, single nucleotide polymorphisms (SNPs) or larger substitutions (Nerkar et al., 2022). CRISPR (Clustered Regularly Interspaced Palindromic Repeats) and Cas (CRISPR associated) system uses guide RNAs to target a specific location in the genome (Ran et al., 2013). The target site is cleaved and repaired through Non-Homologous End Joining (NHEJ) or Homology Directed Repair (HDR) pathways to result in genome modification (Ran et al., 2013). Off-target mutations can occur with CRISPR/Cas9 with one study showing that 3% of potential sites containing the target sequence were mutated (Holme et al., 2019).

Base editing and prime editing allow DNA modification at a single-base level and can generate specific edits with reduced off target effects compared to the CRISPR/Cas system (Molla et al., 2021). CRISPR/Cas9 genome editing has been used to mutagenize wheat *GW2* homoeologs to result in a 5.5% increase in Thousand Grain Weight (TGW), defined as the weight of 1,000 seeds (Wang et al., 2018b). Prime editing can introduce specific insertions or deletions (indels) with reduced off-target mutations (Molla et al., 2021). Prime editing has been successfully demonstrated in both wheat and rice and could be an important tool for crop breeding to introduce targeted mutations and alleles into crop species (Lin et al., 2020).

1.5 Root gravitropism

Root system architecture is shaped by a combination of genetic and environmental factors, including light, gravity and nutrient and water availability (Morris et al., 2017). One of the most important environmental factors is gravity which is a constant and uniform influence on plants (Rich et al., 2020). Gravity sensing occurs in the root cap spatially separated from the resulting gravitropic response in the root elongation zone (Su et al., 2020). Two hypotheses central to the root gravitropic pathway are the starch-statolith hypothesis and the Cholodny-Went hypothesis. The starch-statolith hypothesis proposes that starch-filled statoliths falling to the lower side of the cell will trigger a stimulus to be transmitted to the elongation zone to result in altered root growth (Su et al., 2020). Statoliths

are starch-filled amyloplasts which are thought to have evolved to localise to the root apex in flowering plants and gymnosperm seed plants, as they are not present in basal plant lineages (Zhang et al., 2019). Statoliths are located in root cap columella cells, and the columella cells are thought to be the main site of gravity sensing (Su et al., 2020). A change in gravity stimulus causes statolith sedimentation in the direction of gravity (Su et al., 2020).

Statolith sedimentation triggers a lateral gradient of unequally distributed auxin (indole-3-acetic acid, IAA) resulting in plant organ bending and this process is known as the Cholodny-Went hypothesis (Went and Thimann, 1937). The signal following statolith sedimentation which triggers asymmetric auxin flow is as yet unknown (Su et al., 2017). Auxin accumulates on the lower side of the root elongation zone and inhibits lower side cell elongation which results in downwards root curvature (Band et al., 2012). An additional gravity sensing pathway is thought to be active in plant roots as the starchless *phosphoglucomutase-1* (*pgm-1*) mutant displays a reduced gravity response rate at a third of the rate of wild-type roots, which suggests there is an additional starch-independent gravity sensing mechanism (Wolverton et al., 2011) This additional mechanism may act outside the root cap as maize seedling roots with root caps removed were still able to respond to gravistimulation (Mancuso et al., 2006).

1.6 Auxin transport and reporters

Auxin is the major hormone involved in the gravitropic response pathway and acts in transcriptional regulation through the TIR1/AFB-Aux/IAA-ARF system (Mockaitis and Estelle, 2008). Auxin binds to the auxin-binding pocket of TIR1 in the SCF^{TIR1} E3 ubiquitin ligase complex which is composed of TIR1 F-box, CUL1 and SKP1-like proteins (Kepinski and Leyser, 2005). Auxin binding allows Aux/IAA transcriptional repressor proteins to bind to the SCF complex for ubiquitination and 26S proteasomal-mediated degradation (Maraschin et al., 2009). Aux/IAA protein degradation allows de-repression of the ARF (Auxin Response Factor) transcription factor family. ARFs specifically bind to auxin-response elements (AuxREs) present in the promoters of auxin-responsive genes (Hagen and Guilfoyle, 2002). Auxin binding, Aux/IAA degradation and de-

repression of ARFs allow ARF-mediated transcription of auxin-responsive genes (Maraschin et al., 2009).

Auxin transport occurs via non-directional transport in the phloem or through cell-to-cell polar auxin transport (Adamowski and Friml, 2015). Auxin molecules in the acidic protoplast are protonated (IAAH) and diffuse into cells or are transported though AUX/LAX influx carrier proteins (Adamowski and Friml, 2015). Auxin (IAA-) molecules dissociate in the neutral cell cytoplasm and are transported out through PIN (PIN-FORMED) efflux transporters (Adamowski and Friml, 2015).

PIN polarity determines the direction of auxin flow and PIN2, PIN3, PIN4 and PIN7 are the main PIN proteins in the root tip (Kleine-Vehn et al., 2010). Auxin is concentrated at the root tip quiescent centre cells and is transported up through the root towards the elongation zone by PIN2 (Kleine-Vehn et al., 2010). PIN3 is polarised to the lower side of the columella cells following gravistimulation, which redirects auxin flow to the lower side of the root and leads to cell elongation inhibition (Kleine-Vehn et al., 2010). This asymmetric flow of auxin from the statocytes causes differences in cell elongation between the upper and lower sides which results in differential organ growth (Nakamura et al., 2019).

Auxin was first isolated from oat coleoptiles; however, auxin related processes have since been predominantly characterised in Arabidopsis (Balzan et al., 2014). Genes important in auxin pathways have been identified in cereals such as the ARF genes, with the wheat genome found to contain 23 ARF genes (Qiao et al., 2018). PIN transporter proteins are present and structurally conserved in wheat, rice and maize, although not all Arabidopsis PINs have homologs in these cereal species (Singh et al., 2019). Auxin reporters can be used to visualise auxin flow, signalling and distribution throughout plant architecture (Brunoud et al., 2012). Auxin reporter lines were first developed in Arabidopsis and the creation of reporters in other plant species has improved the understanding of the diversity of auxin signalling processes (Yang et al., 2017, Mir et al., 2017). One of the first auxin-sensitive reporter systems developed was Arabidopsis DR5-GUS composed of a synthetic auxin response element from the *GH3* gene in soybean (*Glycine max*) fused to a CaM35S-GUS reporter gene (Ulmasov et al., 1997). A newer version named DR5v2 was generated using a higher affinity binding site sequence for improved visualisation of auxin responses (Liao et al., 2015).

The DII-VENUS auxin reporter developed by Brunoud et al. (2012) consists of the DII auxin-binding domain of AtAux/IAA28 fused to VENUS yellow fluorescent protein and an N7 nuclear localisation signal, under the control of the CaMV35S promoter. DII-VENUS is degraded in the presence of auxin through association with the auxin-TIR1 complex with the lack of DII-VENUS fluorescence indicating the presence of auxin (Brunoud et al., 2012). The mDII-VENUS control reporter line has a mutation in the DII degron which does not bind TIR1 leaving mDII-VENUS auxin-insensitive so that DII-VENUS and mDII-VENUS expression can be compared to visualise auxin distribution in plant tissues. The Arabidopsis DII-VENUS reporter revealed that auxin redistribution occurs in minutes following a change in gravity stimulus (Band et al., 2012). DII-VENUS expression patterns have also been used to model auxin diffusion through plasmodesmata in Arabidopsis root tips (Mellor et al., 2020). The R2D2 auxin reporter combines DII-VENUS with mDII-ntdTomato in the same construct to allow direct relative quantitative analysis of the DII/mDII fluorescence ratio which is an improvement over previous versions of auxin reporters (Liao et al., 2015).

These auxin reporters have now been translated into some cereal species including rice, maize and barley (Yang et al., 2017, Mir et al., 2017, Dao et al., 2023). The DII-VENUS and DR5 reporters have been successfully transformed into maize and used to discover differences in auxin signalling during cell cycle of leaf epidermal cells (Mir et al., 2017). Rice DII-VENUS and DR5-VENUS reporters have been generated and used for reporting auxin distribution during rice spikelet and root development (Yang et al., 2017). Expression of a DR5v2:ntdTomato/DR5:n3GFP ratio reporter in maize and barley leaf tissues via particle bombardment found DR5v2 to be responsive to exogenous auxin treatment in both species (Dao et al., 2023). The R2D2 reporter has also been demonstrated to function in maize and responsive to auxin application through transient expression (Dao et al., 2023). Despite the advances in other cereals, no auxin reporter lines have yet been generated in wheat.

1.7 Gravitropic setpoint angles in Arabidopsis and cereal species

Auxin is the primary plant hormone involved in gravitropic setpoint angle (GSA) maintenance, which is "the angle with respect to gravity at which an organ is

maintained by gravitropism" (Digby and Firn, 1995). Arabidopsis primary roots growing vertically downwards would have a GSA of 0°, however, lateral roots are predominantly maintained at non-vertical GSAs due to the balance between the angle-dependent gravitropic response and the counter-acting upward anti-gravitropic auxin flux (Roychoudhry et al., 2023).

This balance in auxin flux at GSA is due to a balance of PIN3 and PIN7 in columella cells (Roychoudhry et al., 2023). The non-vertical GSAs displayed by lateral roots may be beneficial for resource capture in the surrounding soil environment. The GSA of a plant organ will change over time during plant development and in response to environmental stimuli such as light (Digby and Firn, 1995). For example, Arabidopsis lateral root GSA becomes more vertical with age (Roychoudhry et al., 2013). Reorientation of Arabidopsis roots will cause either upwards or downwards root bending to return to the original GSA of the root. Root responses to reorientation are angle dependent with greater reorientation angles leading to a faster response to return to the original GSA (Roychoudhry et al., 2013).
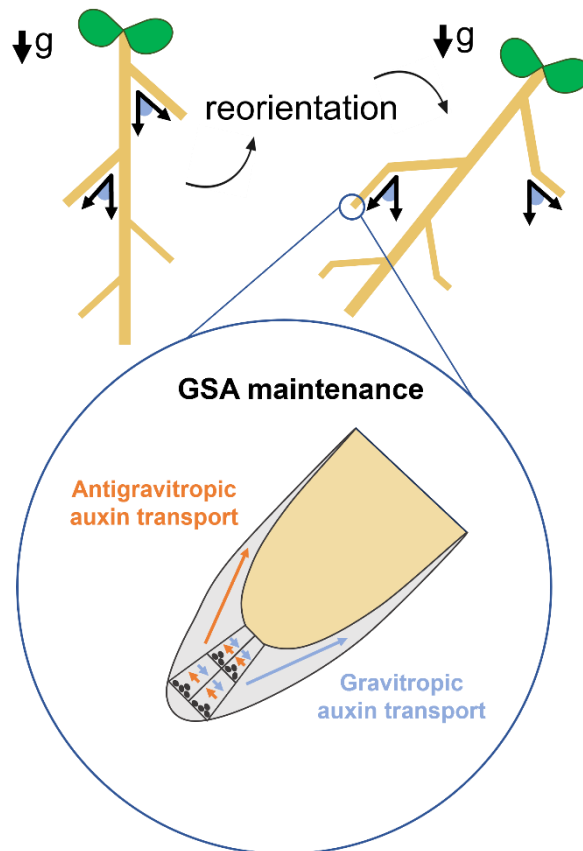
Figure 1.3: Arabidopsis lateral root gravitropic setpoint angle maintenance.

Gravitropic setpoint angles (GSAs) are determined by an angle-dependent gravitropic mechanism acting against an angle-independent antigravitropic offset, these auxin fluxes are balanced when the root is at GSA (Roychoudhry et al., 2023), g = direction of gravity, angle symbols = lateral root at GSA, inset orange arrows = antigravitropic offset, inset blue arrows = gravitropic auxin transport, diagram not to scale.

Limited research has been performed in wheat or other cereals on GSA maintenance, gravitropism and root growth angle control. Early cereal gravitropism research on the gravitropic responses of oat, wheat, rice and maize coleoptiles found that cereal coleoptiles respond to a change in gravity stimulus in an angle-dependent manner (Iino et al., 1996, Tarui and Iino, 1997). A study of maize root gravitropic setpoint angles found differences in GSA between maize cultivars and in different root types (Hund, 2010). The non-vertical growth of cereal roots was originally described as "plagiogravitropic" and the root growth direction was suggested to be determined by the emergence angle and the gravitropic responses of the cereal plant (Oyanagi et al., 1993a). Kaye (2018) found that both rice and wheat non-vertical seminal roots have an active antigravitropic offset mechanism and are capable of GSA maintenance.

1.8 *LAZY* genes: regulators of shoot and root growth angle

The molecular basis of crop shoot and root architecture can be important to understand when investigating methods for optimising plant growth and improvements in crop yields. A crossing experiment between shallow and steep rooting wheat cultivars resulted in a now disproven theory that wheat root gravitropic responses were controlled by a single dominant gene (Oyanagi et al., 1993a). Root gravitropism is now known to be a complex molecular pathway, and several genes involved in wheat gravitropism have since been identified such as *EGT1* (*ENHANCED GRAVITROPISM 1*), *EGT2* and the *LAZY* gene family (Kirschner et al., 2021, Fusi et al., 2022, Rasool et al., 2023).

LAZY genes contain five conserved domains and functionin shoot and root growth angle control (Waite and Dardick, 2021). The first *LAZY* gene to be identified was *LAZY1* (*LA1*) in rice, which has functions in shoot gravitropism and rice tiller angle regulation (Li et al., 2007). There are six *LAZY* genes identified in Arabidopsis; *AtLAZY1*, *AtLAZY2*, *AtLAZY3*, *AtLAZY4*, *AtLAZY5* and *AtLAZY6*, and *AtLAZY2* and *AtLAZY4* are involved in root growth angle control and root gravitropism (Yoshihara and Spalding, 2017). The *LAZY* genes are part of the wider IGT family which also includes the *TAC1* (*TILLER ANGLE CONTROL 1*) genes involved in regulation of shoot growth angle in plant species including Arabidopsis, rice and peach (*Prunus persica*) (Yu et al., 2007, Dardick et al., 2013).

LAZY genes are highly conserved and present in a wide range of plant species including rice, Arabidopsis, maize, soybean (*Glycine max*), *Lotus japonicus* and *Medicago truncatula* (Yoshihara et al., 2013, Ge and Chen, 2016). The wheat *LAZY* gene family has been identified (Ashraf et al., 2019, Rasool et al., 2023, Kitomi et al., 2020), but there has been limited research into the functions of these wheat genes. Sequence alignment analysis of rice *LAZY1* with other cereal genomes first discovered wheat *LAZY1* along with orthologs in sorghum (*Sorghum bicolor*) and maize (Li et al., 2007). Wheat *DRO1-like* (*TaDRO1*) homoeologs were identified as *LAZY* genes and found to interact via a C-terminus EAR motif with TOPLESS proteins, a repressor of auxin-regulated genes (Ashraf et al., 2019). A further triad of wheat *LAZY* genes were named *TaqSOR1-A*, *TaqSOR1-B* and *TaqSOR1-D* after the rice *qSOR1* (*quantitative trait locus for*

SOIL SURFACE ROOTING 1) gene (Kitomi et al., 2020). Sequence alignment of the wheat *DRO1* and *qSOR1* homoeologs showed these genes are most similar to Arabidopsis *LAZY2* and *LAZY4* (Appendix 2) (Kitomi et al., 2020). The entire wheat *LAZY* gene family is thought to have been identified, although investigation of wheat *LAZY* molecular interactions has been limited to the *TaDRO1* homoeologs (Ashraf et al., 2019, Rasool et al., 2023).

Arabidopsis *LAZY2* and *LAZY4* have predominantly root-specific expression in root statocyte columella cells and root vasculature (Taniguchi et al., 2017, Furutani et al., 2020). LAZY2 and LAZY4 proteins are localised in the direction of gravity on the plasma membrane of columella cells and repolarise following a change in gravity stimulus in lateral root columella cells (Furutani et al., 2020). *AtLAZY3* is also expressed in root statocytes and functions in root gravitropism, with Arabidopsis *lazy2 lazy3 lazy4* triple mutants exhibiting negative gravitropism with upwards growing roots (Yoshihara and Spalding, 2017, Taniguchi et al., 2017, Ge and Chen, 2019). This *lazy* triple mutant phenotype could be explained by reversal of PIN3 polarity and auxin flow in response to gravistimulation (Ge and Chen, 2019). *LAZY4* overexpression results in deeper rooting phenotypes in Arabidopsis and plum (*Prunus domestica*) (Guseman et al., 2017).

Rice *LAZY1* regulates rice tiller angle (Li et al., 2007) and similarly Arabidopsis *LAZY1* mainly functions in shoot gravitropism with *lazy1* loss-of-function mutants having more horizontal shoot branch angles (Yoshihara et al., 2013). The loss of *LAZY1* in rice alters polar auxin transport and shoot auxin distribution (Li et al., 2007) and *LAZY1* is thought to act in the gravitropism pathway between gravity sensing and auxin redistribution (Yoshihara et al., 2013). LAZY1 is cell membrane and nuclear localised and is essential for the redistribution of auxin following gravitropic stimulation in rice, maize and Arabidopsis (Li et al., 2007, Dong et al., 2013, Nishimura et al., 2023). Introducing point mutations into domain V of *AtLAZY1* gives a downwards bending, positively gravitropic shoot phenotype (Yoshihara and Spalding, 2020). A horizontal, spreading tiller phenotype can also be seen in a *lazy1* rice mutant with a mutation in a predicted transmembrane domain region of *OsLAZY1* (Chen et al., 2022a).

LAZY1 and *TAC1* have overlapping expression patterns in Arabidopsis shoots and *TAC1* is suggested to negatively regulate *LAZY1* in the shoot as the *lazy1*

mutant phenotype is epistatic to the *tac1* shoot phenotype (Dardick et al., 2013, Hollender et al., 2020). Another LAZY1-interacting protein is BRXL4 (BREVIS RADIX LIKE 4) found to interact with domain V of LAZY1 with at the plasma membrane (Che et al., 2023). BRXL4 proposed to negatively regulate LAZY1 by reducing the amount of plasma membrane localised LAZY1 where LAZY1 may function in gravity signalling (Che et al., 2023).

There are five *LAZY* conserved domains and Arabidopsis *LAZY1*, *LAZY2*, *LAZY4* and *LAZY6* contain all five of these domains (Yoshihara et al., 2013). Conserved domain I at the N-terminus is required for LAZY1 localisation to the plasma membrane and control of shoot branch angle (Yoshihara and Spalding, 2020). Domain II contains a conserved 'IGT' [GφL(A/T)IGT] motif which is present in amino acid sequences of all *LAZY* and *TAC1-like* genes in the IGT family (Dardick et al., 2013). *LAZY* domains III and IV are less well conserved and inducing mutations in domains III or IV in *LAZY1* had a lesser effect on shoot phenotype than mutating domains I, II or V (Yoshihara and Spalding, 2020). *LAZY2* and *LAZY4* contain a longer version of domain III named extended domain III (D3X) (Binns, 2022). A dominant gain-of-function point mutation in D3X of *AtLAZY4* (*lazy4D*) or in *LAZY2* (*lazy2D*) was found to cause a steeper lateral root angle phenotype showing that D3X is important in Arabidopsis lateral root growth angle control (Binns, 2022). This mutant phenotype contrasts with Arabidopsis knockout *lazy2* and *lazy4* mutants which have more horizontal lateral root growth angles (Guseman et al., 2017).

LAZY domain V has high sequence similarity in all LAZY proteins and so was named CCL (conserved C terminus in LAZY1 family proteins) (Taniguchi et al., 2017). The *LAZY* CCL domain interacts with the BRX domain of RCC1-like domain (RLD) proteins to recruit RLD from the cytoplasm to the plasma membrane following gravistimulation (Furutani et al., 2020). The CCL domain contains an EAR-like motif (ethylene-responsive element binding factor-associated amphiphilic repression), which is one of the most common transcriptional repression motifs in plants (Chow et al., 2023). This domain V EAR motif is not present in *TAC1-like* genes (Yoshihara and Spalding, 2017). EAR motif-containing proteins negatively regulate genes that have many different functions in plant growth and development (Chow et al., 2023). The EAR motif

was found to be essential for *LAZY4* function, as overexpressing *LAZY4* gives a steeper rooting phenotype but overexpressing a truncated *LAZY4* lacking an EAR motif yields a wildtype phenotype (Guseman et al., 2017). Expressing only the C-terminal region in Arabidopsis *lazy* mutants was able to reverse the primary root growth direction back to wildtype (Taniguchi et al., 2017).

LAZY genes were proposed to act downstream of gravity perception and upstream of auxin gradient formation in the gravity signalling pathway as asymmetrical auxin gradients did not form in the *atlazy1 lazy2 lazy3* triple mutant (Yoshihara and Spalding, 2017, Taniguchi et al., 2017). GFP-tagged LAZY proteins were shown to be plasma membrane localised in root columella cells (Ge and Chen, 2019). LAZY proteins have now been demonstrated to act as signal transmitters of statolith localisation and gravity direction in the gravitropic pathway by localising to amyloplast sites on the plasma membrane (Nishimura et al., 2023). LAZY proteins diffuse to statoliths at the plasma membrane following LAZY phosphorylation and statolith sedimentation (Chen et al., 2023).

Gravistimulation induces MAPK-mediated (Mitogen-Activated Protein Kinase) phosphorylation of Arabidopsis LAZY proteins in root columella cells which facilitates LAZY protein localisation at statolith sites (Chen et al., 2023) (Fig. 1.4). *LAZY* extended domain III (D3X) is likely to be important during this pathway as mutating *LAZY4* D3X (*lazy4D* mutation) is hypothesised to increase LAZY4 binding to statoliths or *LAZY4* stability at statoliths and D3X may be the site of interaction between *LAZY4* and statoliths (Binns, 2022). At the plasma membrane, Arabidopsis LAZY4 has been shown to recruit RLD proteins for PIN3 re-localisation and polar auxin flow in the direction of gravity (Furutani et al., 2020, Nishimura et al., 2023). LAZY re-polarisation resulting in asymmetric auxin distribution causes changes in cell elongation and differential growth (Fig. 1.4) (Chen et al., 2023).
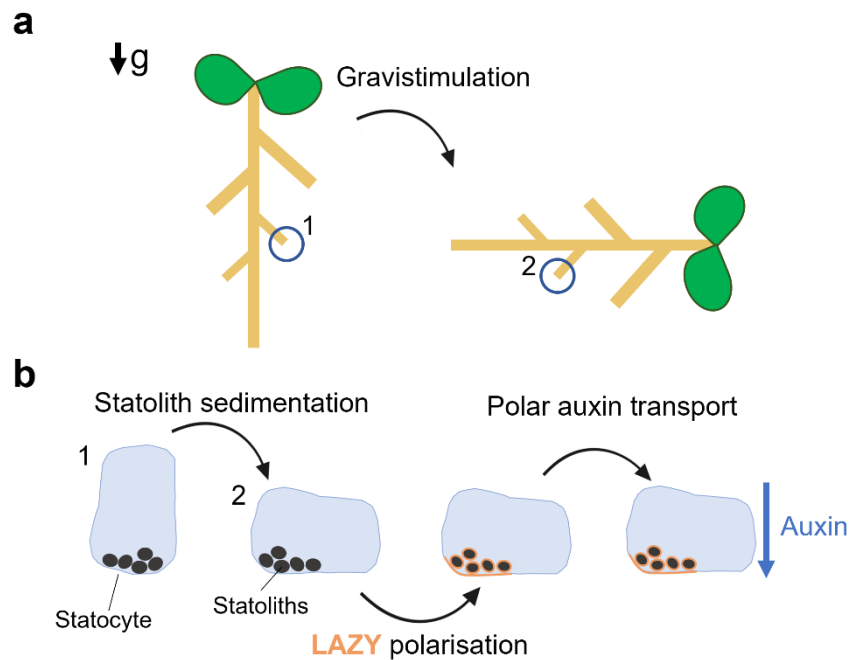
Figure 1.4: The role of LAZY proteins in the gravitropic response pathway.

(a) Arabidopsis seedling reorientated by 90° (b) Diagram showing statolith sedimentation in lateral root columella cells. Statoliths sediment to the new lower side of the cell following gravistimulation, this causes LAZY polarisation (orange shading) to statoliths and results in changes in polar auxin transport (blue arrow), g = direction of gravity (Furutani et al., 2020, Chen et al., 2023).

1.9 The potential of the *LAZY* gene family in crop breeding

LAZY genes are promising candidates for use in future crop improvement as root growth angle modification is proposed to optimise nutrient uptake and improve crop yields (Lynch, 2013). Shallower crop root systems are thought to be advantageous in saline or phosphorus-limited environments (Lynch, 2013). Therefore, root growth angle is a major root trait that can be targeted for optimising crop performance under certain environmental conditions. Rice cultivars grown in irrigated growth conditions often have shallower root systems whereas a steeper root system may be beneficial for upland rice varieties grown in non-flooded conditions which can experience drought (Boonjung and Fukai, 1996). *DRO1* (*DEEPER ROOTING 1*) is a rice *LAZY* gene identified through QTL analysis of a rice population generated from a cross between an upland, deep rooting cultivar and a shallow rooting cultivar (Uga et al., 2011). Overexpression of *DRO1* in rice has been shown to cause a steeper root system phenotype showing that *OsDRO1* functions in root growth angle regulation (Uga et al., 2013).

DRO1 plants were found to have more vertical root growth angles and increased root biomass in deep soil layers which resulted in improved drought avoidance and increased grain yield in water-limited conditions (Uga et al., 2013).

A homolog of rice *DRO1* associated with root angle control was identified and named *qSOR1* (*quantitative trait locus for SOIL SURFACE ROOTING 1*) (Kitomi et al., 2020). Rice *qSOR1* is expressed in root columella cells and rice plants with a loss-of-function *qsor1* allele have shallower root angles and soil surface roots (Kitomi et al., 2020). Rice *qsor1* plants with soil surface roots were better at adapting to growth in saline rice paddies and had increased yield compared to cultivars without the *qsor1* allele (Kitomi et al., 2020). These studies show that plants may have different optimal root angles depending on the growth environment and that *LAZY* family genes are promising candidates to use in crop breeding for modification of root system architecture.

1.10 Project aims

Steeper and deeper crop root systems are proposed to increase crop yields in a changing climate through improving uptake of water and nutrients (Lynch, 2013). This work will investigate potential strategies to achieve the 'steep' phenotype within the 'steep, cheap and deep' ideotype proposed by Lynch (2013).Re-engineering root system architecture in crop breeding programmes could lead to improved yields in low input agricultural systems. The goal of this work was to gain further understanding of cereal root architecture development and the *LAZY* genes in wheat to work towards achieving steeper crop root systems.

Firstly, this work trialled methods for quantifying root system architecture and comparisons of different growth environments to investigate the diversity of wheat root system architecture as root system architecture phenotyping is a difficult challenge (Atkinson et al., 2019). The second objective was to understand whether wheat and rice lateral roots were capable of GSA maintenance which would further the understanding of cereal root gravitropism and contribute towards root system architecture modification. Arabidopsis lateral roots can maintain gravitropic setpoint angles (Roychoudhry et al., 2013, Digby and Firn, 1995), however, the ability of non-vertical cereal lateral roots to maintain gravitropic setpoint angles is unknown.

Next, this work aimed to generate a wheat DII-VENUS auxin reporter to provide a valuable tool for furthering auxin and gravitropism research in wheat. Auxin is the main plant hormone in the gravitropic response pathway, and many other developmental processes and auxin reporters are important tools for visualising auxin distribution, signalling and responses in plants. DII-VENUS is an auxin reporter first developed in Arabidopsis and later generated in maize, rice and barley. A wheat auxin reporter did not yet exist despite wheat being an important cereal species.

The second and third aims were to translate Arabidopsis root gravitropism and *LAZY* gene family research into wheat using crop transformation and other sources of wheat genetic diversity. This work is important as the current understanding of the functions of the wheat *LAZY* gene family is limited and *LAZY* genes could be valuable tools for use in crop breeding. Through their roles in the gravity signalling pathway and regulating the development of root systems, *LAZY* genes have potential applications in crop breeding for modification of root system architecture.

In summary, the aims and objectives of this project were to:

1. Investigate root gravitropism and auxin signalling in cereals to work towards improvement of crop root system architecture.
   a) Explore wheat root system architecture variation in different growth environments and within wheat cultivars and landraces.
   b) Establish if wheat and rice lateral roots have the capacity to maintain gravitropic setpoint angles.
   c) Create a wheat DII-VENUS auxin signalling reporter and determine a wheat root confocal imaging protocol.

2. Examine the functions of the wheat *LAZY* genes to determine if these genes and the *lazy4D* mutation could be used for modifying wheat root system architecture.
   a) Analyse wheat *LAZY* family homoeolog sequence conservation and expression within the shoots and roots of wheat.
   b) Determine if the *lazy4D* mutation in wheat influences lateral root branching angle.

3. Investigate the functions of *LAZY* extended domain III (D3X) in wheat root growth angle control by screening wheat lines with *TaqSOR1* D3X mutations.

    a) Perform root system architecture phenotyping of wheat TILLING lines with *qSOR1* D3X mutations.

    b) Create transformed Arabidopsis lines with mutations introduced from a *qSOR1* extended domain III mutant; Cadenza1761.

    c) Generate backcrossed Cadenza1761 BC_2F_2 plants and perform root growth angle analysis.

Chapter 2

Materials and Methods

Chapter 2: Materials and Methods

2.1 Plant lines and growth conditions

2.1.1 Plant lines

The wheat (*Triticum aestivum*), rice (*Oryza sativa*) and *Arabidopsis thaliana* lines used in this work are listed below. The wheat BC_2F_2 *Taqsor1-B R132*, *R132W$^{+/-}$* and *R132W* lines were developed from backcrossing the Cadenza1761 EMS TILLING line twice to wheat cv. Cadenza.

Table 2.1: List of wheat, rice and Arabidopsis plant lines used in this project.

Plant species	Plant line	Background	Source
Triticum aestivum	Bobwhite		Kepinski lab, University of Leeds
Triticum aestivum	Cadenza		Germplasm Resources Unit, John Innes Centre, Norwich
Triticum aestivum	Fielder		Crop Transformation, John Innes Centre, Norwich
Triticum aestivum	YoGI landrace panel x 285 lines		Harper lab, University of York
Triticum aestivum	*ZmUbi:DII-VENUS-N7*	Fielder	This project and NIAB, Cambridge
Triticum aestivum	*ZmUbi:mDII-VENUS-N7*	Fielder	This project and NIAB, Cambridge
Triticum aestivum	*qSOR1-A:qSOR1-A*	Fielder	This project and Crop Transformation, John Innes Centre, Norwich
Triticum aestivum	*qSOR1-A:qsor1-A (R136K)*	Fielder	This project and Crop Transformation, John Innes Centre, Norwich

Triticum aestivum	*ZmUbi:qsor1-D* (*R135A*)	Fielder	This project and Crop Transformation, John Innes Centre, Norwich
Triticum aestivum	Cadenza0220	Cadenza	Germplasm Resources Unit, John Innes Centre, Norwich
Triticum aestivum	Cadenza1761	Cadenza	Germplasm Resources Unit, John Innes Centre, Norwich
Triticum aestivum	Cadenza1761 x Cadenza BC$_2$F$_2$ *R132*	Cadenza	This project
Triticum aestivum	Cadenza1761 x Cadenza BC$_2$F$_2$ *R132W$^{+/-}$*	Cadenza	This project
Triticum aestivum	Cadenza1761 x Cadenza BC$_2$F$_2$ *R132W*	Cadenza	This project
Oryza sativa ssp. *japonica*	Nipponbare		Aneesh Lale, University of Nottingham
Arabidopsis thaliana	Col-0		Kepinski lab, University of Leeds
Arabidopsis thaliana	*lazy2*	Col-0	(SALK_149134C) Kepinski lab, University of Leeds
Arabidopsis thaliana	*LAZY2:LAZY2*	Col-0	Kepinski lab, University of Leeds
Arabidopsis thaliana	*LAZY2:lazy2D* (*R143A*)	Col-0	Kepinski lab, University of Leeds
Arabidopsis thaliana	*LAZY2:lazy2 1761* (*R144W*)	Col-0	This project
Arabidopsis thaliana	*lazy4D*	Col-0	Kepinski lab, University of Leeds

2.1.2 Seed sterilisation

Arabidopsis and wheat seeds were sterilised with chlorine gas prior to growth. Seeds were placed in 1.5 ml microcentrifuge tubes and the open tubes were placed inside a desiccator under a fume hood. Chlorine gas was generated by adding 3 ml of 37% hydrochloric acid to 100 ml of liquid bleach and the seeds were exposed to this in the desiccator for 2 – 3 hours. The seeds were transferred to a laminar flowhood for 1 hour for ventilation. For rice, the seed husk was removed from the seed which was then surface sterilised by washing with 20% sodium hypochlorite (2 minutes), 70% EtOH (2 minutes) followed by three washes with distilled dH_2O.

2.1.3 Plant media preparation

Arabidopsis seeds were sown onto 120 x 120 mm square plates on 45 ml autoclaved Arabidopsis Thaliana Salts (ATS) media (Table 2.2) (Wilson et al., 1990), containing 1% w/v sucrose and 0.8% plant agar (Duchefa Biochemie). Seeds were stratified on plates at 4°C for 48 hours.

Table 2.2: ATS media preparation

Macronutrients	mM
Potassium dihydrogen monophosphate (KH_2PO_4) (pH 5.5)	2.5
Potassium nitrate (KNO_3)	5
Calcium nitrate ($Ca(NO_3)_2$)	2
Magnesium sulphate ($MgSO_4$)	2
Micronutrients	**µM**
Iron ethylenediaminetetraacetic acid (Fe-EDTA)	50
Orthoboric acid (H_3BO_4)	70
Manganese chloride ($MnCl_2$)	14
Sodium chloride (NaCl)	10
Copper sulphate ($CuSO_4$)	0.5
Zinc sulphate ($ZnSO_4$)	1
Sodium molybdate ($NaMoO_4$)	0.2
Cobalt chloride ($CoCl_2$)	0.01

Hoagland's No. 2 nutrient solution (Hoagland and Snyder, 1933) was used for wheat experiments, in Hoagland's solution for pouches or on Hoagland's agar for plates. Hoagland's solution was prepared with 1.6g of Hoagland's stock added to 1 L of dH_2O before use (Table 2.3). Hoagland's agar for wheat plate experiments was made by adding 1% w/v sucrose and 0.8% w/v plant agar to Hoagland's solution. Wheat seeds were stratified on wet filter paper in petri dishes at 4°C for 48 hours before plating on 245 x 245 mm square plates containing 200 ml Hoagland's agar. Wheat pouch experiments were set up with seeds placed in individual CYG seed germination pouches (Mega International) standing in Hoagland's No. 2 solution.

Table 2.3: Hoagland's No. 2 preparation.

Reagent	mg/litre
Potassium nitrate (KNO_3)	606.6
Calcium nitrate ($Ca(NO_3)_2$)	656.4
Magnesium nitrate $Mg(NO_3)_2$	240.76
Ammonium dihydrogen phosphate ($NH_4H_2PO_4$)	115.03
Manganese chloride tetrahydrate ($MnCl_2.4H_2O$)	1.81
Boric acid (H_3BO_3)	2.86
Molybdenum trioxide (MoO_3)	0.016
Zinc sulphate heptahydrate ($ZnSO_4.7H_2O$)	0.22
Copper sulphate pentahydrate ($CuSO_4.5H_2O$)	0.08
Ferric tartrate ($Fe_2(C_4H_4O_6)_3$)	5

Rice seeds were stratified on wet filter paper in petri dishes at 4°C for 48 hours and then moved to 27°C, 12-hour photoperiod for a further 48 hours before plating. Rice plants were grown on 50 ml Yoshida's agar prepared with 1.25 ml of each macronutrient solution and the micronutrients stock solution added to 1 L of dH_2O before use (Table 2.4) (Yoshida et al., 1976). The plates were prepared with 1% w/v sucrose and 0.8% w/v plant agar on 120 x 120 mm square plates.

Table 2.4: Yoshida's media preparation.

Macronutrients	g/litre
Ammonium nitrate (NH$_4$NO$_3$)	91.4
Sodium dihydrogen phosphate dihydrate (NaH$_2$PO$_4$·2H$_2$O)	40.3
Potassium sulphate (K$_2$SO$_4$)	71.4
Calcium chloride (CaCl$_2$)	88.6
Magnesium sulphate pentahydrate (MgSO$_4$.7H$_2$O)	324
Micronutrients*	**g/litre**
Manganese chloride tetrahydrate (MnCl$_2$.4H$_2$O)	1.5
Ammonium molybdate tetrahydrate ((NH$_4$)$_6$Mo$_7$O$_{24}$.4H$_2$O)	0.074
Boric acid (H$_3$BO$_3$)	0.934
Zinc sulphate heptahydrate (ZnSO$_4$.7H$_2$O)	0.035
Copper sulphate pentahydrate (CuSO$_4$.5H$_2$O)	0.031
Iron (III) chloride hexahydrate (FeCl$_3$.6H$_2$0)	7.7
Citric acid monohydrate	11.9

*Micronutrients were mixed with 50 ml H$_2$SO$_4$ and made up to 1 L with dH$_2$O.

2.1.4 Plant growth conditions

Arabidopsis plates, wheat plates and wheat pouches were grown vertically in controlled environment rooms under long day conditions (16 hours light/8 hours dark) at a temperature of 20°C with 60% humidity and light intensity of approximately 350 µmol m^{-2}. Rice plates were grown vertically in controlled environment cabinets at 27°C under 12 hours light/12 hours dark conditions. Arabidopsis and wheat plants grown for seed, crossing or shoot phenotype analysis were grown on plates or pouches and transferred to compost (Petersfield No. 2) in 9 cm square pots. Wheat plants grown for root angle phenotyping were grown in large compost-filled pots containing a 20 cm diameter colander placed so the top was level with the compost surface. Plants were grown in glasshouses under long day conditions (16 hours light / 8 hours dark) at 20 – 25°C. Wheat plants grown for seed or crossing experiments were grown under speed breeding conditions (22 hours light/2 hours dark) at 22°C.

2.1.5 Wheat transformation

Wheat DII-VENUS and mDII-VENUS auxin reporter lines were developed by expressing Arabidopsis DII-VENUS and mDII-VENUS constructs codon-optimised for wheat under the control of the maize ubiquitin-1 (*ZmUbi*) promoter in wheat cv. Fielder (see 2.2.9 for details). The constructs were created and sent to NIAB (Cambridge) for transformation into wheat cv. Fielder. The *TaqSOR1-A:qSOR1-A*, *TaqSOR1-A:qsor1-A* (*R136K*) and *ZmUbi:qsor1-D* (*R135A*) wheat constructs (see 2.2.10 for details) were transformed into wheat cv. Fielder by Crop Transformation at the John Innes Centre (Norwich).

2.1.6 *Agrobacterium*-mediated Arabidopsis transformation

Arabidopsis plants were transferred from plates into 9 cm square pots with 5 seedlings per pot and grown for 4 – 6 weeks prior to transformation, where three pots were used for each transformation. A 2 ml culture of Luria-Bertini (LB) media was inoculated with a single colony of *Agrobacterium tumefaciens GV3101* straincontaining the construct for transformation. This culture was used to inoculate 2 x 250 ml LB media containing gentamycin (25 µg/ml), rifampicin (100 µg/ml) and spectinomycin (70 µg/ml). The cultures were grown overnight at 28°C shaking at 140 rpm. Agrobacterium cells were isolated with centrifugation at 8,000 rpm for 12 minutes at room temperature and resuspended in 250 ml of floral dipping solution (5% w/v sucrose, 10 mM $MgCl_2.6H_2O$ and 25 µl Silwet L-77). Arabidopsis inflorescences were dipped in the solution for 2 – 3 minutes and sealed in a transparent autoclave bag for 24 hours (Clough and Bent, 1998). The bag was opened after 24 hours, and the plants were grown for 4 – 6 weeks before harvesting of T_1 seeds.

2.1.7 Selection of transgenic plants with seed coat fluorescence

Arabidopsis seeds transformed with an Alligator V vector that displayed seed coat fluorescence in T_1 were selected using an Olympus SZX12 stereo microscope. The T_2 seeds from self-pollinated T_1 plants with a 3:1 fluorescent:non-fluorescent ratio were selected as they were likely to contain a single insertion in T_1. The T_3 lines with 100% seed coat fluorescence were selected for use as homozygous single insertion lines. Three independent T_3 lines from three different T_1 plants were used for phenotyping.

2.2 Molecular biology

2.2.1 Wheat *LAZY* gene family and EMS mutant identification

The full-length protein sequences for the Arabidopsis *LAZY* gene family; *AtLAZY1* (AT5G14090), *AtLAZY2* (AT1G17400), *AtLAZY3* (AT1G19115), *AtLAZY4* (AT1G72490), *AtLAZY5* (AT3G24750) and *AtLAZY6* (AT3G27025) were downloaded from EnsemblPlants (https://plants.ensembl.org) and used in reciprocal BLAST searches to identify orthologs in the wheat genome. Wheat and Arabidopsis amino acid sequences were aligned with CLUSTAL-Omega, T-Coffee and Boxshade (https://www.ebi.ac.uk/Tools/msa/). Since this work, the wheat *LAZY* genes have been identified and published under several names (Ashraf et al., 2019, Kitomi et al., 2020, Rasool et al., 2023).

The 'Genetic Variation' tool within EnsemblPlants was used to search for lines in the wheat cv. Cadenza EMS TILLING population with mutations in extended domain III of the three wheat *qSOR1* homoeologs. Seeds were ordered from the Germplasm Resources Unit (Norwich) for selected mutants.

2.2.2 Wheat genomic DNA extraction

Wheat leaf tissue was harvested at the two-leaf stage and frozen in liquid nitrogen. Genomic DNA extraction was performed using a protocol adapted from the Cotton Lysis Buffer (CLB) protocol (Paterson et al., 1993). Frozen leaf tissue was ground with a micropestle and incubated in CLB at 65°C for 45 minutes. The sample was spun for 5 minutes with 375 µl chloroform isoamyl alcohol, supernatant removed and spun with 300 µl for 30 minutes at 8,000 rpm to form a pellet. The supernatant was discarded, and the pellet washed with 70% EtOH, air dried and resuspended in 50 µl dH_2O.

2.2.3 Polymerase Chain Reaction (PCR)

The Phusion High-Fidelity DNA Polymerase Kit (NEB) was used for cloning the *TaqSOR1-A* promoter according to the manufacturer's instructions. The reaction components (Table 2.5) were added to 0.2 ml PCR tubes on ice with Phusion polymerase added last. The tubes were briefly spun down to mix and transferred from ice to a thermocycler preheated to 98°C in the following thermocycling conditions (Table 2.6).

Table 2.5: Phusion PCR reaction components.

Component	Volume (µl) per 20 µl reaction
5X Phusion HF buffer	4
Forward primer (10 µM)	1
Reverse primer (10 µM)	1
dNTP (10 mM)	0.4
Phusion DNA polymerase	0.2
Template gDNA	1
dH$_2$O	12.4

Table 2.6: Thermocycling conditions for *TaqSOR1-A* promoter cloning

Step	Temperature (°C)	Time
Initial denaturation	98	30 seconds
35 cycles	98	10 seconds
	64	30 seconds
	72	90 seconds
Final extension	72	10 minutes
Hold	4	∞

GoTaq G2 DNA polymerase was used for genotyping wheat lines for the *TaqSOR1-B R132W* SNP according to the manufacturer's instructions. The reaction components (Table 2.7) were added to 0.2 ml PCR tubes on ice. The tubes were briefly spun down to mix and transferred from ice to a thermocycler preheated to 95°C in the following thermocycling conditions (Table 2.8).

Table 2.7: GoTaq G2 PCR reaction components.

Component	Volume (µl) per 20 µl reaction
5X Green GoTaq reaction buffer	4
Forward primer (10 µM)	0.5
Reverse primer (10 µM)	0.5
dNTP (10 mM)	0.4
GoTaq G2 DNA polymerase	0.2
Template gDNA	2
dH$_2$O	12.4

Table 2.8: Thermocycling conditions for *Taqsor1-B R132W* SNP genotyping.

Step	Temperature (°C)	Time
Initial denaturation	95	2 minutes
35 cycles	95	30 seconds
	60	30 seconds
	72	1 minute
Final extension	72	5 minutes
Hold	4	∞

2.2.4 Agarose gel electrophoresis

Agarose gel electrophoresis was used for PCR product analysis. Agarose was dissolved in TAE (1X Tris-acetate-EDTA; 40 mM Tris-base, 20 mM acetic acid, 1 mM EDTA at pH 8) buffer at a 1% w/v concentration and 1X Gel-Red nucleic acid added. 5 µl PCR product (and 1 µl loading dye for Phusion PCR products) loaded onto the gel with 8 µl 1 kb+ DNA ladder (ThermoFisher) and run for 50 minutes at 80 V in 1X TAE buffer in a Bio-Rad gel tank, then visualised with a UV gel imager.

2.2.5 Agarose gel extraction

DNA was extracted from agarose gel with a scalpel under a UV illuminator and purified with an Invitrogen PureLink Quick Gel Extraction Kit. An Eppendorf with 3 volumes of Gel Solubilization Buffer for 1 volume gel incubated in a 50°C waterbath for 10 minutes until dissolved. One volume of isopropanol was added,

then the dissolved gel slice was transferred to a quick extraction column inside a wash tube and centrifuged for 1 minute. The flowthrough was discarded, and the column washed with 500 μl Wash Buffer 1, centrifuged, flowthrough discarded and column centrifuged again. The sample was eluted with 30 μl Elution Buffer into a recovery tube and stored at -20°C.

2.2.6 PCR purification

PCR products were purified using a QIAquick PCR purification kit (Qiagen). 5 volumes of Buffer PB were added to 1 volume of PCR product and mixed. The mix was transferred to a QIAquick column and centrifuged for 60 seconds, before discarding the flowthrough. The column was washed with 750 μl Buffer PE and centrifuged for 60 seconds before discarding the flowthrough. The QIAquick column was centrifuged for 60 seconds and placed into a 1.5 ml microcentrifuge tube. The purified DNA was eluted with 30 μl Buffer EB by centrifugation for 60 seconds and stored at -20°C.

2.2.7 *Escherichia coli* (*E. coli*) transformation and growth conditions

A 30 μl aliquot of DH5α *E. coli* competent cells was thawed on ice before 5 μl of plasmid DNA added and incubated on ice for 30 minutes. The cells were heat shocked for 42°C for 30 seconds and placed back on ice for 2 minutes. LB (Luria-Bertani) was prepared with 10 g/L tryptone, 10 g/L NaCl and 5 g/L yeast extract (liquid) and the addition of 1.5% agar for LB agar. The aliquot had 1 ml of liquid LB added and then incubated at 37°C at 200 rpm for 1 hour. The solution was spread on LB agar plates with the correct antibiotic and incubated overnight at 37°C. *E. coli* transformed with pDONR 221 P1-P5r, pDONR 221 P5-P2 or pGGG vectors were incubated with kanamycin (40 μg/ml). The pAlligator V destination vector was selected with spectinomycin (70 μg/ml) and the pDONR 207 entry vector was selected with gentamycin (25 μg/ml).

2.2.8 Site-directed mutagenesis

Site-directed mutagenesis to introduce the *R144W* mutation into *AtLAZY2* was performed on a pDONR P5-P2 entry vector containing the Arabidopsis *LAZY2* gene sequence using a Q5 Site-Directed Mutagenesis Kit (NEB). The reaction mix (Table 2.9) was amplified in a PCR thermocycler (Table 2.10), and then 1 μl of the PCR product was mixed with 5 μl 2X KLD Reaction Buffer, 1 μl KLD

Enzyme Mix and 3 µl dH$_2$O. 5 µl of the KLD mix was added to 50 µl of chemically competent *E. coli* cells and incubated on ice for 5 minutes. 950 µl SOC media added to the cells and incubated at 37°C for 1 hour with shaking, before spreading onto LB agar plates with kanamycin (40 µg/ml) and incubated overnight at 37°C. The presence of the *R144W* mutation was confirmed with Sanger sequencing (Genewiz).

Table 2.9: Site-directed mutagenesis reaction components.

Component	Volume (µl)
Q5 Hot Start High-Fidelity 2X Master Mix	12.5
Forward primer (10 µM)	1.25
Reverse primer (10 µM)	1.25
Template DNA	1
dH$_2$O	9

Table 2.10: Thermocycling conditions for site-directed mutagenesis.

Step	Temperature (°C)	Time
Initial denaturation	98	30 seconds
25 cycles	98	10 seconds
	59	30 seconds
	72	2 minutes
Final extension	72	2 minutes
Hold	4	∞

2.2.9 Gateway cloning

Gateway cloning was used to create the DII-VENUS and mDII-VENUS vectors for wheat transformation, and for the *lazy2 R144W* Arabidopsis transformation. Gateway cloning was used as specific Gateway destination vectors were required for the respective wheat and Arabidopsis transformation experiments. The Gateway cloning system uses site-specific recombination to create destination vectors for transformation. Entry vectors are created by a BP recombination reaction between a pDONR vector and an *attB* flanked PCR product to create an

entry vector with *attL* sites. The final vector is generated by an LR recombination reaction between the entry vectors and a destination vector.
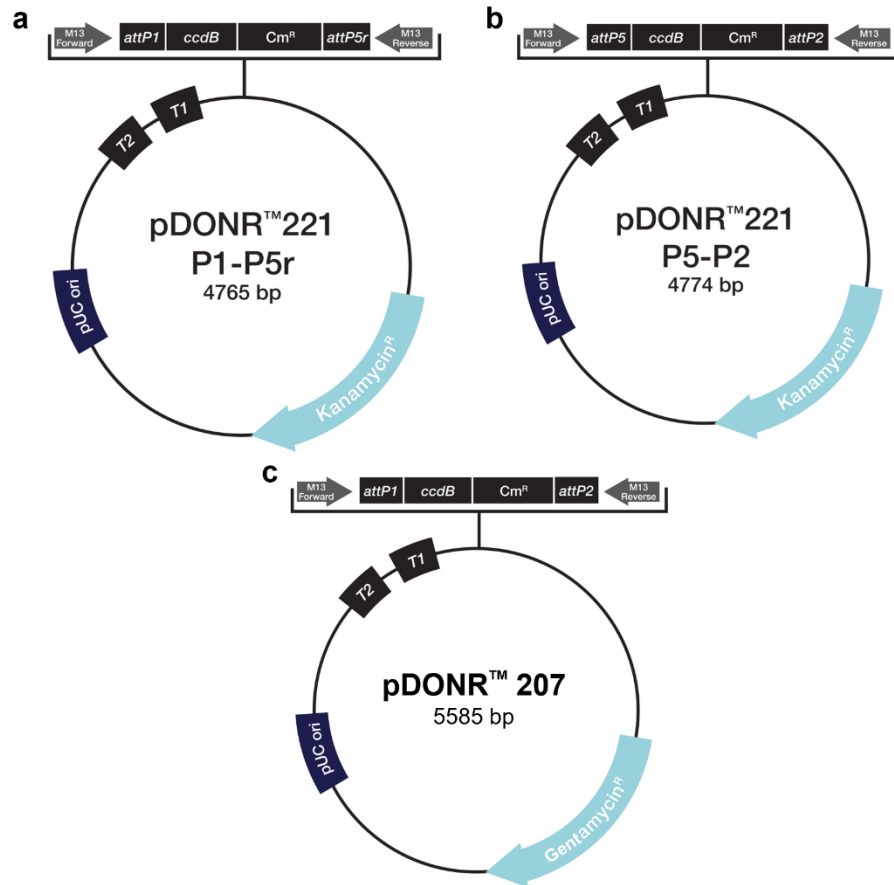
Figure 2.1: Maps of vectors used in Gateway cloning.

Plasmid maps of (a) pDONR221 P1-P5r, (b) pDONR221 P5-P2 and (c) pDONR207 (Invitrogen). The *attP* recombination sites recombine with *attB* sites to create *attL* sites. *ccdB*: lethal gene exchanged with gene of interest during BP reactions, Cm^R: Chloramphenicol resistance gene. M13 Forward and M13 Reverse: priming sites. pUC ori: origin of replication. *T1* and *T2*: *rmB* transcription termination sequences.

To create the DII-VENUS and mDII-VENUS vectors, the published Arabidopsis DII-VENUS and mDII-VENUS sequences were codon-optimised for wheat using an online codon optimisation tool. These DII-VENUS and mDII-VENUS sequences were gene synthesised as entry vectors (Genewiz) and the sequences were each introduced into pDONR207 vectors via a BP reaction (Fig. 2.1c). The reaction (Table 2.11) was centrifuged and incubated at 25°C overnight. 1 µl of Proteinase K (Invitrogen) was added to inactivate the BP Clonase II and incubated at 37°C for 10 minutes. The BP reaction was transformed into chemically competent *E. coli* cells and selected with gentamycin (25 µg/ml). The entry vector was extracted from single colonies grown and digested and

sequenced to confirm correct vector construction. These DII-VENUS and mDII-VENUS entry vectors were sent to NIAB (Cambridge) for assembly into destination vectors for wheat transformation.

Table 2.11: Components for BP reaction.

Component	Volume (µl)
Synthesised DNA with *attB* sites (15-150 ng)	2
pDONR 207 vector (150 ng/µl)	1
TE Buffer pH 8.0	5
BP Clonase II	2

Two-way multisite Gateway cloning was used for creation of the Arabidopsis *LAZY2:lazy2* (*R144W*) construct (Fig. 2.1a, b). The pDONR221 P1-P5r and P5-P2 entry vectors containing the *LAZY2* promoter and mutagenized *lazy2 R144W* gene sequences were recombined in an LR recombination reaction (Table 2.12) into the pAlligator V destination vector, a modified pF1P101 vector (Bensmihen et al., 2004). The components were incubated overnight at 25°C, before the addition of 2 µl Proteinase K. The reaction was incubated at 37°C for 10 minutes, transformed into *E. coli* cells and selected with spectinomycin (70 µg/ml).

Table 2.12: Components for LR reaction.

Component	Volume (µl)
pDONR221 P1-P5r *LAZY2* promoter entry vector (10 fmoles)	1
pDONR 221 P5-P2 *lazy2* (*R144W*) entry vector (10 fmoles)	1
pAlligator V destination vector (20 fmoles)	0.55
TE Buffer pH 8.0	5.45
LR Clonase II	2

2.2.10 Golden Gate cloning

Golden Gate cloning allows the assembly of multiple inserts into a vector in one reaction. The inserts have fragment-specific sequence overhangs to allow simultaneous assembly of multiple fragments. Golden Gate cloning was used to

generate the *TaqSOR1-A:qSOR1*-A, TaqSOR1-*A:qsor1-A* (*R136K*) and *ZmUbi:qsor1-D* (*R135A*) vectors for wheat transformation. Goldengate cloning was used as this was the preferred cloning method for Crop Transformation (John Innes Centre) which transformed these constructs into wheat.The *TaqSOR1-A* promoter sequence was amplified from Fielder gDNA, and the gene sequences were gene synthesised. The *ZmUbi* promoter, NosT terminator and pGoldenGreenGate (pGGG) destination vector were obtained from Crop Transformation at the John Innes Centre. The 10 µl reaction mix (Table 2.13) was run in a thermocycler (Table 2.14) and then transformed into chemically competent *E. coli* cells and plated on LB agar with kanamycin (40 µg/ml), X-gal and IPTG (isopropyl β-D-1-thiogalactopyranoside) and incubated overnight at 37°C. Blue-white screening was used to identify successful recombination. The β-galactosidase enzyme is produced via α-complementation by the *lacZ* gene within the *lac* operon present in non-recombinant plasmids in *E. coli* cells (Julin, 2018). β-galactosidase hydrolyses X-gal to form a blue pigment. The recombinant colonies do not produce a functional β-galactosidase enzyme and so appear white as a blue pigment is not formed in the presence of X-gal (Julin, 2018). Single white colonies were selected for inoculation of overnight LB and kanamycin cultures for plasmid extraction. The miniprepped plasmid was digested and sequenced with Sanger sequencing (Genewiz) to confirm correct vector construction before being sent to Crop Transformation at the John Innes Centre for wheat transformation (Hayta et al., 2021).

Table 2.13: Golden Gate reaction components.

Component	Volume (µl)
pGGG destination vector (100 ng/µl)	1
Gene promoter (50 ng/µl)	2
Gene coding sequence (100 ng/µl)	1
NosT terminator (100 ng/µl)	1
T4 DNA Ligase Buffer (10X)	1.5
T4 Ligase	0.5
BsaI (Eco31)	0.5
dH$_2$0	7.5

Table 2.14: Golden Gate reaction thermocycling conditions.

Temperature (°C)	Time
37	5 minutes
16	5 minutes
Go to step 1, 10 times	
37	7 minutes
80	10 minutes
4	∞

2.2.11 Agrobacterium transformation and growth conditions

A 50 µl aliquot of chemically competent *Agrobacterium tumefaciens* GV3101 strain cells was thawed and up to 1 µg of plasmid DNA was added. The cells were heat shocked at 37°C for 5 minutes and 750 µl of liquid LB was added to the aliquot. The aliquot was incubated at 28°C and with 140 rpm shaking for 4 hours. The aliquot was spread on LB agar plates containing rifampicin (100 µg/ml), gentamycin (25 µg/ml) and spectinomycin (70 µg/ml). The plates were incubated at 28°C for up to 3 days, and then single colonies were used to inoculate 5 ml of liquid LB and antibiotics, and incubated at 28°C and 140 rpm for up to 2 days. 2 ml was transferred to 250 ml of liquid LB and antibiotics in 1 L flasks and incubated overnight at 28°C and 140 rpm.

2.2.12 Plasmid miniprep

Single *E. coli* colonies were used for inoculation of 5 ml liquid LB cultures containing appropriate antibiotics. The cultures were incubated overnight at 37°C and 200 rpm before plasmid isolation was performed with the Plasmid Mini Kit (Qiagen). Pelleted bacterial cells were obtained from the 5 ml liquid culture centrifuged for 10 minutes at 8000 rpm. The pelleted cells were resuspended in 250 µl Buffer P1 and transferred to a microcentrifuge tube. The resuspension had 250 µl Buffer P2 added and mixed by inversion, before addition of 350 µl Buffer N3 and centrifugation for 10 minutes at 13,000 rpm. 800 µl of the supernatant was added to a QIAprep 2.0 Spin Column, centrifuged for 30 seconds and washed with 500 µl Buffer PB. The column was then washed with 750 µl Buffer PE and centrifuged for 60 seconds, flowthrough discarded and centrifuged again

for 60 seconds. The DNA was eluted in 50 µl Buffer EB into a 1.5 ml microcentrifuge tube by centrifugation for 60 seconds.

2.2.13 Restriction digest

Restriction digests of plasmids and DNA fragments were used for genotyping or to check for correct vector construction. A typical digest (Table 2.15) was set up and incubated at 37°C for 3 hours (reagents from NEB and ThermoFisher). 2 µl of loading dye was added to the digest reaction and analysis of the fragments performed with agarose gel electrophoresis on a 1% agarose gel.

Table 2.15: Restriction digest reaction components.

Component	Volume (µl) for a 20 µl reaction
Digest buffer	2
Restriction enzyme 1	0.5
Restriction enzyme 2	0.5
DNA (<1 µg)	5
dH$_2$O	12

2.2.14 Wheat *TaqSOR1-B R132* SNP genotyping

DNA was extracted from wheat leaf tissue harvested at the two-leaf stage. An 879 bp DNA fragment across the SNP site in *TaqSOR1-B* was amplified and digested with BshTI (ThermoFisher) (Table 2.16). The BshTI restrict site present in plants with *R132W* point mutation would result in 2 fragments of 412 bp and 467 bp, whereas DNA fragments from *R132* plants would remain undigested (879 bp). Confirmation of the genotyping was performed with Sanger sequencing (Genewiz) of undigested 879 bp DNA fragments.

Table 2.16: BshTI digestion of *TaqSOR1-B* fragments.

Component	Volume (µl) for a 10 µl reaction
10X FastDigest Buffer	1
BshTI (AgeI)	0.2
PCR product (<1 µg)	5
dH$_2$O	3.8

2.2.15 RNA extraction and cDNA synthesis

Wheat cv. Fielder plants were grown on Hoagland's agar in 245 x 245 mm square plates for 10 days. Three biological replicates of ~50 pooled lateral root tips, ~50 pooled seminal root tips and wheat shoot tissue sections were harvested with a scalpel, frozen in liquid nitrogen and stored at -80°C. Samples were ground with a Tissue Lyser (Qiagen) and RNA was extracted using an E.Z.N.A. Plant RNA kit (Omega Bio-tek). 500 µl RB Buffer and 2-mercaptoethanol was added to the samples and vortexed to mix. The lysate was transferred to a Homogenizer Mini Column in a 2 ml collection tube and centrifuged at 13,000 rpm for 5 minutes. The cleared lysate was transferred to a 1.5 ml microcentrifuge tube, 1 volume 70% EtOH added and vortexed to mix. 700 µl of the sample was transferred to a HiBind RNA Mini Column and centrifuged at 13,000 rpm for 1 minute, this was repeated to transfer all of the sample. DNA was removed from the sample with on-membrane DNase I digestion; 73.5 µl E.Z.N.A. DNase Digestion Buffer, 1.5 µl RNase-free DNase 1 per sample. 500 µl RNA Wash Buffer I was then added and centrifuged for 30 seconds, The sample was washed twice with 700 µl RNA Wash Buffer II, centrifuged at 13,000 rpm for 2 minutes to dry the column and eluted with 30 µl nuclease-free water into a 1.5 ml microcentrifuge tube and stored at -80°C.

cDNA synthesis from 1 µg of RNA was performed using a SuperScript VILO cDNA Synthesis kit (Invitrogen). 4 µl of SuperScript MasterMix and nuclease-free water were added to the RNA sample to make the reaction volume up to 20 µl. The reaction was incubated at 25°C for 10 minutes, 50°C for 10 minutes and 85°C for 5 minutes and stored at -20°C.

2.2.16 Quantitative PCR (qPCR)

Wheat homoeolog-specific primers were designed using the Primer3Plus online tool and BLAST. Each wheat homoeolog primer was designed to be specific by containing more than one unique base within the sequence compared to the other two homoeologs within the triad. Primer sequence specificity to the wheat homoeolog sequence was checked using PCR with pooled wheat cDNA as a template to ensure the primer pairs were amplifying a single amplicon.. The reference gene qPCR primers used were *TaActin* (Iquebal et al., 2019) and *TaEF* (Wu et al., 2015). Primer efficiencies were tested using a 4-point 1:4 dilution

series of pooled cDNA samples with the efficiency equation: $E = -1 + 10^{-1/x}$ where E is the primer efficiency and x is the line gradient of Ct against log cDNA concentrations (Rasmussen, 2001). cDNA was diluted 1:20 and amplified by qPCR in 15 µl reactions in 96-well plates (Table 2.17). The plate was spun for 30 s at 10,000 rpm before the qPCR program was run in a Bio-Rad CFX96 qPCR machine (Table 2.18).

Table 2.17: Quantitative PCR reaction components.

Component	Volume (µl) per 15 µl reaction
SsoFast EvaGreen Supermix (Bio-Rad)	7.5
Forward primer (10 µM)	0.75
Reverse primer (10 µM)	0.75
cDNA (synthesised from 1 µg of RNA)	1
dH$_2$O	5

Table 2.18: Thermocycling conditions for qPCR.

Step	Temperature (°C)	Time
Initial denaturation	95	5 minutes
45 cycles	95	5 seconds
	60	10 seconds
	72	10 seconds
Melt curve	65 - 97	

All reactions were performed in triplicate for three biological replicates per tissue type. The mean Ct values from three qPCR technical replicates for each homoeolog were normalised against the geometric mean of the *TaActin* (Iquebal et al., 2019) and *TaEF* (Wu et al., 2015) reference genes to calculate the normalised relative expression. Statistical analysis was based on the log transformed normalised expression per sample (Taylor et al., 2019).

2.2.17 List of primers

Table 2.19: List of primers used in this project.

Use	Target	Orientation	Sequence (5' - 3')	Source
qPCR	*TaLAZY1-Un*	FW	TCGGTGAACTGTTCATGCGT	This project
		RV	CCGGCACCTTTCTCATCCTT	
	TaLAZY1-B	FW	GGCCACGAAGACTATGACGTC	This project
		RV	ATGTCATCTTTCTCCGCGATG	
	TaLAZY1-D	FW	GTTCGCCGCCATTAATGTCC	This project
		RV	GGCGACGTCATCTTTTTCCG	
	TaDRO1-A	FW	ACCGGTAGTAGCTCCACACT	This project
		RV	ATCGGGATGTGGGAATGAGC	
	TaDRO1-B	FW	AAACTCATGACCCGCACGAT	This project
		RV	GAAGCAACTGATCTCGGCTTG	
	TaDRO1-D	FW	AACTACTCATGCGCAAGGGT	This project
		RV	GCTCATCCGGCTTCCAGTCT	
	TaqSOR1-A	FW	CCGGTCCGGGAGAATAGT	This project
		RV	CACCTCCTCGATGGTGAAGT	
	TaqSOR1-B	FW	GGGGGTGTCAAGCAGAAT	This project
		RV	GGCGCTCATCTTCTTTTGAA	
	TaqSOR1-D	FW	CGAGGAGGAGGAAGAGGATT	This project
		RV	CAATGAAATCTGAATCTGTTTTGTC	
	TaActin	FW	CAAATCATGTTTGAGACCTTCAATG	Iquebal et al., 2019
		RV	ACCAGAATCCAACACGATACCTG	
	TaEF	FW	CAGATTGGCAACGGCTACG	Wu et al., 2015
		RV	CGGACAGCAAAACGACCAAG	
Genotyping	*TaqSOR1-B*	FW	ACTGGGTGCAGAATCGGCTA	This project
		RV	GGCGCTCATCTTCTTTTGAA	
Cloning	*TaqSOR1-A* promoter	FW	ggctacggtctcaggagTGTCAAAAACGCTCTTAC	This project
		RV	ggctacggtctctcattCGATCCCTACTCTCTTCAAG	
Site-directed mutagenesis	*AtLAZY2*	FW	GGTCGATAGATGGATCAGTAACGC	This project
		RV	TCAAGACTCGAAGGACAATTC	
Sequencing	*M13*	FW	CAGGAAACAGCTATGAC	Messing, 1983
		RV	CGCCAGGGTTTTCCCAGTCACGAC	
	AtLAZY2	FW	ATGAAGTTCTTCGGGTGGATG	This project
		RV	TCATATCTCGAGAACTATGAAATCAGAATC	

2.3 Phenotyping experiments

2.3.1 Analysis of wheat root system architecture

RootNav software (Pound et al., 2013) was used for root system architecture analysis of wheat plants grown in pouches and on agar plates. Pouches were imaged with a tripod-mounted RICOH GR II camera and agar plates were imaged with an Epson Perfection V370 or V800 scanner. The images were processed to reduce the size below the 5-megapixel threshold required for RootNav. RootNav software was used to generate RSML (Root System Markup Language) files which represent root system architecture data (Lobet et al., 2015). RootNav Portal was used to extract the following root system traits: number of seminal roots, seminal root length, seminal root emergence angle, seminal root tip angle, convex hull area and root system width/depth ratio. The pixels/mm value for the

images was obtained from ImageJ and used to covert the length measurements from pixels to millimetres. The mean length of the primary and first pair of seminal roots (first three roots), mean first pair seminal emergence angle and mean first pair seminal tip angle measurements were calculated using Excel.

Wheat root systems grown in compost-filled square plates were imaged with an Epson Perfection V370 scanner and analysis was performed with ImageJ to measure the angle from vertical of the widest pair of crown roots visible at 50 mm from root emergence.

2.3.2 Arabidopsis lateral root and wheat seminal and lateral root growth angle analysis

Arabidopsis plants grown on ATS agar plates and imaged with an Epson Perfection V370 or V800 scanner. Lateral root growth angle was measured using ImageJ as the angle from vertical at Stage III (0.5 – 1 mm) and Stage IV (2.5 – 3 mm) away from the lateral and primary root junction.

5-day old wheat plants grown on CYG germination pouches were used for seminal root growth angle analysis. Seminal angle was measured as degrees from vertical at certain intervals measured from root emergence with ImageJ. Wheat plants were grown for 9 days for lateral root growth angle analysis. The angle from vertical was measured for six lateral roots per plant with the lateral roots measured being the first three lateral roots on both sides of the primary seminal root. Wheat lateral root growth angle was measured 0.5 – 1 mm away from the lateral and seminal root junction using ImageJ.

2.3.3 Wheat and rice reorientation experiments

Wheat and rice plants were grown vertically on agar plates for 9 days before being reorientated by 30° with respect to gravity. Plates were imaged with an Epson Perfection V370 or V800 scanner prior to reorientation and then imaged every 12 or 24 hours. For the analysis, downwards bending roots were roots reorientated above their original growth angle whereas upwards bending roots were reorientated below their original growth angle. Lateral root angle was measured using ImageJ as the angle in degrees from vertical of the last 1 mm section of the root. Changes in wheat and rice lateral root growth angle over time

were analysed by measuring lateral root tip angle from images of non-reorientated plates imaged at 0, 24 and 48 hours.

2.3.4 Compost colander experiments

Quantification of wheat root growth angle was performed using a colander method first described in Oyanagi et al. (1993b). Wheat seeds were germinated on wet filter paper in petri dishes and transferred after 2 days into the centre of 20 cm plastic colanders set into compost-filled pots. The colanders were removed from the pots after 8 weeks and the compost from the outside of the colanders removed without disturbing the emerging roots. The number of roots that emerged from each layer of holes in the colander were counted and the percentage of total roots emerging at each hole layer was calculated and plotted against the angle that the roots emerged from the colander. The ratio of deep rooting as described in Uga et al. (2013) was calculated by dividing the number of roots that emerged between 40° and 0° from vertical (0° = vertically growing roots), by the total number of roots that emerged from the colander. A higher deep rooting ratio value shows that a greater proportion of roots grew downwards and represents a steeper root system.

2.3.5 Wheat shoot phenotyping

Wheat plants were grown to 16 or 18 weeks for shoot phenotyping analysis. The number of tillers and the number of spikelets for each tiller were recorded and the tiller length of the main tillers were measured from shoot emergence from the compost surface to the top of the wheat spike.

2.4 Microscopy

2.4.1 DIC microscopy

Rice and wheat seminal root tips were imaged with a Differential Interference Contrast (DIC) Zeiss Scope A1 microscope at 10x magnification. Roots were treated with Lugol solution (Sigma) to stain starch present in the roots and mounted on glass slides with chloral hydrate solution (8:3:1 choralhydrate:water:glycerol) for imaging.

2.4.2 Confocal microscopy

Wheat DII-VENUS and mDII-VENUS seminal roots were imaged with 488 nm (GFP) and 555 nm (PI) lasers using a vertical stage Zeiss LSM 800 confocal microscope at 10x magnification. Wheat plants were grown vertically for 3 days on ATS agar plates and then transferred into Lab-Tek borosilicate coverglass chamber slides. The root cell walls were stained with propidium iodide (PI) prior to imaging.

A horizontal stage Zeiss LSM880 confocal microscope at 10x magnification was used to image 4-day old wheat DII-VENUS and mDII-VENUS seminal roots cleared and fixed with ClearSee for 3 days. Wheat seminal roots were mounted on slides with water prior to imaging, and all images were processed with ImageJ.

2.4.3 Lattice light-sheet imaging

A Zeiss Lattice Lightsheet 7 microscope was used for imaging of 4-day old wheat DII-VENUS and mDII-VENUS primary seminal roots cleared and fixed with ClearSee for 4 days. The roots were mounted in water on glass slides and imaged at 60x magnification with a GFP channel to create a Z-stack. Representative images from the Z-stack were processed with ImageJ.

2.4.4 Auxin treatment

Wheat DII-VENUS and mDII-VENUS plants were grown vertically for 3 days on agar plates. Auxin treatment of DII-VENUS and mDII-VENUS wheat plants was performed by laying the plates horizontally and treating with 1 µM IAA (indole-3-acetic acid) in 50 ml liquid ATS. A stock solution of IAA was prepared by addition of indole-3-acetic acid (Sigma) to dimethyl sulfoxide (DMSO), which was then added to liquid ATS solution to make a 1uM concentration. Mock-treated plants were treated with liquid ATS containing the same volume of DMSO. The plants were treated for 3 hours and then transferred to chamber slides before imaging with a vertical stage Zeiss LSM 800 confocal microscope at 10x magnification (488nm GFP and 555 nm PI channels). Images of 3 – 4 primary seminal root tips of DII-VENUS and mDII-VENUS (mock and IAA-treated) were used for analysis. The nuclei fluorescence of root cap cells was measured with ImageJ, with a circle of the same area measured for each nucleus.

2.5 Data analysis

All data analysis and data visualisation were performed with Python in a Jupyter notebook. Data was plotted using Seaborn and matplotlib data visualisation libraries. Data was first tested for normality using the Shapiro-Wilk test and normally distributed data was analysed with parametric tests: a student's t-test (t) (2 groups) or a one-way analysis of variance (ANOVA) (F) (more than 2 groups) followed by Tukey's honestly significant difference (HSD) post-hoc tests. If the Shapiro-Wilk test for normality showed that the data was not normally distributed then the data was analysed using non-parametric Mann-Whitney U (U) or Kruskal-Wallis (H) tests followed by Dunn's post-hoc tests. Correlation analysis of wheat root system traits in the landrace panel was performed using the non-parametric Spearman's rank correlation coefficient (r) as the phenotypic data were not normally distributed.

Chapter 3

Cereal root system architecture & root gravitropism

Chapter 3: Cereal root system architecture & root gravitropism

3.1 Introduction

Improving nutrient and water uptake is a crucial challenge in crop production as the outputs of current global agriculture are largely dependent on high inputs of fertilisers and irrigation (Gomiero et al., 2011). The intensive nature of the system increases soil erosion, lowers water use efficiency and reduces biodiversity (Gomiero et al., 2011). Following on from the Green Revolution that began in the 1960s, a 'second Green Revolution' was called for to increase yields whilst reducing the use of fertilisers and other inputs to lower the negative impacts of modern agriculture (Gomiero et al., 2011). Climate change is leading to higher global temperatures, increased CO_2 levels and an increase in extreme weather events (Lobell and Gourdji, 2012).

Improving the extent and depth of plant root systems is proposed to increase carbon capture and sequestration, to help mitigate some of the impacts of intensive agriculture and climate change (Kell, 2012). The deeper and more vertical root system phenotype with few, long lateral roots is known as the 'steep, cheap and deep' root system ideotype. This ideotype is hypothesised to optimise water and nitrogen uptake from soil (Lynch, 2013). Integrating these traits into elite crop cultivars could enhance carbon sequestration and nutrient-use efficiency under lower input conditions for adaptation to changing climates (Gao, 2021, Lynch, 2013).

Important sources of genetic diversity and beneficial traits include wild crop relatives, and landraces, which are crop varieties cultivated and adapted to the environmental conditions of a geographical area (Casañas et al., 2017). Modern cultivars and elite crop varieties have reduced genetic diversity and may have lost important traits found in more diverse varieties (Wingen et al., 2017). Landraces can be sources of beneficial traits that are not present in the current elite germplasm. For example, the yield-improving *Rht* dwarfing alleles introduced into wheat cultivars during the Green Revolution originated from 'Shiro Daruma', a Japanese wheat landrace (Cseh et al., 2021). An allele of the maize *Opaque-2* transcriptional activator gene present in a Peruvian landrace was found to improve protein quality through increasing lysine and tryptophan production (Dwivedi et al., 2016, Henry et al., 2005).

These traits can be introduced into current elite cultivars via introgression breeding programmes, although this is a long-term process which can take 5 to 6 generations (Palmgren et al., 2015). Marker-assisted selection can reduce the length of the breeding programme where DNA markers associated with target traits are selected (Palmgren et al., 2015). Identification of trait alleles can be performed with quantitative trait loci (QTL) analysis or genome-wide association studies (GWAS) to increase breeding efficiency (Yang et al., 2016). For example, a QTL on chromosome 6A of durum wheat (*Triticum durum*) was found to influence seminal root growth angle in response to water limitation (Alahmad et al., 2019).

Improving crop root system architecture is proposed to increase soil resource uptake and crop yields, as roots are crucial for the uptake of soil nutrients and water resources, particularly in water-limited and low nutrient environments (Lynch, 2013). Root system architecture or the spatial arrangement of plant roots in soil determines the efficiency of soil resource uptake as water and nutrients are not distributed uniformly within the soil (Orman-Ligeza et al., 2013). The development of root system architecture has a substantial genetic basis but environmental factors including water availability, light, temperature and gravity have roles in root system architecture formation (Rich and Watt, 2013). Understanding the mechanisms and processes which shape plant root system architecture is key for optimising plant root systems and improving crop yields under water- and nutrient-limited conditions.

Root phenotyping is a challenge within root system architecture research, particularly when plants are grown in a soil environment. Root phenotyping within a 2D controlled growth environment such as agar plates or pouch systems can allow whole seedling root system visualisation but may not be representative of root growth in soil. As an alternative, growing plants around the edge of soil-filled clear pots or soil-filled thin containers allows visualisation of root growth in soil but is still limited to young plants and a 2D growth environment (Richard et al., 2015). Root system phenotyping of plants grown in field conditions gives the best representation of root system architecture. However, current field phenotyping methodology can be destructive, time-intensive and impractical on a large scale. Invasive field methods include soil coring and 'shovelomics' where mature root crowns are excavated for root system phenotyping, data collection and analysis

(York et al., 2019). Growing plants in mesh baskets in the soil and then quantifying the angles that plant roots emerge from the mesh allows analysis of plant root growth angle (Oyanagi et al., 1993b, Uga et al., 2013). A non-invasive root phenotyping method involves using X-ray computed tomography (X-ray CT) scanning to image plant roots at a high resolution that were grown in soil columns or grown in the field and transferred into cylinders for scanning (Urfan et al., 2022). The multiple factors influencing root development mean that growing plant species in both controlled and field conditions is important for understanding the different phenotypes shown in different growth environments (Fiorani and Schurr, 2013).

Understanding the mechanisms underlying root gravitropic response pathways in cereals is essential for crop root system improvement. Gravity is a uniform and constant force with a large influence in shaping plant root systems through the root gravitropic response pathway (Rich and Watt, 2013). Plant roots are positively gravitropic and exhibit downwards growth in the direction of gravity. The site of root gravity sensing is in the root cap columella cells where starch-filled amyloplasts known as statoliths act in gravity perception and signalling (Su et al., 2020). Statoliths localise in the root apex in flowering plants and gymnosperm seed plants but root apex-localised statoliths are not present in basal plant lineages, indicating that this feature of the root gravitropic pathway evolved in seed plants (Zhang et al., 2019). There is spatial separation of gravity sensing and response sites within the root gravitropism pathway with gravity sensing occurring in the root cap and the gravitropic response in the root elongation zone (Su et al., 2020).

In the gravitropic response pathway, statolith sedimentation occurs in the direction of gravity and triggers a lateral gradient of unequally distributed auxin resulting in plant organ bending, which is known as the Cholodny-Went hypothesis (Went and Thimann, 1937). Auxin (indole-3-acetic acid, IAA) is the major hormone involved in gravitropism and many other developmental processes (Mockaitis and Estelle, 2008). Auxin transport occurs via non-directional transport in the phloem or through cell-to-cell polar auxin transport (Adamowski and Friml, 2015). Auxin is transported out of cells through PIN-FORMED (PIN) protein efflux transporters and PIN polarity determines the direction of auxin flow. The main PIN proteins found in the root tip are PIN2, PIN3,

PIN4 and PIN7 (Kleine-Vehn et al., 2010). Asymmetric flow of auxin from statocytes causes differences in cell elongation between the upper and lower sides which results in differential organ growth (Nakamura et al., 2019). The accumulation of auxin on the lower side of the root elongation zone inhibits lower side cell elongation and results in downwards root curvature (Band et al., 2012).

Roots which grow vertically downwards such as Arabidopsis primary roots can be described as having a gravitropic setpoint angle of 0°. Gravitropic setpoint angle (GSA) is "the angle with respect to gravity at which a plant organ is maintained at by gravitropism" (Digby and Firn, 1995). The GSA of a plant organ will change during plant development, for example, the GSA of Arabidopsis lateral roots became more vertical over time (Digby and Firn, 1995, Roychoudhry et al., 2013). Lateral roots and shoots are predominantly maintained at non-vertical GSAs due to the balance between the angle-dependent gravitropic response auxin flux and the counter-acting upward anti-gravitropic auxin flux (Roychoudhry et al., 2023). In cereals, wheat and rice seminal roots have been shown to maintain GSAs but the capacity of cereal lateral roots to maintain GSAs has not been investigated (Kaye, 2018).

The development of auxin reporters in Arabidopsis have allowed visualisation of auxin flow, signalling and distribution and insight into the gravitropic response pathway (Brunoud et al., 2012). Auxin reporters have now been generated in maize, rice and barley but not yet in wheat (Mir et al., 2017, Yang et al., 2017, Dao et al., 2023). In plants, the presence of auxin induces degradation of Aux/IAA transcriptional repressor proteins, which enables transcription of ARF-mediated auxin responsive genes (Maraschin et al., 2009). The Arabidopsis DII-VENUS auxin signalling reporter contains a degron motif from Aux/IAA28 Domain II (DII) fused to VENUS, a yellow fluorescent protein, which undergoes ubiquitination and degradation in the presence of auxin (Brunoud et al., 2012). The Arabidopsis DII-VENUS reporter has been used to demonstrate that auxin redistribution in roots occurs within minutes following a change in gravity stimulus (Band et al., 2012).

A large proportion of root gravitropism and root growth angle research has been performed in Arabidopsis, however, crop plants such as monocot cereal species differ in root types and root system development compared to the dicotyledonous

plants (dicots) such as Arabidopsis. Dicots have a primary taproot system from which lateral roots emerge, and adventitious roots may emerge later in plant development (Atkinson et al., 2014). Cereals including wheat (*Triticum aestivum*), rice (*Oryza sativa*) and maize (*Zea mays*) have fibrous root systems where embryonic roots first emerge from the seed followed by post-embryonic lateral, crown and adventitious roots which will form most of the monocot root system (Atkinson et al., 2014). Adventitious roots in dicots constitute a smaller proportion of the root system compared to cereal plants (Rich and Watt, 2013). In wheat, up to seven embryonic seminal roots will form, followed by post-embryonic lateral and crown roots which initiate from root endodermis or pericycle cells (Orman-Ligeza et al., 2013, Rich and Watt, 2013). These root system architecture differences between Arabidopsis and cereals means there are likely to be differences in the root gravitropic response pathway between these species. This chapter aimed to investigate root system architecture, root gravitropic setpoint angle maintenance, and auxin signalling in cereals to work towards the improvement of crop root system architecture.

The objectives of this chapter were to:

1. Explore wheat root system architecture variation in different growth environments and within wheat cultivars and landraces.
2. Establish if wheat and rice lateral roots have the capacity to maintain gravitropic setpoint angles.
3. Create a wheat DII-VENUS auxin signalling reporter and determine a wheat root confocal imaging protocol.

3.2 Results

3.2.1 Effects of growth medium on the root system architecture of three wheat varieties

There are many tools that can be used for root system architecture analysis, with the Quantitative Plant software database listing 42 different software tools for plant root system analysis (Lobet et al., 2013). RootNav and ImageJ have mainly been used for this project due to these software tools being relatively high throughput and able to measure a wide range of root traits (Pound et al., 2013). The three spring bread wheat cultivars 'Bobwhite', 'Cadenza' and 'Fielder' were grown vertically on germination pouches (Adeleke et al., 2020) for 5 days to investigate any root system architecture differences between wheat cultivars with this growth system. The chosen germination pouch growth system was used due to the high-throughput capability of this method, although it is recognised that this method is not guaranteed to reflect the eventual mature wheat root system architecture.These wheat varieties were chosen as they were either used for other experiments in this project, are commonly used in wheat research or for wheat gene editing and transformation (Sato et al., 2021, Fernández-Gómez et al., 2020, Pellegrineschi et al., 2002).

Six root system traits were analysed as these traits represent many important root system architecture characteristics; number of seminal roots, convex hull area, width/depth ratio, first pair seminal root emergence and tip angles, and mean length of the first three seminal roots to emerge (primary and first pair of seminal roots). Convex hull area was defined as the area encompassing all root material of a given plant. When grown in germination pouches, Bobwhite and Cadenza had similar root system traits in all six traits analysed (Fig. 3.1a) whereas Fielder had a larger root system, shallower root angles and an increased number of seminal roots (Fig. 3.1a - g). Seminal root number ranged between 3 – 6 for all three varieties matching previous studies of wheat embryonic root systems (Rich et al., 2020). Root system width/depth ratio is a ratio between the maximum width and maximum depth (Fig. 3.1b) and this trait was found to reflect the seminal emergence and tip angle results (Fig. 3.1f, g). Width/depth ratio is a standard measurement used in root system analysis and indicates the angle of

the root system, for example, a shallower root system will have a higher width/depth ratio (Iyer-Pascuzzi et al., 2010).

Although 2D high throughput methods are useful to screen large numbers of plants, the root architecture data may not always reflect the phenotypes of plants grown in other growth environments or in field conditions (Wasson et al., 2012). To explore the root system architecture of wheat plants in different growth conditions, the same three varieties were grown in agar plates (Fig. 3.2e - h) and compost-filled plates (Fig. 3.2i - l) for comparison with the germination pouch data (Fig. 3.2a - d). Fielder had a shallower root system than Bobwhite when grown on agar or in pouches, however, the root system of Cadenza became wider than Bobwhite when grown on agar. There were no significant differences between the plant root systems when grown for 4 weeks in compost-filled plates (Fig. 3.2i – l). Germination pouches, agar plates and soil growth methods are three of several different methods that can be used to image seedling root systems (Richard et al., 2015). Out of the three growth methods used, the germination pouch method was the best in terms of high throughput set up and efficiency, ease of imaging and analysis. Comparison of the seedling data obtained from these methods with mature plant field data would be required to identify the seedling phenotyping method that best reflects the root phenotype when grown in field conditions.
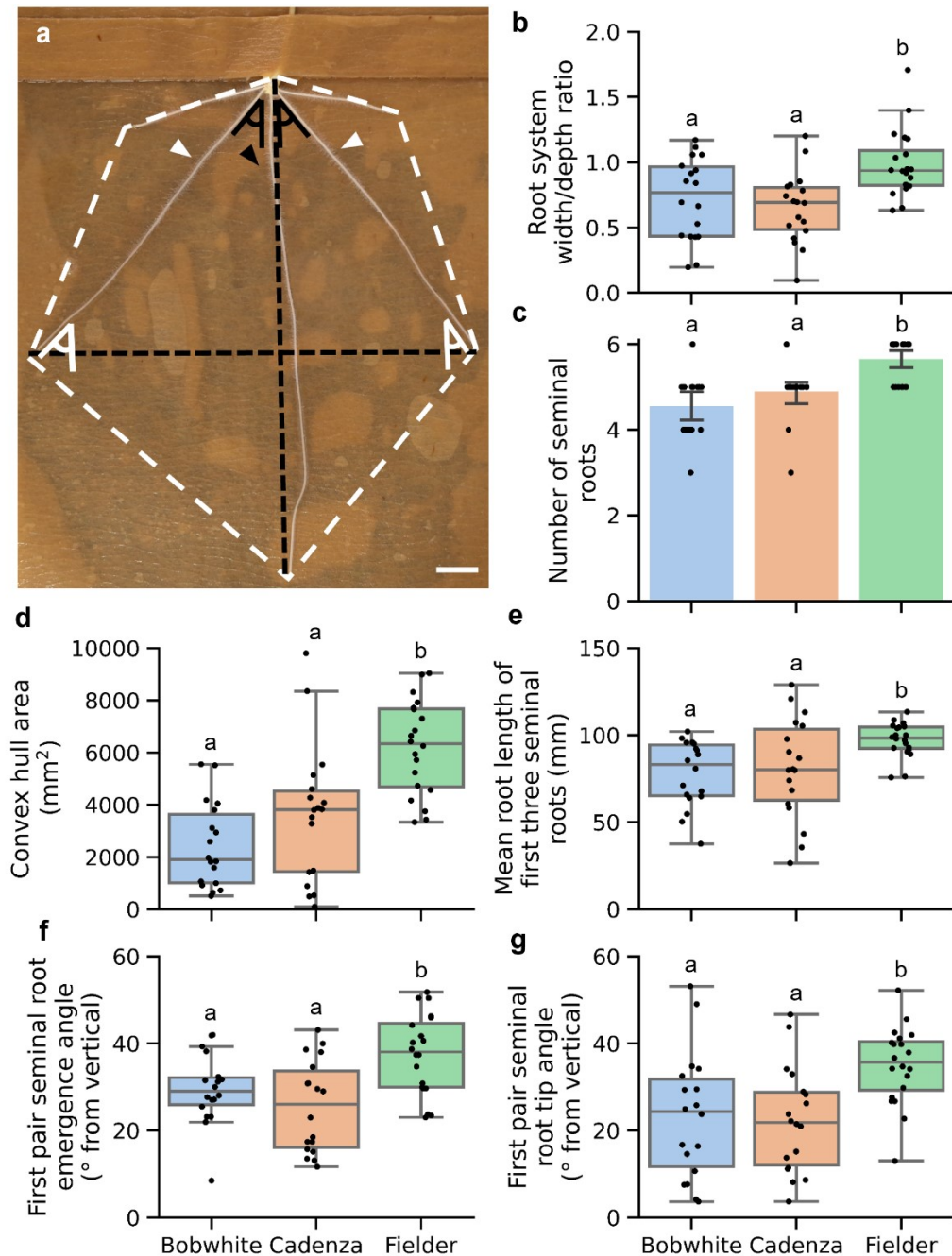
Figure 3.1: Differences in root system architecture between three wheat varieties.

Root system analysis of 5-day wheat varieties 'Bobwhite', 'Cadenza' and 'Fielder' performed with RootNav (a) 5-day old wheat seedling grown vertically on a germination pouch, scale bar = 10 mm. Black dashed line represents root system maximum width and maximum depth used to generate (b) width/depth ratio, $F = 7.531$, $p = 0.00132$. (c) number of seminal roots, $H = 24.193$, $p = 5.580 \times 10^{-6}$, (d) convex hull area (mm^2) indicated by white dashed line, $F = 16.831$, $p = 2.192 \times 10^{-6}$. (e) mean root length of first three (primary and first pair) seminal roots (black and white arrows respectively), $F = 5.003$, $p = 0.0102$. (f) first pair seminal emergence angles (degrees from vertical) shown by black angles, $F = 8.198$, $p = 7.90 \times 10^{-4}$ and (g) first pair seminal tip angles (degrees from vertical) shown by white angles, $F = 6.780$, $p = 0.00239$. Statistical analysis was performed with Shapiro-Wilk and one-way ANOVA and Tukey's post-hoc tests (b, d – g) or Kruskal-Wallis and Dunn's post-hoc tests (c). Letters show significant differences for each plot; $p < 0.05$, n = 18 – 20 plants per wheat variety.
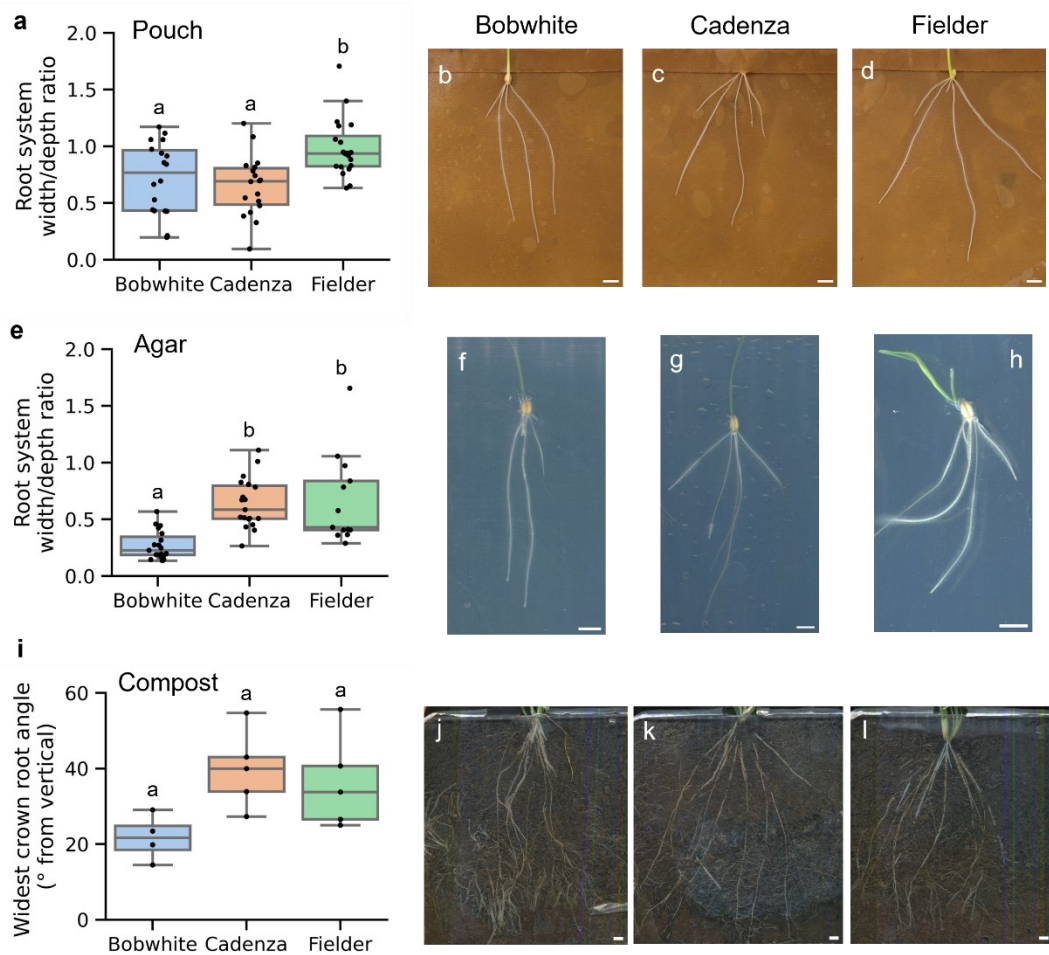
Figure 3.2: Effects of growth medium on wheat root system architecture.

Wheat cv. 'Bobwhite' (b, f, j), 'Cadenza' (c, g, k) and 'Fielder' (d, h, l). (a) Root system width/depth ratio of 5-day old pouch grown plants (b - d), F = 7.531, p = 0.00123, n = 18 – 20 plants per variety. (e) Root system width/depth ratio of 5-day old plants grown on Hoagland's agar (f - h), H = 24.424, p = 4.971 x 10^{-6}, n = 13 – 19 plants per variety. (i) Widest crown root angle analysis of 35-day wheat plants grown in compost-filled plates (j - l), F = 3.762, p = 0.0569, n = 4 – 5 plants per variety. Statistical analysis was performed with Shapiro-Wilk and one-way ANOVA and Tukey's post-hoc tests (a, i) or Mann-WhitneyU and Dunn's post-hoc tests (e), scale bars = 10 mm.
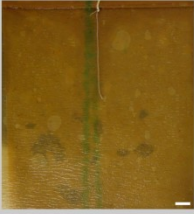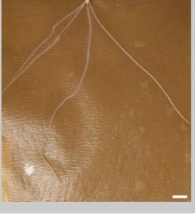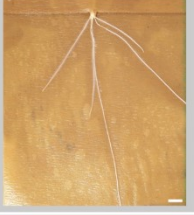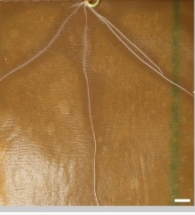
3.2.2 Root system architecture analysis of a wheat landrace panel

The YoGI wheat landrace panel represents a wide range of wheat lines from different environmental conditions and regions of origin, and the modern wheat cultivar Paragon was included for comparison (Barratt et al., 2023). The aim of this analysis was to explore the variation in root system architecture and create a root trait dataset for the YoGI landrace panel. The wheat lines from this panel were grown in germination pouches for root system imaging and analysis using RootNav software (Pound et al., 2013). The same six root system traits were analysed as the previous experiment (Fig. 3.1); number of seminal roots, convex hull area, width/depth ratio, first pair seminal root emergence and tip angles, and mean length of the first three seminal roots to emerge (Table 3.1). There was a wide phenotypic range in these traits within the landrace panel, as demonstrated by the minimum and maximum trait example images and data plots (Table 3.1, Fig. 3.4). The landrace panel had an approximately equal split between spring and winter varieties (Fig. 3.3a, c, e) and representation from six continents (Fig. 3.3b, d, f).

Correlation analysis of the landrace trait data showed that that some traits were highly correlated, for example, mean root length and convex hull area ($r_s = 0.85$) (Fig. 3.4). First pair seminal emergence and tip angles were not well correlated ($r_s = 0.16$), showing that root emergence angle was not a predictor of root tip angle in this experiment. The modern cultivar 'Paragon' was included for comparison within the panel of landraces (Fig. 3.4). Paragon is an elite bread wheat cultivar commonly grown in the UK (Wingen et al., 2017). Paragon had fewer and longer seminal roots and a larger root system than many of the landraces (Fig. 3.4), which could be an indicator of the elite cultivar root system phenotype.

Table 3.1: Wheat root system architecture traits.

Example trait images of 5-day old wheat landraces grown on germination pouches, scale bars = 10 mm.

Trait	Units	Description	Minimum trait example	Maximum trait example
Number of seminal roots		Total number of seminal roots		
Convex hull area	mm^2	Area encompassing all root material of a given plant		
Root system width/depth ratio		Root system maximum width divided by maximum depth		
Mean root length of first three seminal roots	mm	Mean root length of primary seminal root and first pair of seminal roots to emerge		
First pair seminal root emergence angle	(° from vertical)	Mean angle of first pair seminal root tips relative to vertical		
First pair seminal root tip angle	(° from vertical)	Mean emergence angle of first pair seminal roots relative to vertical		
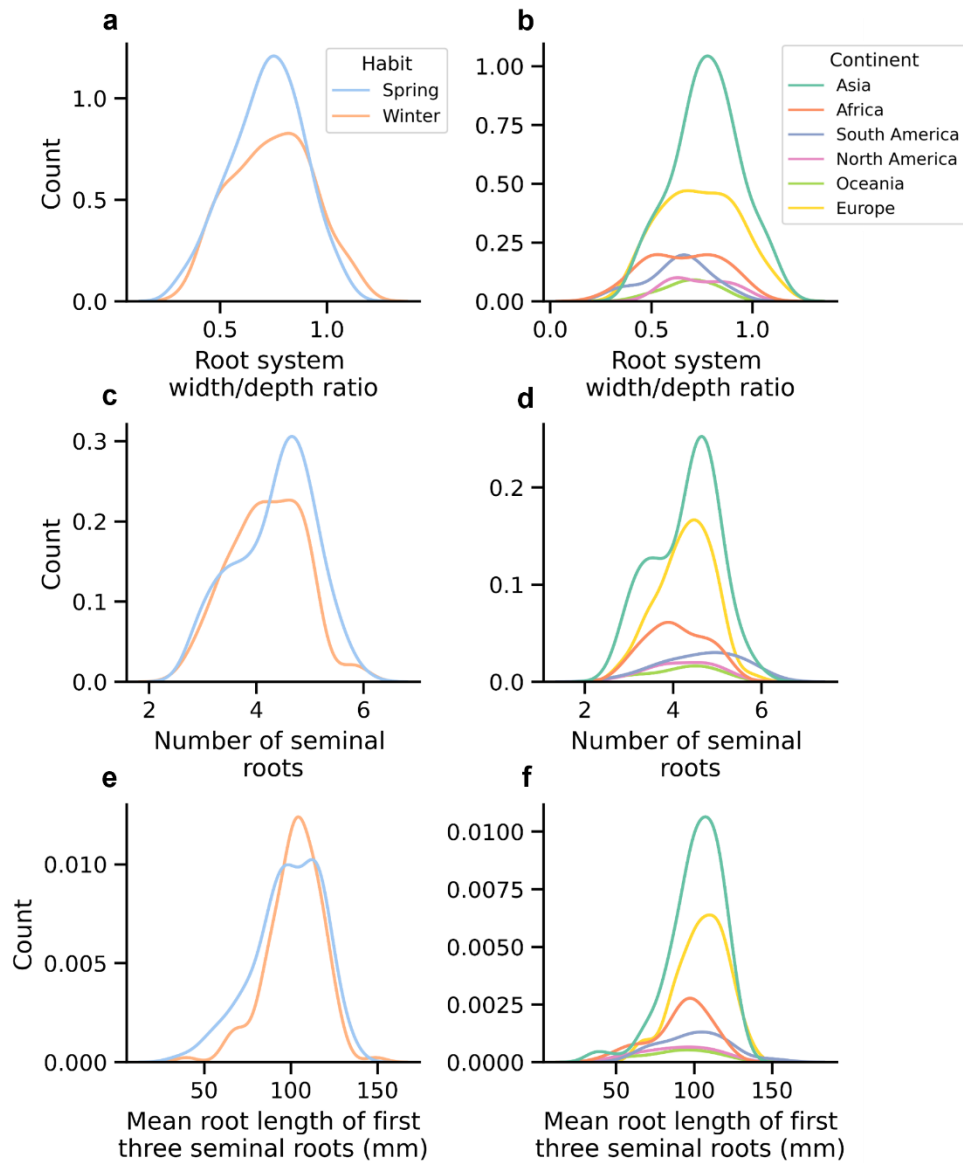
Figure 3.3: Continent of origin and growth habit distribution in wheat landrace root system traits.

Distribution plots of three landrace root system traits divided by growth habit (a, c, e) and continent of origin (b, d, f). (a, c, e) growth habit: 'Spring' n = 152, 'Winter' n = 119. (b, d, f) continent of origin: 'Asia' n = 121, 'Africa' n = 33, 'South America' n = 21, 'North America' n = 12, 'Oceania' n = 9, 'Europe' n = 75. Selected traits plotted for comparison (a, b) root system width/depth ratio, (c, d) number of seminal roots and (e, f) Mean root length of first three seminal roots (primary and first pair of seminal roots), n = 285 landraces, 3 – 10 plants per landrace.
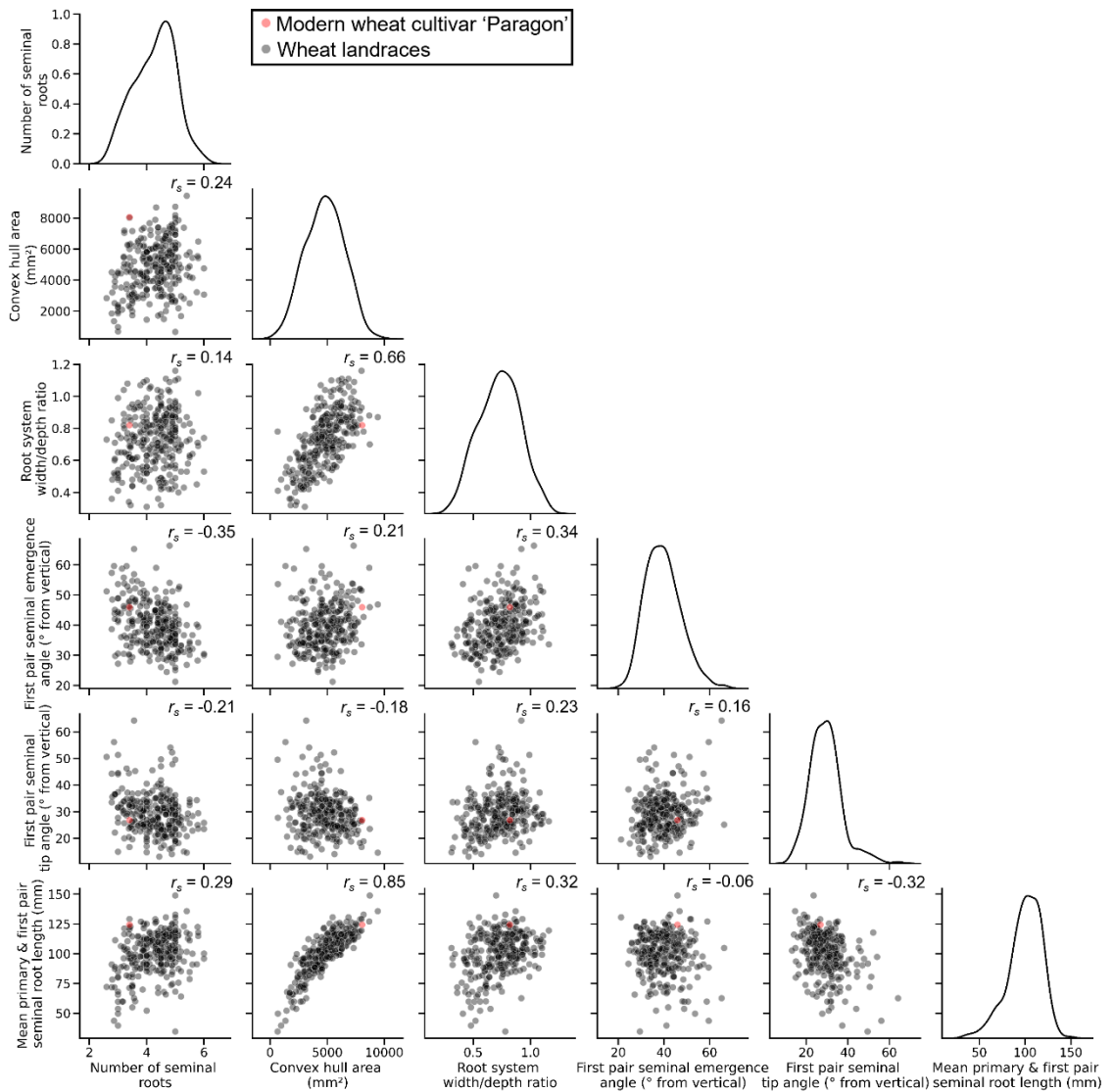
Figure 3.4: Root system architecture correlation analysis of a wheat landrace panel.

285 wheat landraces from the YoGI bread wheat landrace panel (Barratt et al., 2023) were grown in germination pouches and imaging and root system analysis performed at 5 days with RootNav and ImageJ (n = 3 – 10 plants per landrace). Grey circles represent landraces and pink circles represent modern wheat cultivar 'Paragon'. Trait distribution shown with kernel density estimate plots along the diagonal. Statistical analysis was performed with Spearman's rank correlation test and values are shown in upper right-hand side of each scatter plot (r_s).

Three steep rooting and three shallow rooting landraces were selected based on width/depth ratio, seminal emergence angle and tip angle data to understand the differences in root angle profiles between steep and shallow rooting landraces. The root growth angles of the first pair of seminal roots were analysed in degrees from vertical at 10 mm intervals along each root (Fig. 3.5). Paragon had an approximately median root angle so was plotted for comparison (grey lines, Fig.

3.5). The steep root angle landraces (Fig. 3.5a, c, e) had root emergence of approximately 40° and root angle become more vertical down to approximately 20° at the root tip. In comparison, the shallow rooting landraces had similar root angles at root emergence and at the root tip of 45 – 65° (Fig. 3.5b, d, f). The root system analysis of this landrace panel displays the diversity in root system architecture and in root growth angle in wheat, and the potential for using wheat landraces to incorporate advantageous root traits in breeding programmes.
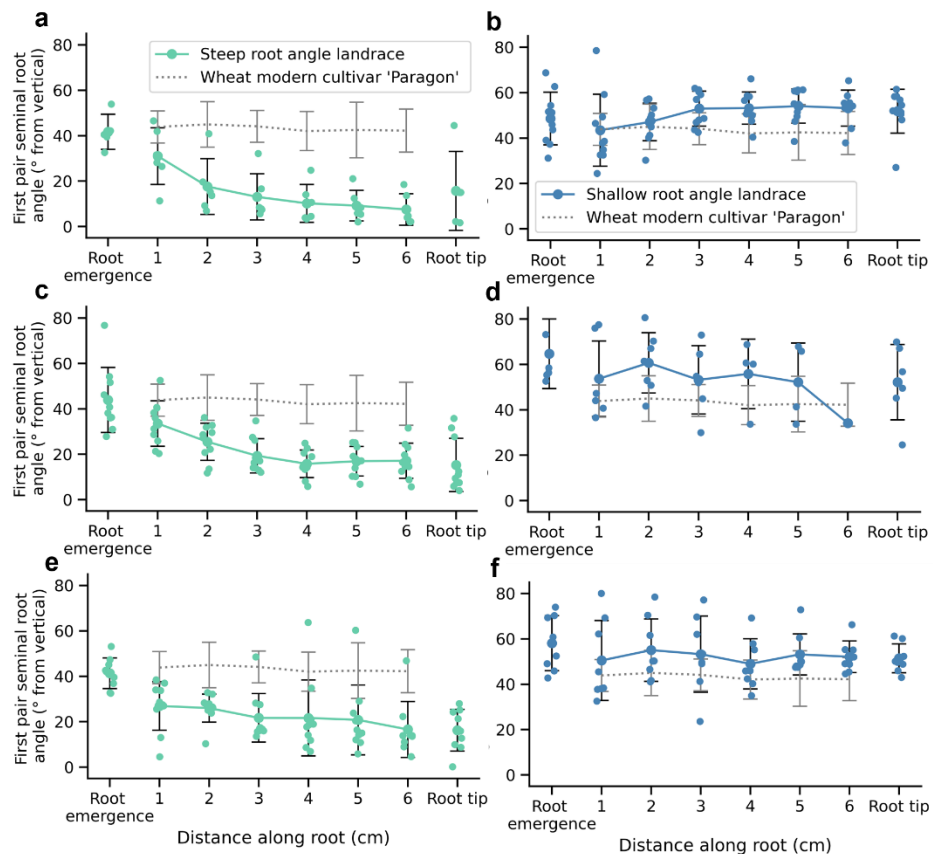
Figure 3.5: Root growth angle analysis of steep and shallow rooting wheat landraces.

(a, c, e) 3 steep landrace root systems (YoGI 141, 271 & 320) and (b, d, f) 3 shallow root systems (YoGI 065, 112 & 300) selected for further root angle analysis using ImageJ, n = 4 – 10 plants per landrace. Seminal root angle from vertical measured every 10 mm for 60 mm along each first pair of seminal roots. Mean data plotted with root emergence and root tip angle data measured with RootNav. Grey dashed lines show modern wheat cultivar 'Paragon' (YoGI 350) for comparison to steep rooting landraces (green) and shallow root angles (blue).

3.2.3 Wheat and rice root system development & lateral gravitropic setpoint angles

Wheat and rice are both monocotyledonous plant species with fibrous root systems, mainly composed of nodal and lateral roots in mature plants (Ouyang et al., 2020). There are anatomical differences in the roots between the species, with rice roots found to have larger xylem size and increased endodermis suberization and lignification (Ouyang et al., 2020). Both species initially form embryonic roots from the seed; wheat seminal roots (Fig. 3.6a - d) or rice seminal roots (Fig. 3.6g - j) with post-embryonic lateral and crown/nodal roots forming later in development (Fig. 3.6d, j).

Lateral roots form a considerable proportion of root system architecture and function in nutrient and water uptake from the soil (Ouyang et al., 2020). The lateral roots of Arabidopsis can maintain gravitropic setpoint angles, which are specific angles maintained with respect to gravity, due to a balance between gravitropism and an anti-gravitropic offset mechanism (Roychoudhry et al., 2013). Arabidopsis lateral root GSA becomes more vertical over time as the lateral roots emerge near horizontal and curve towards the vertical during root elongation (Mullen and Hangarter, 2003). Wheat and rice plants were grown on agar for 10 days and then imaged at 24-hour intervals to characterise lateral root growth angle over time and understand whether this phenomenon occurs in cereal species. Wheat and rice plants were grown for 10 days as lateral emergence occurs 6 – 10 days after germination in wheat (Wang et al., 2018a). Analysis of rice and wheat root systems showed that rice had more horizontal lateral roots and a larger range in lateral root angle than wheat (Fig. 3.7). Wheat lateral roots (Fig. 3.7a) became slightly more vertical over time compared to rice laterals (Fig. 3.7b) which maintained a more horizontal angle throughout the timeframe.

Wheat cv. Bobwhite

Rice cv. Nipponbare
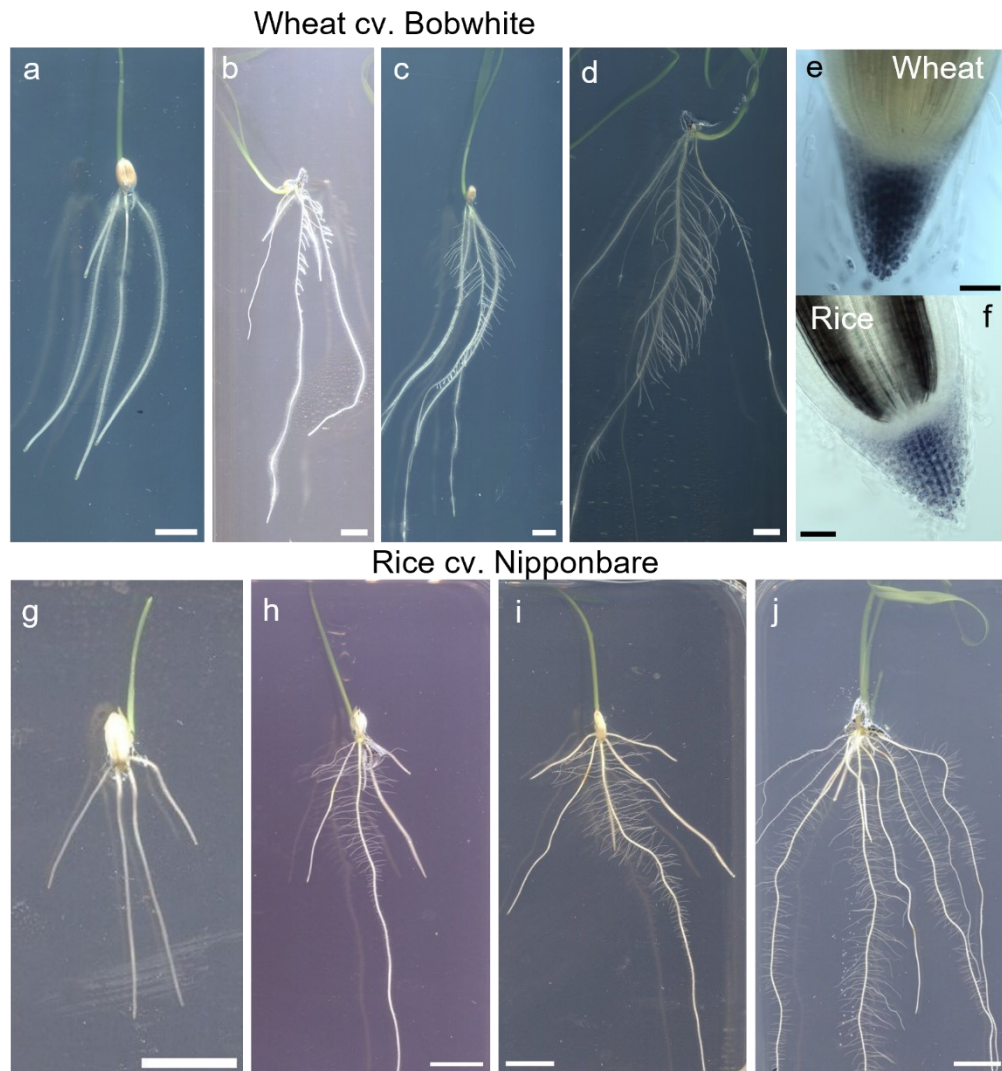
Figure 3.6: Wheat and rice root types and root system development.

(a – d) Wheat grown on Hoagland's agar growth medium; (a) 5 days (b) 7 days (c) 9 days (d) 11 days. (e) Wheat seminal root tip and (f) 8-day old rice seminal root tip after Lugol staining. (g – j) Rice grown on Yoshida's agar growth medium; (g) 2 days (h) 5 days (i) 6 days (j) 12 days. Scale bars (a – d, g – j) = 10 mm and scale bars (e, f) = 100 µm.

The reorientation of Arabidopsis lateral roots relative to gravity triggers a gravitropic response which returns the roots to their original GSA (Roychoudhry et al., 2013). Lateral root reorientation analysis of wheat and rice showed the lateral roots of both species were able to return towards their original root growth angles in upwards and downwards bending roots (Fig. 3.8). These results show that wheat and rice lateral roots are both capable of GSA maintenance. Wheat downwards bending lateral roots were able to reach their original growth angle after 24 hours (Fig. 3.8a – c), whereas wheat upwards bending roots and rice lateral roots only returned partially towards their original angles (Fig. 3.8).
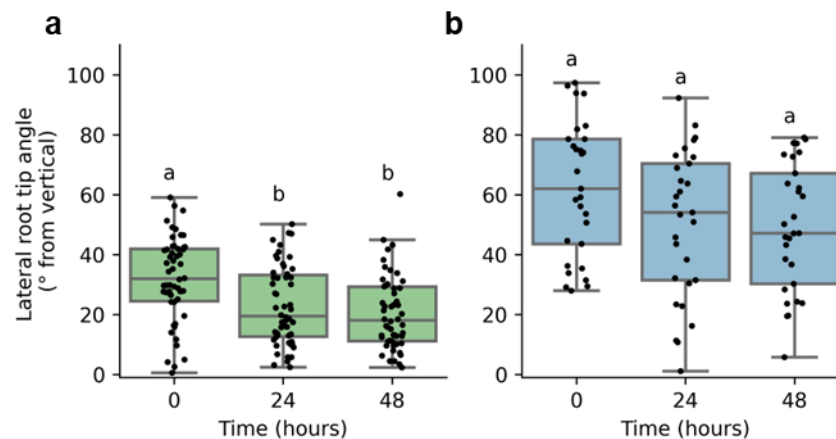
Figure 3.7: Change in wheat and rice lateral root growth angles over time.

Wheat and rice plants grown on agar plates for 10 days and (a) wheat lateral root tip angles and (b) rice lateral root tip angles measured over 48 hours. Statistical analysis performed within a one-way ANOVA and post-hoc Tukey's tests, (a) $F = 568$, $p = 2.814 \times 10^{-6}$ and (b) $F = 15.471$, $p = 3.219 \times 10^{-7}$, n = 29 – 54 roots.

Further reorientation experiments were performed over 48 hours with imaging every 12 hours, to understand whether the roots of both species would regain their original GSAs over a longer timeframe (Fig. 3.9). Wheat lateral roots had already returned to their original GSAs after only 12 hours from reorientation and then became progressively more vertical at successive timepoints in downwards bending roots or maintained an angle of approximately 20° in upward bending roots (Fig. 3.9a, b). In rice, downwards bending lateral roots did not return to their original GSAs and but maintained an angle more vertical than the reorientated angle at 0 hours post-reorientation (Fig. 3.9c). Upwards bending rice lateral roots regained their original GSA at 36 hours after reorientation (Fig. 3.9d). These findings suggest that both wheat and rice lateral roots show GSA maintenance but there are likely to be species-specific differences in achieving GSA maintenance, as wheat lateral roots displayed a more vertical root growth angle phenotype and a faster return to GSA was observed in comparison to rice lateral roots.
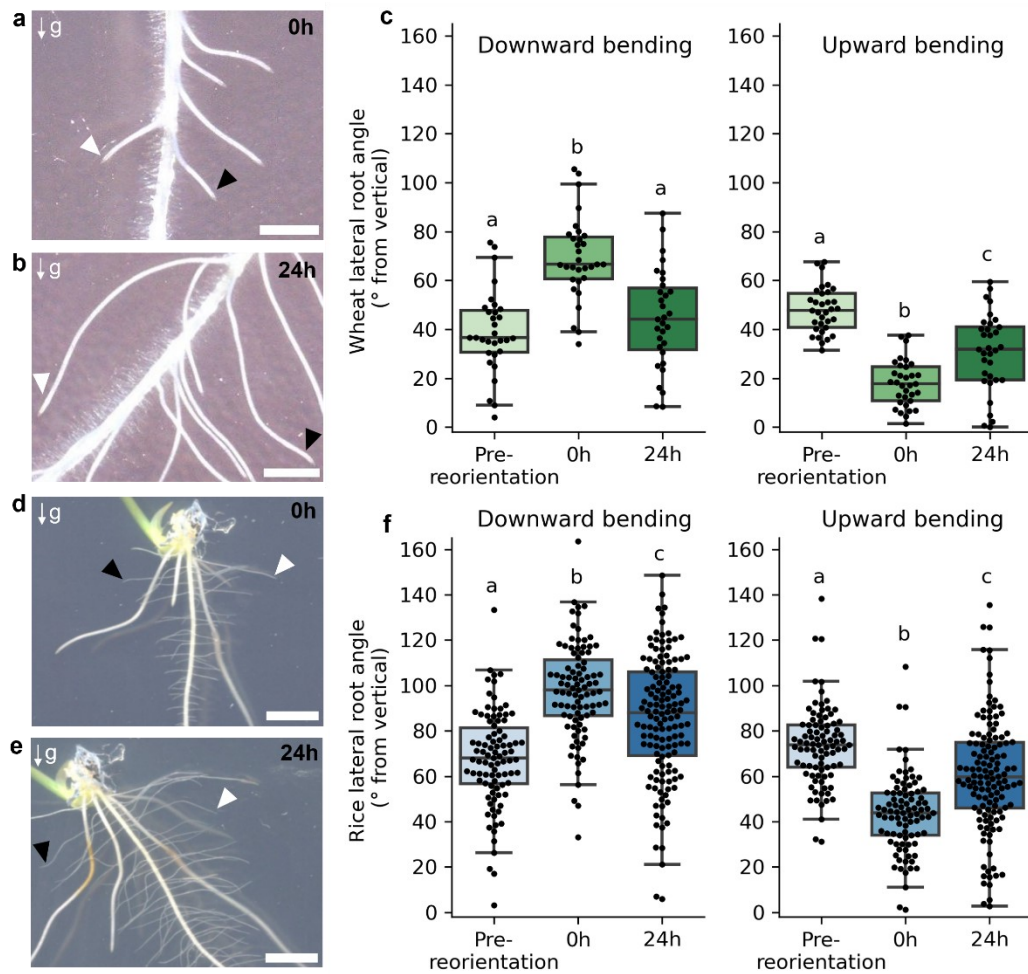
Figure 3.8: Wheat and rice lateral roots return towards their original growth angles after reorientation.

Wheat 'Bobwhite' (a – c) and rice 'Nipponbare' (d – f) plants grown on agar for 10 days and reorientated by 30° for 24 hours. Plants were imaged at 0 hours (a, d) and 24 hours (b, e) and root angle analysis performed with ImageJ (c, f), n = 31 – 136 roots from 3 replicates. Upward bending lateral roots are shown by black arrows and downward bending roots indicated with white arrows. 'g' = direction of gravity. Statistical analysis was performed with one-way ANOVA and Tukey's post-hoc tests, letters show significant differences for each plot, p < 0.05, scale bars = 3 mm.
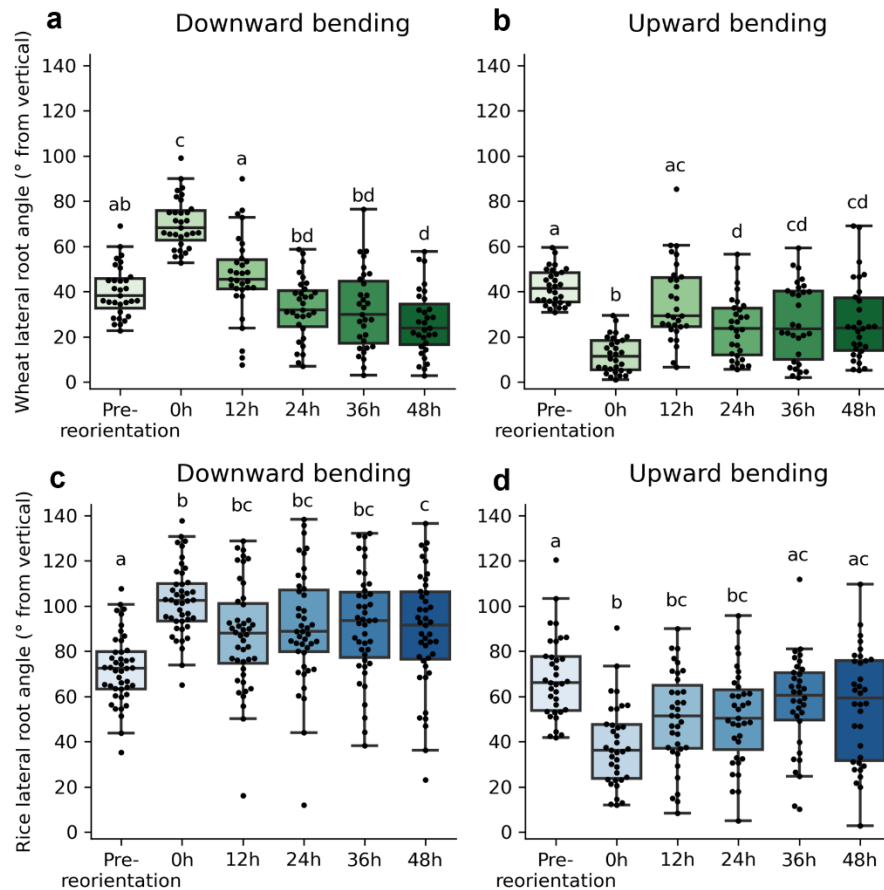
Figure 3.9: Wheat and rice lateral root growth angle responses to 30° reorientation over a 48-hour time course.

Wheat 'Bobwhite' (a, b) and rice 'Nipponbare' (c, d) plants grown on agar and reorientated by 30° for 48 hours with imaging every 12 hours. Lateral root angles were analysed with ImageJ for downwards bending (a, c) and upwards bending (b, d) roots, n = 30 – 44 roots from 3 replicates. Statistical analysis was performed with one-way ANOVA and Tukey's post-hoc tests, letters show significant differences for each plot, p < 0.05.

3.2.4 Visualising auxin fluxes in wheat with a DII-VENUS auxin signalling reporter

Auxin is the major hormone involved in many developmental processes including root gravitropism (Mockaitis and Estelle, 2008). Auxin reporters are important tools to monitor auxin response in plant species (Jedličková et al., 2022). DII-VENUS is a degron-based reporter developed in Arabidopsis which reports auxin input and shows auxin concentration and distribution (Jedličková et al., 2022). In the auxin signalling pathway, Aux/IAAs are ubiquitinated and degraded in the presence of auxin to allow auxin-inducible gene expression (Jedličková et al., 2022). The DII-VENUS reporter consists of Domain II of AUX/IAA28 (DII) fused to VENUS, a fast-maturing yellow fluorescent protein. AUX/IAA28 was originally chosen as this AUX/IAA protein has a relatively long half-life (Brunoud et al., 2012). The absence of DII-VENUS signal indicates that auxin is present as the presence of auxin causes DII-VENUS degradation. The mDII-VENUS control line has a mutation in the degron of domain II and so does not undergo auxin-sensitive degradation.

DII-VENUS reporters have been generated in rice (Yang et al., 2017) and maize (Mir et al., 2017), but a DII-VENUS reporter did not yet exist in wheat. The aim of this part of the project was to create a wheat DII-VENUS reporter to visualise auxin distribution in wheat roots, particularly during gravitropism. The DII-VENUS sequence from the published Arabidopsis reporter (Brunoud et al., 2012), was codon-optimised for wheat using an online codon optimisation tool. The sequences were synthesised into as entry vectors (Genewiz) for cloning downstream of the maize ubiquitin-1 promoter (*ZmUbi*). Species-specific codon optimisation can increase transgene expression in cereals (Feike et al., 2019) and the *ZmUbi* promoter is known to have good constitutive expression in wheat although some variability between lines has been reported (Rooke et al., 2000). The DII-VENUS and mDII-VENUS constructs (Fig. 3.10a) were introduced into pDONR207 using Gateway cloning. Restriction digests (Fig. 3.10b) and sequencing were performed to check correct assembly before wheat cv. 'Fielder' transformation and copy number evaluation was performed at NIAB (Cambridge). The single copy number DII-VENUS and mDII-VENUS lines were screened for fluorescence using confocal microscopy and the lines with strong VENUS signal were used for further experiments.
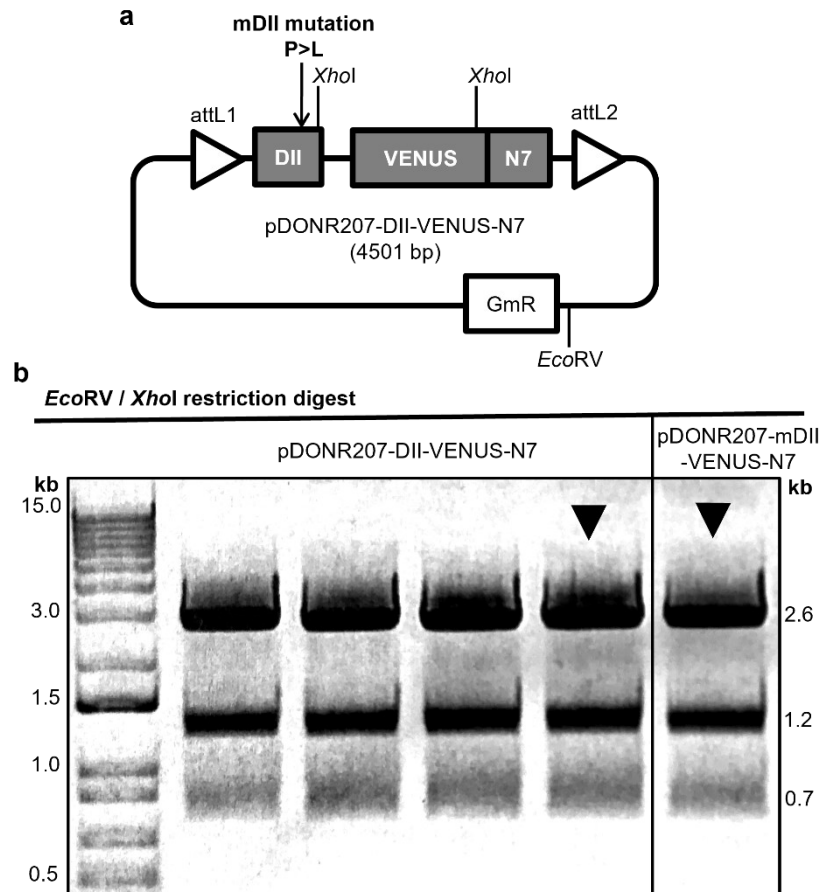
Figure 3.10: Schematic diagram of DII-VENUS plasmid DNA fragments from EcoRV and XhoI double restriction digest.

(a) pDONR207 backbone with DII-VENUS-N7 insert at attL1 and attL2 site. DIII: AtIAA28 degron, VENUS: yellow fluorescent protein, N7: a nuclear localisation sequence, GmR: Gentamycin resistance. P > L indicates DII degron mutation site in mDII-VENUS which prevents auxin-dependent degradation. Labelled restriction sites indicate enzymes used in double digestion (EcoRV, XhoI). (b) Agarose gel showing restriction digest fragments of pDONR207-DII-VENUS and pDONR207-mDII-VENUS plasmids from independent miniprepped colonies. The left-hand side shows 1kb+ ladder and right-hand side shows digest fragment sizes. Black arrows: plasmids selected for use in wheat transformation.

Transgene products or position effects of overexpression constructs transformed into wheat can have deleterious side effects and pleiotropic phenotypes such as dwarfing or chlorosis (Brunner et al., 2011). To check the DII-VENUS wheat phenotypes, transformed lines with strong DII-VENUS signal were grown to maturity for phenotyping. The DII-VENUS, mDII-VENUS and non-transformed control plants showed no differences in number of tillers or number of spikelets (Fig. 3.11a, c). The transformed DII-VENUS and mDII-VENUS lines had shorter tillers than the control but no difference between the two transformed lines (Fig. 3.11b).
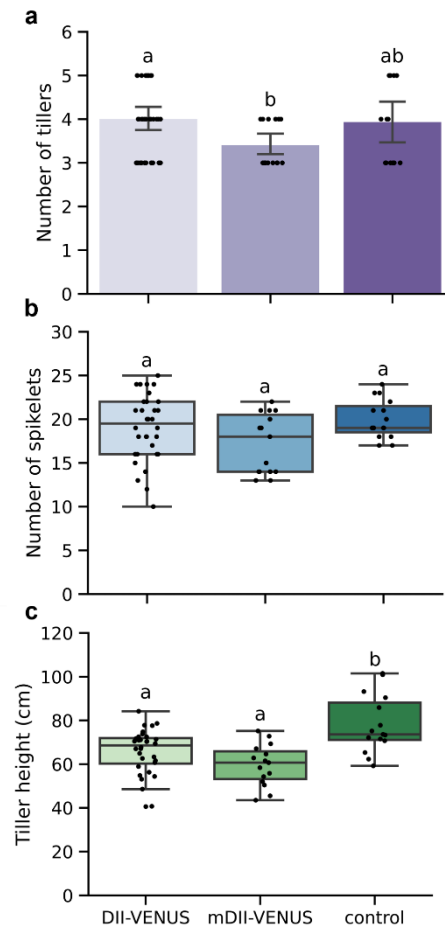
Figure 3.11: No differences in the shoot phenotypes of wheat DII-VENUS and mDII-VENUS lines.

The (a) number of tillers, (b) number of spikelets and (c) tiller height were measured from DII-VENUS, mDII-VENUS and Fielder (untransformed background) plants at 18 weeks (n = 15 – 32 plants). Error bars in (a) = 95% confidence interval. Statistical analysis was performed with one-way ANOVA and Tukey's post-hoc tests, letters show significant differences for each plot, p < 0.05.

Confocal imaging of live wheat roots is a difficult challenge compared to Arabidopsis due to the thickness of the roots even at the seedling stage. Plant species with thicker root systems are often fixed and sectioned for confocal fluorescence imaging of cell structures (Dyachok et al., 2016), but this does not allow for live cell imaging. Wildtype wheat cv. 'Fielder' seedlings were grown in chambered slides on agar to trial a method for live wheat root imaging. Once the first three seminal roots had emerged, the roots were stained with propidium iodide (PI) and imaged on a horizontal stage confocal at 3 days (Fig. 3.12a). This set up allowed vertical confocal imaging of the root tip, but signal was restricted

to the outer edge of the root when imaging at the centre of the root (Fig. 3.12b, c).
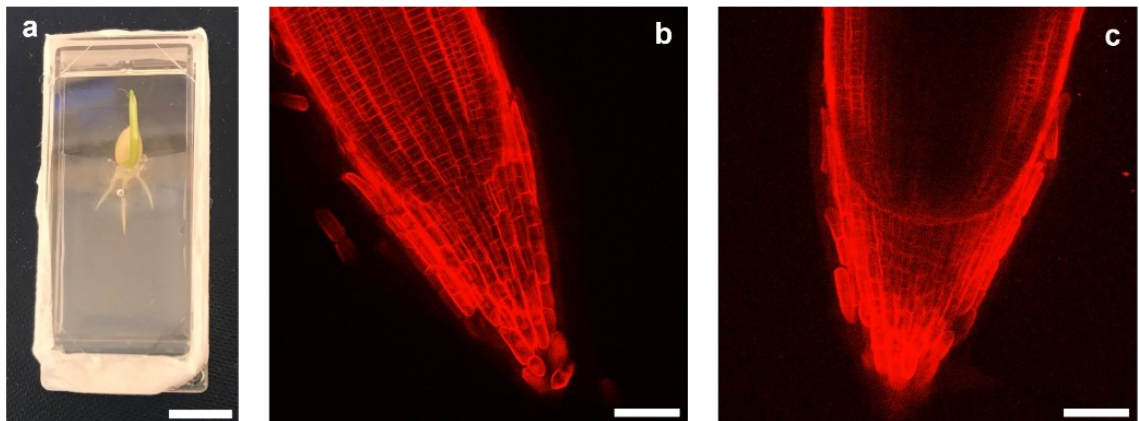
Figure 3.12: Developing a technique for wheat root confocal microscopy imaging.

(a) 3-day old wildtype 'Fielder' wheat seedling on ATS agar within a chambered slide (Lab-Tek 1.0). (b, c) Seminal roots imaged at 3 days following PI staining. Scale bars = (a) 10 mm, (b, c) 100 μm.

To confirm that VENUS fluorescence could be seen with this confocal set up trialled with wildtype wheat cv 'Fielder' (Fig. 3.12), DII-VENUS and mDII-VENUS plant primary seminal roots were imaged with PI staining to visualise the plant cell walls (Fig. 3.13). The confocal imaging was unable to reach the centre of the root due to root thickness, so imaging was restricted to the root epidermis to be able to observe DII-VENUS signal. Strong nuclear-localised signal could be seen in the mDII-VENUS lines throughout the root tip (Fig. 3.13d, while the DII-VENUS signal was predominantly found in the root cap columella cells (Fig. 3.13a, b) or the root epidermis (Fig. 3.13c). No signal was seen in the non-transformed control plant seminal roots (Fig. 3.13f – h).

Clearing and fixing root tissue was hypothesised to allow improved imaging into the centre of the root, so DII-VENUS, mDII-VENUS and non-transformed control plants were fixed and incubated for 3 days with ClearSee clearing solution. ClearSee reduces chlorophyll autofluorescence whilst maintaining stability of fluorescent proteins including VENUS (Kurihara et al., 2015). Confocal imaging of these samples showed similar fluorescence patterns as the imaging of live roots (Fig. 3.13). DII-VENUS signal was restricted to the root cap and root epidermis (Fig. 3.14a – c), whilst strong signal was seen throughout the mDII-VENUS roots (Fig. 3.14d – f). The control roots showed some possible

autofluorescence signal along the outer root edges, but no nuclear-localised signal was observed (Fig. 3.14g, h).
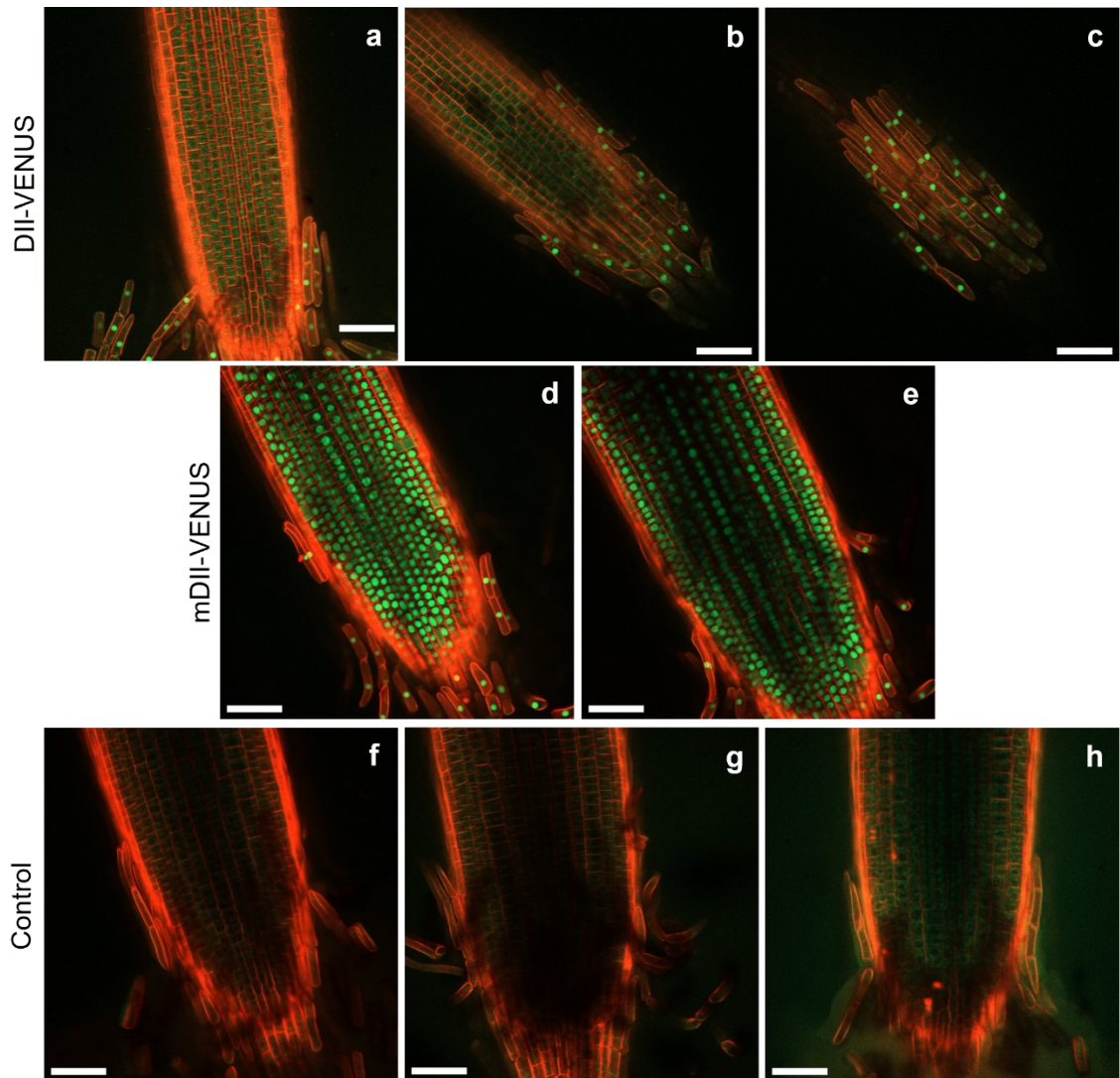
Figure 3.13: Visualising wheat DII-VENUS root tips with confocal imaging.

Vertical stage confocal (LSM800) imaging of 3-day old 'Fielder' wheat seedlings transformed with DII-VENUS (a – c) or mDII-VENUS (d – e) constructs, and non-transformed control plants (f - h). Plants were grown on ATS agar plates and transferred on agar into chamber slides for seminal root imaging following PI staining, scale bars = 100 μm.
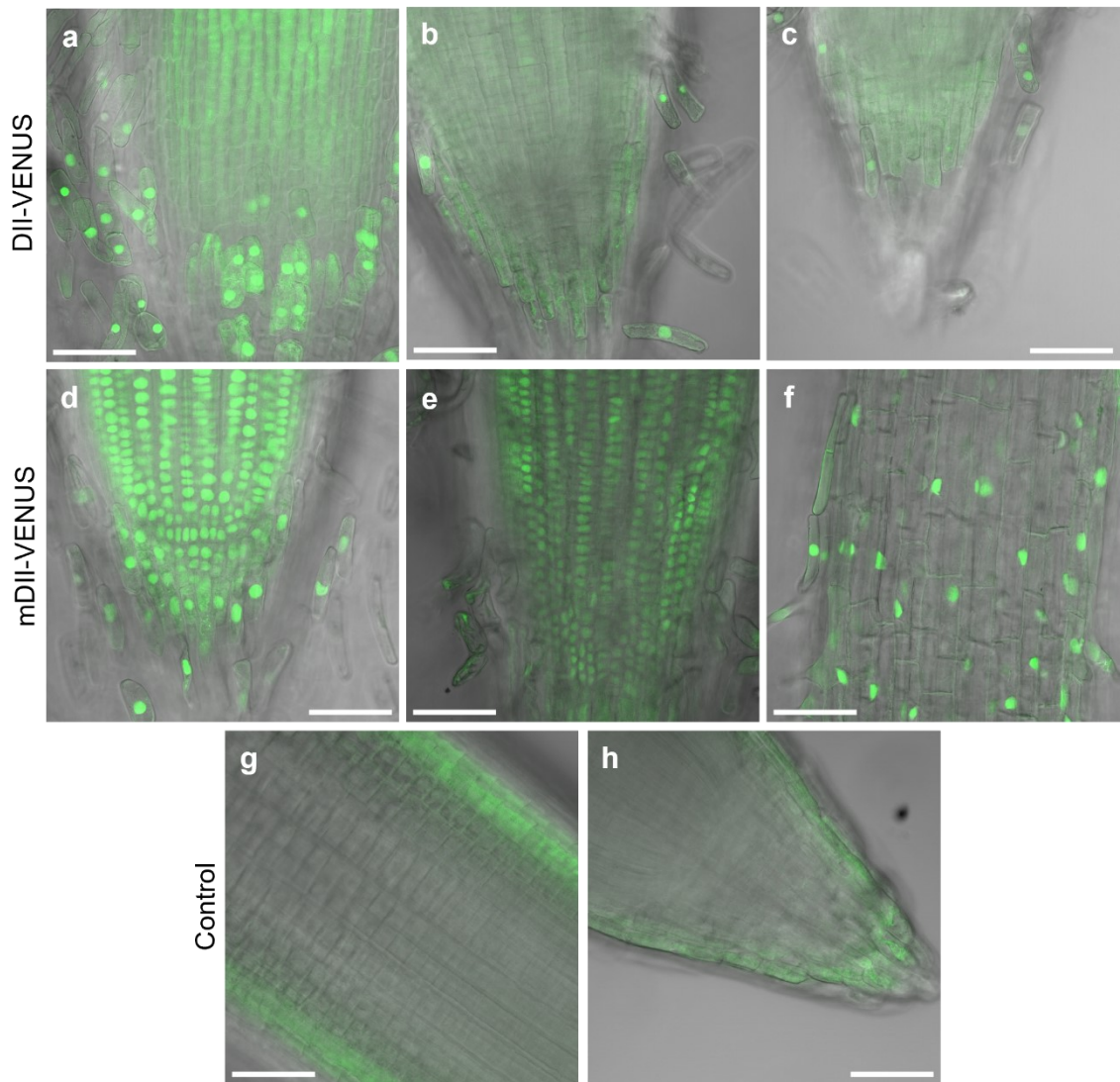
Figure 3.14: Wheat DII-VENUS and mDII-VENUS seminal roots fixed and incubated with ClearSee.

4-day old plants were fixed and incubated with ClearSee for 3 days. Seminal roots were imaged on slides with horizontal stage confocal (LSM880). (a – c) DII-VENUS (d – f) mDII-VENUS (g – h) control non-transformed wheat cv. Fielder roots, scale bars = 100 µm.

Lattice light-sheet microscopy allows high speed and low phototoxicity three-dimensional (3D) imaging at a very high resolution (Chen et al., 2014). Fixed and cleared DII-VENUS and mDII-VENUS seminal roots were imaged using a lattice light-sheet to generate a 3D reconstruction of the roots. This imaging method allowed deeper imaging of the seminal roots, but the same limited signal distribution was seen in DII-VENUS with nuclear signal on the root epidermis (Fig. 3.15a) but not further in the root (Fig. 3.15b). There is potential cell wall fluorescence within the DII-VENUS root, which was not present in mDII-VENUS (Fig. 3.15c) or the control roots (Fig. 3.15d).
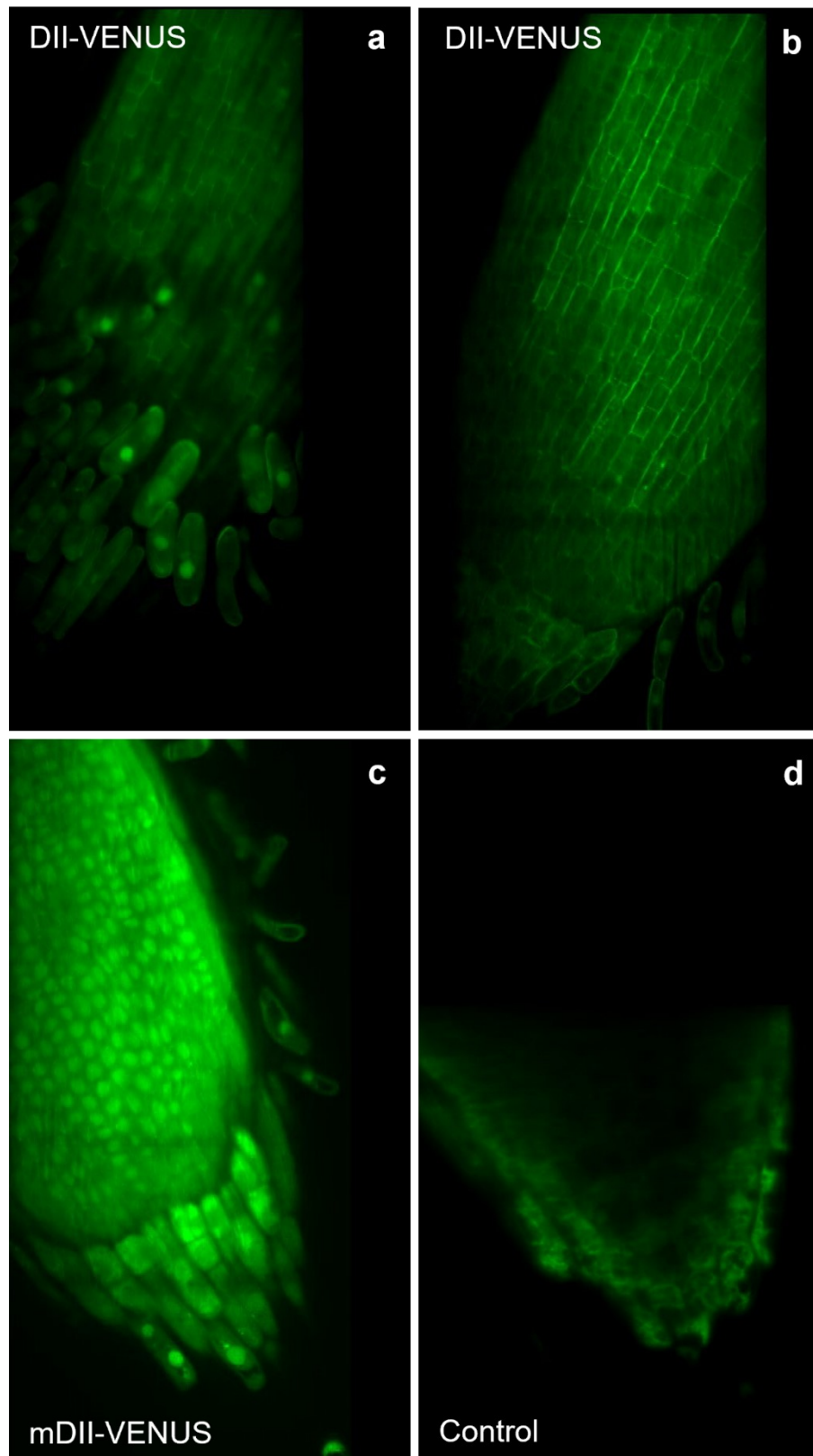
Figure 3.15: Lattice light-sheet imaging of wheat DII-VENUS and mDII-VENUS seminal roots.

4-day old seminal roots expressing (a, b) DII-VENUS, (c) mDII-VENUS or (d) non-transformed control roots fixed and incubated in ClearSee for 4 days before 60x imaging (Zeiss lattice lightsheet 7).

These imaging experiments trialled a wide range of techniques to image transformed fluorescent wheat root tissue. The lack of improvement in imaging nuclear signal in DII-VENUS roots with fixing and clearing or the lattice light-sheet microscopy indicates that DII-VENUS signal may be restricted to the root cap and root epidermal cells. Therefore, DII-VENUS roots were treated with IAA and the nuclear fluorescence analysed to test the sensitivity to auxin in the root cap, due to the lack of signal elsewhere within the root.

Nuclear-localised signal was present in non-treated DII-VENUS roots, but no signal was found in DII-VENUS roots treated with 1 µm IAA (Fig. 3.16a, b). mDII-VENUS roots showed consistent strong signal with or without presence of IAA treatment (Fig. 3.16c, d). Analysis of nuclei fluorescence within the root cap cells showed a clear reduction in fluorescence of IAA-treated DII-VENUS seminal roots (Fig. 3.16e). These results suggest that the wheat DII-VENUS reporter line responds to auxin application by degradation of VENUS-tagged DII protein and that the reporter can be used to visualise auxin distribution. The constant mDII-VENUS signal shows the reliability of this line as a control for the DII-VENUS reporter.
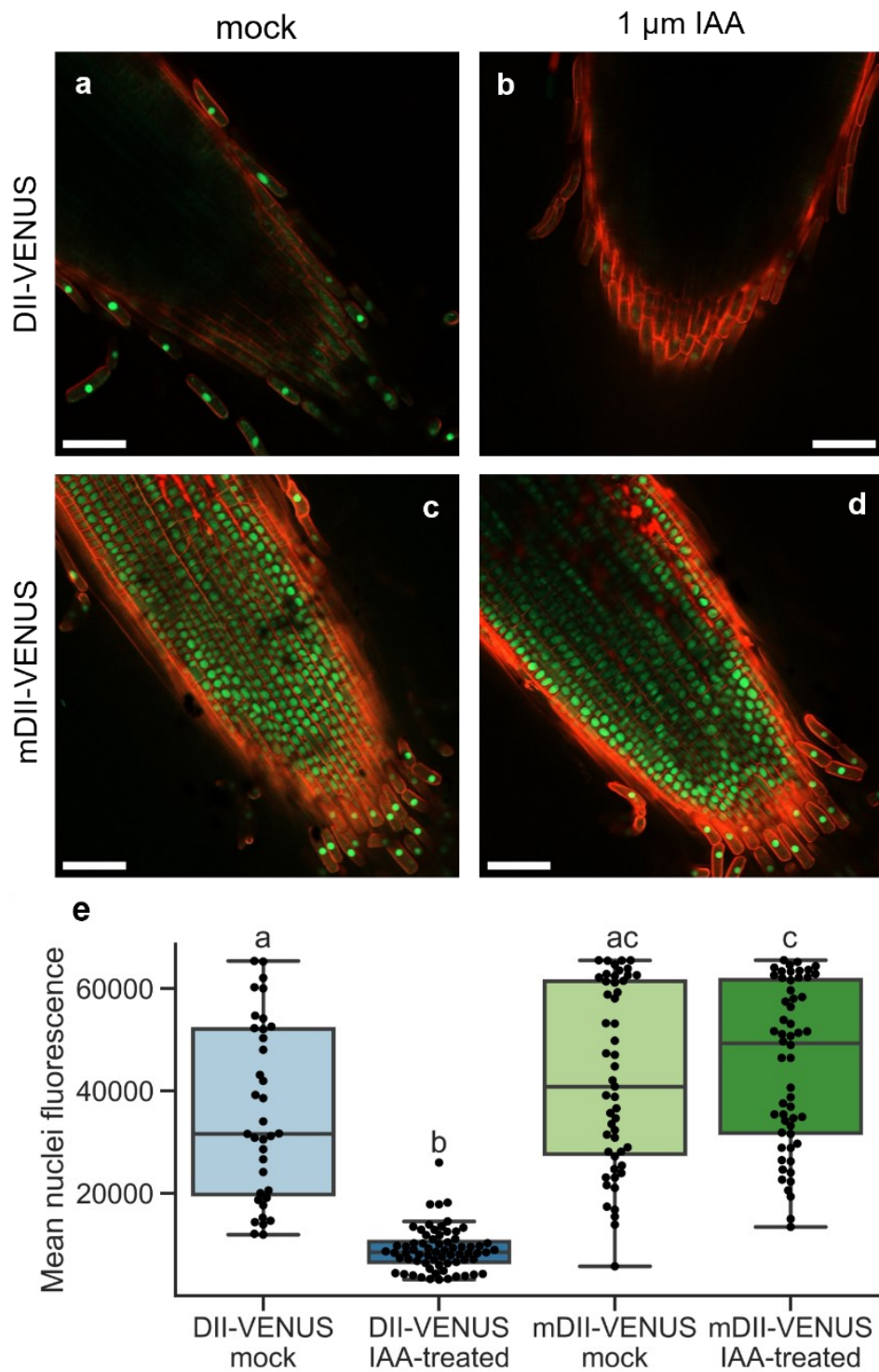
Figure 3.16: IAA treatment removes nuclear DII-VENUS fluorescence.

Nuclear fluorescence of wheat root cap cells (n = 36 – 68) measured for 3 – 4 wheat primary seminal roots per treatment and genotype. DII-VENUS (a, b) and mDII-VENUS (c, d) roots treated with DMSO (mock; a, c) or 1 µm IAA (b, d), scale bars = 100 µm. (e) nuclei fluorescence analysis of mock and 1 µm IAA treated DII-VENUS and mDII-VENUS roots using ImageJ. Statistical analysis was performed with one-way ANOVA and Tukey's post-hoc tests, letters show significant differences, $p < 0.05$.

3.3 Discussion

3.3.1 Variation within wheat root system architecture

There are many factors that influence root development and shape root system architecture. Roots are the interface between the plant and the soil environment and play a major role in nutrient uptake and plant yield. The interactions between environmental and genetic factors result in unique architecture and variation within the same plant species (de Dorlodot et al., 2007). Three UK hexaploid spring wheat varieties; Bobwhite, Cadenza and Fielder were grown to investigate variation in root system architecture between these varieties, which are widely used in research and crop transformation (Sato et al., 2021, Fernández-Gómez et al., 2020, Pellegrineschi et al., 2002). Root system analysis showed the root system of wheat cv. 'Fielder' was shallower and covered a larger surface area compared to the other two varieties (Fig. 3.1).

Growing the same wheat variety using three growth methods; hydroponic germination pouches, agar plates and compost-filled clear plates, showed differences in root system architecture (Fig. 3.2). This experiment focused on root system width/depth ratio as maximum width and depth are the simplest measurements to summarise the root system, and so a valuable trait to describe root system structure (Lobet et al., 2017). A previous study found genotype-specific modulation of root architecture when grown in different mediums and hypothesised that the homogenously available nutrients in the hydroponic culture could cause root architecture differences between this growth method and soil systems (Sinha et al., 2018). The germination pouch and agar plate growth methods would both have had homogenously distributed nutrients but there were differences seen in root architecture between these growth methods. Bobwhite maintained a similar root system width/depth ratio when grown on pouches or on agar plates, whereas Cadenza had a relatively shallower root system when grown on plates. These root trait differences between the varieties means that other environmental or genetic factors may have influenced the root phenotypes as well as the growth method used.

Germination pouches were found to be the best growth method for further large-scale root phenotyping experiments as they required less space and were quick to set up. The scarcity of high-throughput root phenotyping methods is a barrier

for root architecture research and root system improvement in crop breeding (Ober et al., 2021). Plant root traits grown under controlled conditions do not always translate to field conditions, and seedling root phenotypes are not always seen in mature plants (Ober et al., 2021). However, it is often not possible to phenotype large numbers of plants in 3D soil environment due to the resources and facilities required (de Dorlodot et al., 2007). Root system architecture traits are not often focussed on within modern crop breeding programmes due to root phenotyping challenges (Mathew and Shimelis, 2022). Root system architecture is a key plant trait so understanding cereal seedling root architecture under controlled conditions is still a valuable aim whilst working towards improving crop yields.

The YoGI wheat landrace panel represents wheat diversity from across the world (Barratt et al., 2023). The 281 landraces screened here show a wide variation in root traits including seminal root number, root system convex hull area and seminal root growth angle (Fig. 3.4). Landraces with steepest or shallowest seminal emergence and tip angles were identified for further seminal root angle analysis, which showed clear differences in growth angle along the root profiles between the steep and shallow rooting landraces (Fig. 3.5). Root growth angle determines overall root system architecture phenotype, and a steeper root system is proposed to optimize water and nitrogen uptake from deeper soil layers (Lynch, 2013). Alternatively, shallow root systems have been shown to increase shoot biomass in common bean (*Phaseolus vulgaris*) in a phosphorus-limited environment (Miguel et al., 2015). The natural variation found in landraces is an important source of beneficial traits which could be introduced into elite cultivars via introgression line development (Ober et al., 2021).

3.3.2 Gravitropic setpoint angle maintenance between wheat and rice lateral roots

Arabidopsis non-vertical roots and shoots are maintained at gravitropic setpoint angles (GSAs) due to an interaction between the gravitropic response and angle-independent antigravitropic offset (Roychoudhry et al., 2023). This chapter found that wheat and rice lateral roots both showed GSA maintenance (Fig. 3.8), which fits with previous findings that non-vertical wheat seminal roots and rice crown roots can maintain GSAs (Kaye, 2018). Wheat lateral roots showed a faster return

to their original growth angle (12 hours or less) compared to 36 hours in rice and rice lateral roots had a more horizontal growth angle than wheat (Fig. 3.9). These differing lateral root phenotypes could be due to differences in their growth habit leading to change in root gravitropic responses. Nipponbare is a Japanese lowland rice cultivar (Fukuoka and Okuno, 2001), usually grown in waterlogged soils whereas wheat is usually grown in drier conditions. Lowland rice varieties have been documented as having shallow root systems with high numbers of thin roots (Courtois et al., 2013), so further insight into rice root gravitropic responses could be gained from comparing these Nipponbare lateral root GSA findings with upland rice cultivars.

3.3.3 Challenges and opportunities of developing a wheat DII-VENUS reporter

The final section of this chapter reports on the creation of a wheat DII-VENUS auxin reporter line (Fig. 3.16), which have previously been developed in Arabidopsis (Brunoud et al., 2012), maize (Mir et al., 2017) and rice (Yang et al., 2017). Auxin regulates many aspects of wheat development and there are 23 Auxin Response Factors (*TaARF*s) present in wheat (Qiao et al., 2018). One study found that overexpressing an auxin biosynthetic gene (*TaTAR2.1-3A*) in wheat increased plant height and grain yield, so having a wheat auxin reporter would be greatly beneficial to understand auxin concentration and distribution in wheat. Crossing wheat DII-VENUS with gravitropic or other auxin-related mutants would allow insight into auxin localisation during gravitropism and further understanding of the cellular processes occurring within the plant. Despite the successful creation of this wheat auxin reporter, the challenges of live imaging thicker tissues need to be addressed to be able to take full advantage of this tool. The lack of DII-VENUS signal within the root tip (outside of the root cap and epidermis) could be due to an inability to image far enough into the root or the presence of auxin degrading any signal within this area. Non-constitutive DII-VENUS expression is a possibility, however, the strong constitutive expression across the mDII-VENUS roots suggests that this is not likely to be the case. Two-photon excitation microscopy (multiphoton microscopy) allows deeper and high-resolution imaging of living tissues compared to confocal microscopy (Mizuta,

2021), which may be required for in depth imaging of this wheat auxin reporter line.

If the native auxin levels within wheat DII-VENUS seminal roots cause DII-VENUS degradation, then an alternative transcriptional auxin reporter such as DR5 may be needed to visualise auxin distribution. DR5 consists of Auxin Response Elements (AuxREs) fused to a reporter such as a fluorescent protein or luciferase to show the sites of transcriptional auxin response (Ulmasov et al., 1997). DII-VENUS only allows semi-quantitative analysis of auxin levels whereas R2D2 combines DII-VENUS and mDII-VENUS within the same plant and allows ratiometric analysis of DII-VENUS and mDII-ntdTomato fluorescence (Liao et al., 2015). An advantage of DII-VENUS and R2D2 reporters is that they can show auxin accumulation that does not lead to gene activation via AuxREs (Liao et al., 2015).

Future wheat auxin research may need to use different reporters; however, wheat DII-VENUS will still be a valuable tool and starting point for further development. For example, crossing wheat DII-VENUS with wheat root growth angle mutants would allow understanding of wheat auxin localisation and whether the root growth angle mutant phenotypes were caused by changes in auxin distribution. In Arabidopsis, DII-VENUS was introduced into an *Atdro1* (*Atlazy4*) mutant to discover that the loss-of-function *dro1* mutation caused an impairment of DII-VENUS gradient establishment (Waite et al., 2020).

This chapter gave insight into the variation that exists with the root system architecture of bread wheat varieties and a landrace panel, and different trait measurements for phenotyping root systems. The reorientation experiments showed the capability and distinctions between wheat and rice lateral root gravitropic setpoint angles and response to reorientation with respect to gravity. Finally, the creation and imaging of a novel wheat DII-VENUS auxin signalling reporter was demonstrated, which will be an important tool for wheat gravitropism research and many other developmental processes. Gaining understanding of the molecular basis underlying cereal root system architecture and root gravitropism will be important to further our knowledge for optimising root systems to improve crop yields.

Chapter 4

Characterising the genetic diversity of the wheat *LAZY* gene family

Chapter 4: Characterising the genetic diversity of the wheat *LAZY* gene family

4.1 Introduction

Understanding the molecular basis of root system architecture is crucial for optimising crop plant growth and improving yields in a changing climate. One gene family involved in shaping root and shoot architecture is the *LAZY* gene family which play important roles in growth angle control and gravitropism (Waite and Dardick, 2021). The first *LAZY* gene to be identified was *LAZY1* (*LA1*) in rice, which has functions in shoot gravitropism and rice tiller angle regulation (Table 4.2) (Li et al., 2007). Other *LAZY* genes including *LAZY2* and *LAZY4* are predominantly associated with root angle control (Yoshihara and Spalding, 2017). The *LAZY* genes are part of the wider IGT family which also includes the *TAC1* (*TILLER ANGLE CONTROL 1*) genes. *TAC1* controls shoot growth angle in plant species including Arabidopsis, rice and peach (*Prunus persica*) (Yu et al., 2007, Dardick et al., 2013).

LAZY genes could be valuable for future crop improvement as overexpression of rice *DRO1* (*DEEPER ROOTING* 1) has been shown to increase root system verticality and improve drought avoidance and grain yield in water-limited conditions (Uga et al., 2013). Rice *DRO1* is a member of the *LAZY* family (Table 4.2), and *OsDRO1* exhibits high expression in rice root tips and plays a crucial role in root growth angle regulation. A rice variety with a truncated version of *DRO1* gives shallow rooting, whereas *DRO1* overexpression leads to increased root verticality (Uga et al., 2013). *LAZY* family genes are good candidates for use in crop breeding as they are highly conserved and have been identified and characterised in a wide range of plant species including rice, Arabidopsis, maize, soybean (*Glycine max*), *Lotus japonicus* and *Medicago truncatula* (Yoshihara et al., 2013, Ge and Chen, 2016).

Despite the global importance of wheat as one of the three main cereal crops contributing almost 50% of calories in the human diet (Milani et al., 2022),, there have been relatively limited studies on the wheat *LAZY* family. A *LAZY1* ortholog in wheat was first identified through sequence alignment with rice *LAZY1*, along with orthologs in sorghum (*Sorghum bicolor*) and maize (Li et al., 2007). More

recently, further wheat genes within the *LAZY* family have been identified. Wheat *DRO1-like* (*TaDRO1*) homoeologs were discovered and found to interact with TOPLESS proteins, a repressor of auxin-regulated gene via a C-terminus EAR motif (Ashraf et al., 2019).

A rice *DRO1* homolog associated with root growth angle was identified and named *qSOR1* (*quantitative trait locus for SOIL SURFACE ROOTING 1*) (Table 4.2) (Kitomi et al., 2020). Rice *qSOR1* is expressed in root columella cells and rice plants with a loss-of-function *qsor1* allele have shallower root angles and soil surface roots. This *qSOR1* gene has orthologs in wheat; *TaqSOR1-A*, *TaqSOR1-B* and *TaqSOR1-D* (Kitomi et al., 2020). Sequence alignment of wheat *DRO1* and *qSOR1* homoeologs shows these genes are similar to Arabidopsis *LAZY2* and *LAZY4* (Appendix 2) (Kitomi et al., 2020). The entire wheat IGT family including *TaTAC1* as well as the wheat LAZY genes; *TaLAZY1*, *TaDRO1* and *TaqSOR1* (*TaDRO2*) homoeologs were identified and characterised for the first time (Rasool et al., 2023). Despite the presence of twelve *LAZY* and *TAC1* homoeologs in wheat, the study of wheat *LAZY* molecular interactions has been limited to only the *TaDRO1* homoeologs (Ashraf et al., 2019). In this chapter, wheat IGT nomenclature from Kitomi et al. (2020) and Rasool et al. (2023) will be used (Table 4.1).

Table 4.1: Wheat *LAZY* gene family nomenclature.

The wheat *LAZY* gene nomenclature used in this thesis will be from Rasool et al. (2023), except for the *TaqSOR1* homoeologs which were first named in Kitomi et al. (2020).

Gene name	Other name(s)	Gene ID
TaLAZY1-Un (*A*) (Rasool et al., 2023)	*TaLA1* (Li et al., 2007)	*TraesCSU02G083100*
TaLAZY1-B (Rasool et al., 2023)		*TraesCS6B02G461400*
TaLAZY1-D (Rasool et al., 2023)		*TraesCS6D02G396500*
TaDRO1-A (Rasool et al., 2023)	*TaADRO1-like* (Ashraf et al., 2019), *TaADRO1* (Kitomi et al., 2020)	*TraesCS5A02G213300*
TaDRO1-B (Rasool et al., 2023)	*TaBDRO1-like* (Ashraf et al., 2019)	*TraesCS5B02G210500*
TaDRO1-D (Rasool et al., 2023)	*TaDDRO1-like* (Ashraf et al., 2019)	*TraesCS5D02G218700*
TaqSOR1-A	*TaAqSOR1* (Kitomi et al., 2020), *TaDRO2-A* (Rasool et al., 2023)	*TraesCS2A02G169900*
TaqSOR1-B	*TaDRO2-B* (Rasool et al., 2023)	*TraesCS2B02G196200*
TaqSOR1-D	*TaDRO2-D* (Rasool et al., 2023)	*TraesCS2D02G177400*
TaTAC1-A (Rasool et al., 2023)		*TraesCS5A02G316400*
TaTAC1-B (Rasool et al., 2023)		*TraesCS5A02G316900*
TaTAC1-D (Rasool et al., 2023)		*TraesCS5D02G322600*

LAZY genes have different expression patterns in different plant tissues. *AtLAZY1* mainly functions in shoot gravitropism with *lazy1* loss-of-function mutants having more horizontal shoot branch angles (Yoshihara et al., 2013). The loss of *LAZY1* in rice alters polar auxin transport and shoot auxin distribution (Li et al., 2007), and *LAZY1* is thought to act in the gravitropism pathway between gravity sensing and auxin redistribution (Yoshihara et al., 2013). LAZY1 is cell membrane and nuclear localised and is essential for the redistribution of auxin following gravitropic stimulation in rice, maize and Arabidopsis shoots (Li et al., 2007, Dong et al., 2013, Che et al., 2023). *AtLAZY2*, *AtLAZY3* and *AtLAZY4* have roles in root gravitropism (Yoshihara and Spalding, 2017) and are expressed in root statocytes (Taniguchi et al., 2017, Furutani et al., 2020). Arabidopsis *lazy2 lazy3 lazy4* triple mutants exhibit negative gravitropism with upwards growing roots (Ge and Chen, 2019). *LAZY4* overexpression leads to deeper rooting phenotypes in Arabidopsis and plum (*Prunus domestica*) (Guseman et al., 2017).

AtLAZY2 and *AtLAZY4* have predominantly root-specific expression in root statocyte columella cells and root vasculature (Taniguchi et al., 2017). In the columella cells, LAZY2 and LAZY4 are located on the plasma membrane in the direction of gravity, and they repolarise following a change in gravity stimulus in the lateral root columella cells (Furutani et al., 2020). Recently, LAZY proteins were shown to specifically localise to amyloplast sites at the plasma membrane and act as signal transmitters of statolith localisation and gravity direction in the gravitropic pathway (Nishimura et al., 2023).

LAZY genes contain up to five conserved domains (Yoshihara et al., 2013). In Arabidopsis there are six *LAZY* genes, with *LAZY1*, *LAZY2*, *LAZY4* and *LAZY6* containing all five conserved domains. Conserved domain I at the N-terminus is needed for LAZY1 localisation to the plasma membrane and control of shoot branch angle (Yoshihara and Spalding, 2020). Domain II contains a conserved 'IGT' [GφL(A/T)IGT] motif which is present in all IGT family genes (Dardick et al., 2013). LAZY domains III and IV are less well conserved, with *LAZY2* and *LAZY4* containing a longer version of domain III named extended domain III (D3X) (Binns, 2022). Mutating domains III and IV in *LAZY1* had a lesser effect on shoot phenotype than domains I, II or V (Yoshihara and Spalding, 2020).

LAZY domain V was named CCL (conserved C terminus in *LAZY1* family proteins) due to the domain's high sequence similarity in all LAZY proteins (Taniguchi et al., 2017). The *LAZY* CCL domain interacts with the BRX domain of RCC1-like domain (RLD) proteins to recruit RLD from the cytoplasm to the plasma membrane following gravistimulation (Furutani et al., 2020). The CCL domain contains an EAR-like motif (ethylene-responsive element binding factor-associated amphiphilic repression), which is one of the most common transcriptional repression motifs in plants (Chow et al., 2023). EAR motif-containing proteins negatively regulate genes that have many different functions in plant growth and development (Chow et al., 2023). The EAR motif was found to be essential for *LAZY4* function, as overexpressing *LAZY4* gives a steeper rooting phenotype but overexpressing a truncated *LAZY4* lacking an EAR motif yields a wildtype phenotype (Guseman et al., 2017). Expressing only the C-terminal region in Arabidopsis *lazy* mutants was able to reverse primary root

growth direction showing that domain V is crucial for *LAZY* function (Taniguchi et al., 2017).

Steeper and deeper root system architecture has been shown to improve water and nitrogen uptake from the soil and improve crop yields in drought conditions (Uga et al., 2013). The *LAZY* genes could help to create improved root phenotypes as demonstrated by the *lazy4D* steeper rooting Arabidopsis mutant (Binns, 2022). The *lazy4D* mutant has a more vertical lateral root phenotype due to a dominant gain-of-function substitution (*R145K*) mutation within *LAZY4* extended domain III (D3X) (Binns, 2022). Arabidopsis *LAZY2* and *LAZY4* both contain this conserved D3X which has been shown to be important in lateral root growth angle control (Binns, 2022). Mutating the same residue in *LAZY2* also gives a steeper lateral root angle phenotype (Binns, 2022), showing that domain III is important for *LAZY2* and *LAZY4* roles in root gravitropism. The dominant nature of the *lazy4D* mutation has great potential for use in hexaploid wheat as the effects of single genome mutations can often be masked by the other genome homoeologs in wheat (Krasileva et al., 2017). The aim of this chapter was to investigate the functions of the wheat *LAZY* genes to determine if these genes and the *lazy4D* mutation could be used for optimising wheat root system architecture.

The objectives of this chapter were to:

1. Analyse wheat *LAZY* family homoeolog sequence conservation and expression within the shoots and roots of wheat.
2. Determine if the *lazy4D* mutation in wheat influences lateral root branching angle.

4.2 Results

4.2.1 Wheat *LAZY* gene family sequence and conserved domain analysis

The defining feature of the IGT gene family which includes the *LAZY* and *TAC1* genes is the conserved 'IGT' [GφL(A/T)IGT motif, thought to be present across plant species (Dardick et al., 2013). Analysis of the wheat *LAZY* family shows that all genes contain [φLxIGTφG], a variation on the original motif (Fig. 4.1, Table 4.2). This may indicate that the residues in the original IGT motif are not all essential for *LAZY* domain II function and that the terminal Glycine residue could also be important within this domain. Domains I, III and IV are less well conserved in comparison to domains II and V across the wheat *LAZY* homoeologs (Fig. 4.1). The D3X domain found in *AtLAZY2* and *AtLAZY4* (Binns, 2022) is highly conserved across all *TaqSOR1* homoeologs but to a lesser extent in *TaDRO1* homoeologs and not present in *TaLAZY1* homoeologs (Fig. 4.1). There are two *TaLAZY1* homoeologs on chromosomes 6B and 6D (Table 4.2) (Rasool et al., 2023). A search of the IWGSC CS RefSeq v2.1 assembly showed that the published *TaLAZY1-Un* homoeolog is located on chromosome 6A.

```
                        I
              ┌─────────────────────────┐
AtLAZY1       1 MKFWGWMHHKFRENSKEPLK-DASTGN-SYSILSAHPSLDSQEVYPTACAGSRYNTGFR
OsLAZY1       1 MKLLGWMHRKLRSNNDVFKE-FNTGGGGAC-NCITGLASPDH---DN------------
TaLAZY1-Un    1 MTLLGWMHRKLRSNNDVFKE-FNTAG-----------ASPDD---E------------
TaLAZY1-B     1 MTLLGWMHRKLRSNNDVFKE-FNTGGGAC-NCIAGLASQDH---E------------
TaLAZY1-D     1 MTLLGWMHRKLRSNNDVFKE-FNTTG-----------ASQDH---E------------
AtLAZY2       1 M-KFFGWMQNKLNGDH--NRT-STSSAS-SHHV------------------------
AtLAZY4       1 MCKIANIIPNILLSID---WL-SDIFVF-SY-L-----------------------
OsDRO1        1 MKIFSWVANKISGKQEANRF-PANSSA-PY--------------------------
OsqSOR1       1 MGIINWMQNRLSTAKQDKRRTEAA-AVASS-A-----------------------
TaDRO1-A      1 MKIFSWMANKISGKQEASRF-PASSSG-PS--------------------------
TaDRO1-B      1 MKIFSWMANKISGKQEASRF-PASSSG-PS--------------------------
TaDRO1-D      1 MKIFSWMANKISRKQEASRF-PASSSG-PS--------------------------
TaqSOR1-A     1 MGIINWVQNRLNTKQEKKRS-AAAAAAGAS-S-----------------------
TaqSOR1-B     1 MGIINWVQNRLNTKQEKKRS-AAA--AGAS-S-----------------------
TaqSOR1-D     1 MGIINWVQNRLNTKQEKKRS-AAAAAAGAS-S-----------------------

                                                            II
                                           ┌──────────────────────────────┐
AtLAZY1      58 KQVNLFQESSFAGPKQYTEE-D-F-------KDERNS-DFFDGFLAIC---TLGGETLLD
OsLAZY1      43 ---DYFSGD---DAAHASPP-V--------TAGDLFT-FGGSGLLTIG---TLGIAAVAI
TaLAZY1-Un   32 ----YYGDDAF-VANNPSPS-V--------NADDLFT-FGGSGLLTIG---TLGFAAVNV
TaLAZY1-B    42 ----YYDDDAF-VANHPSPP-V--------NADDLFT-FGGSGLLTIG---TLGFAAVNV
TaLAZY1-D    32 ----YYDDDAF-VANHPSPP-V--------NADDLFT-FGGSGLLTIG---TLGFAAINV
AtLAZY2      29 --------------KQE------------PREEFS-DWPHALLAIG---TFGTTSNSV
AtLAZY4      28 --------------KQD-----H-------PREEFN-DWPHGLLAIG---TFGNKKQTP
OsDRO1       29 --------------RANVS-D-C-------RKDEFS-DWPQSLLAIG---TFGNKQIEE
OsqSOR1      31 --------------RRRGGGGGESCRQEEARDE-IKIAGD-HLLSIG---TLGNESPPR
TaDRO1-A     29 --------------RSNVP-D-C-------RNDEFS-DWPQSLLAIG---TFGNKQIEE
TaDRO1-B     29 --------------RSKVP-D-C-------RNDEFS-DWPQSLLAIG---TFGNKQIEE
TaDRO1-D     29 --------------RSNVP-D-C-------RNDEFS-DWPQSLLAIG---TFGNKQIEE
TaqSOR1-A    31 --------------VRNAPVRENSCRGQ-ADDE-L--PGDWSMLSIGTIGTLGNEPTP-
TaqSOR1-B    29 --------------VRNAPVREKSCRGQ-GDDE-L--PGDWSMLSIG---TLGNEPTP-
TaqSOR1-D    31 --------------VRNAPVREKSCRGQ-ADDE-L--PGDWSMLSIG---TLGNEPTPA

AtLAZY1     105 EQP-AT-----------------------------PT-------F-------------
OsLAZY1      84 PSGGDD--DDYDIDFE--VDATSDDDGGFTVEDDDADVG-GAVTPTFTFPAATAAEAVVA
TaLAZY1-Un   74 PGE-HVGDGDYDVDDEDCVDIDLDSIDGTIGEVDNGDVEDGAATPTFTFPQLE-----AT
TaLAZY1-B    84 PGE-DDGHEDYDVDDEDCVDIDLDNIDGTIDEVDNGNVDDGALTPTFTFPQLE-----SA
TaLAZY1-D    74 PGE-DEGHEDYDVDDDDCVDIDLDNIDGTIDEVDDGNVDDGALTPTFTFPQLE-----ST
AtLAZY2      57 SEN-ESKNVHEEIE---------AEK---K-----------------------------C
AtLAZY4      57 QTL-DQEVIQEETV---------SNL---H-----------------------------V
OsDRO1       61 VAQ-VE-----------------------------------------------------
OsqSOR1      71 PPA--------------------------------------------------------
TaDRO1-A     61 VAQ-VQ-----------------------------------------------------
TaDRO1-B     61 VAQ-VQ-----------------------------------------------------
TaDRO1-D     61 VAQ-VQ-----------------------------------------------------
TaqSOR1-A    71 -AP--------------------------------------------------------
TaqSOR1-B    66 -AP--------------------------------------------------------
TaqSOR1-D    69 PAP--------------------------------------------------------

AtLAZY1     113 ------GM-SFED-PAIDD-ADVTENDLKLISNELDKFLEAEAK---EGHHQPSGRNSDT
OsLAZY1     139 TVEK--AVAAVEAIAEKDD-DTTTEDDLMVVSAEIEKVLGGVDV---ASARV--------
TaLAZY1-Un  128 ATEK--VMVTVEAIAEKDD-VATTEDDLMLVSAEIEKVLGGSNV---PSARV--------
TaLAZY1-B   138 TAEK--VMVSVEAIAEKDD-IATTEDDLMLVSAEIEKVLGGSDV---PSARV--------
TaLAZY1-D   128 TAEK--VMVSVEAIAEKDD-VATTEDELMLVSAEIEKVLGGSNV---PSARV--------
AtLAZY2      75 TAQS--EQ-EEEPSSSVNLE-DFTPEEVGKLQKELMKLLSR-TKKRKSDVNR--------
AtLAZY4      75 EGRQAQDT-DQELSSSDDLEEDFTPEEVGKLQKELTKLLTRRSKKRKSDVNR--------
OsDRO1       66 ------NS-SDNVQSVQDT-VKFTEEEVDKIRKEFETLLAIKDQ---AEAQR--------
OsqSOR1      74 ----A-----AAATAAEEV-ADFTIEEVKKLQEALNKLLRRAKST-KSGSRR--------
```

```
                        III
AtLAZY1    161 NTIASTIEAIEGVDDEEDNQPMKF-----------PLQEYFFGSLIELPESKIAGKK---
OsLAZY1    185 -----SF---AMGG--G----VDC-----------PLQGFLFGSPV-----SDVESRPEY
TaLAZY1-Un 174 -----SF---AMG--------VDC-----------PLQGFLLGSPV----CSDTESWPE-
TaLAZY1-B  184 -----SF---AMG-------IDC-----------PLQGFLLGSPV----CSDTESWPE-
TaLAZY1-D  174 -----SF---AMG-------IDC-----------PLQGFLLGSPV----CSDTESWPE-
AtLAZY2    122 -----EL--MK-----------N-----------LPLDRFLNCPS----SLEVDRRISN
AtLAZY4    126 -----EL--A-----------N-----------LPLDRFLNCPS----SLEVDRRISN
OsDRO1     107 -----SH---DD-----------------------DQ---VG---------LQKRAD-
OsqSOR1    115 -----GS--TAAEHDAD----ERSSSSSSSGSQLLLPLDRFLNCPS----SLEVDRRVAA
TaDRO1-A   107 -----SH---DD-----------------------EQ---VTS--HKEVDESIN-
TaDRO1-B   107 -----PH---DD-----------------------DQ---VAS--HKNVDESIN-
TaDRO1-D   107 -----SH---DD-----------------------EQ---VTS--HKDVDESIN-
TaqSOR1-A  108 -----GS--TAGAGDEE----QN-----------LPLDRFLNCPS----SLEVDRRLSL
TaqSOR1-B  103 -----GS--TAGAGDEE----QN-----------LPLDRFLNCPS----SLEVDRRLSL
TaqSOR1-D  107 -----GS--TAGAGDEE----QN-----------LPLDRFLNCPS----SLEVDRRLSL
                                              D3X

AtLAZY1    207 -------------DRASLGELFQITEVQDKQ-----SENIY-----------GKKKK--
OsLAZY1    215 LQA---PRDSSGSCGGGGRRTSLGELFMRTRFADEKVALVAVAEGEDGVAGDDGAAAAGV
TaLAZY1-Un 202 -----------KPNGGGRRASLGELFMRTRFTEEKGALVAVQESEDGGEREEGKAG--K
TaLAZY1-B  212 -----------KRNSGGRRASLGELFMRTRFTEEKGALVAVQESEDGGEREEGKVV--K
TaLAZY1-D  202 -----------KPNGGGRRASLGELFMRTRFTEEKGALVAVQESEDGGEREEGKVG--K
AtLAZY2    148 ALSAVVDSS----EENKEEDMERTINVILGR-----CKEISI-------ESKNN-KK---
AtLAZY4    151 ALC-----------DEKEEDIERTISVILGR-----CKAIST-------ESKNKTKKN--
OsDRO1     121 -------GE----DNEKHIRQLINKRIIVSK-----SKNSL---------------GKK--
OsqSOR1    160 ----------------ADGEFSPDTQIILSK-----ARDLLV----------NTNG---
TaDRO1-A   125 ---------------EKHRDQLLNKMVVISK-----AKDSL-----------GKK--
TaDRO1-B   125 ---------------EKHRDQLFNK-IVISK-----AKDSP-----------GKK--
TaDRO1-D   125 ---------------EKHRDQLLNKKVVISK-----AKDSL-----------GKK--
TaqSOR1-A  141 RLQ----GA----DGGQNGEFSPDTQIILSK-----ARELLV----------STNGN--
TaqSOR1-B  136 RLQ----GA----DGGQNGEFSPDTQIILSK-----ARELLV----------STNGN--
TaqSOR1-D  140 RLQ----GA----DGGQNGEFSPDTQIILSK-----ARELLV----------STNGN--
                                                                IV
AtLAZY1    235 QPN-----SAHKSAKHLVK-KVLKKIHPSSRGSVS----GKP--EVDSTKKFQKMVQ-V
OsLAZY1    272 GGDRAGKGGG----YKTVKKRKVKD-E----KGGGGAAGGGMP--ATVT-KSKFQKILQI-
TaLAZY1-Un 248 GGD-----GG---HKRTKKLRVKD-E----KGAGGD---GVP--ASATAKSKFQKILKI-
TaLAZY1-B  258 GGD-----GG---HKRTKKWRVKD-E----KGHGGD---GVP--ANATAKSKFQKILKI-
TaLAZY1-D  248 GGD-----SG---HKRTKKWRVKD-E----KGAGGD---GVP--ASATAKSKFQKILKI-
AtLAZY2    188 KRD-----ISKNSVSYLFKKIFVC------ADGIST--APSPSLRDTLQESRMEKLLKMM
AtLAZY4    186 KRD-----LSKTSVSHLLKKMFVC------TEGFSP--VPRPILRDTFQETRMEKLLRMM
OsDRO1     149 GNT-----LKPRSVASLLK-IFMC------KGGFTS-VVPEP--RNTFPQSRMEKLLKAI
OsqSOR1    185 GGA-----IKQKSFRFLLKKMFVC------RGGFSPSPAPPPTLKDPV-ESRIEKLFRTM
TaDRO1-A   149 AST-----LKPRSVASLFK-LLMR------KGGFAS-AIPDP--RSSFPQSRMEKLLKAI
TaDRO1-B   148 AST-----LKPRSVASLLK-LLMP------KGGFAS-AVPDP--RNSFPQSRMEKLLKAI
TaDRO1-D   149 AST-----LKPRSVASLFK-LLMR------KGGFAS-AVPDP--RSSFPQSRMEKLLKAI
TaqSOR1-A  175 GGG-----VKQKSFKFLLKNMFAC------RGGFP----PQPSLKDPV-ETKLEKLFKTM
TaqSOR1-B  170 GGG-----VKQNSFKFLLKNMFAC------RGGFP----PQPSLKDPV-ETKLEKLFKTM
TaqSOR1-D  174 GGG-----VKQKSFKFLLKNMFAC------RGGFP----PQPSLKDPV-ETKLEKLFKTM

AtLAZY1    282 FHRKVHPEESIM---ETKIYSSVANPKSSKA-NSID-LTFEKV--NH--CHEA------S
OsLAZY1    320 FHRKVYPENTLLTRNLTKKSRNRGATDNGGGAVATGDPDGPLASPVLRCRKDHPMR-GFG
TaLAZY1-Un 289 FHRKVYPESTMLT----KKNRKRGTPDNGGGGGATD-ESVPSP--TP--KKTGPRRLSFG
TaLAZY1-B  299 FHRKVYPESTMLT----KKNRKRGTPDNGGGGGATD-ESVPSP--TP--KKTRPRRLSFG
TaLAZY1-D  289 FHRKVYPESTMLT----KKNRKRGTPDNSGGGGGATD-ESVPSP--TP--KKTGPRRLSFG
AtLAZY2    235 LHKKINAQASSKPTSLTTKRYLQDKKQL----------------------------S
AtLAZY4    233 LHKKVNTQASSKQTS--TKKYLQDKQQL----------------------------S
OsDRO1     194 LQKKIHPQNSST---LVAKRHLDWKPDE----------------------------T
```

```
             v
AtLAZY1     327 KRCIQYE-----LR---SSRSAKNGEHWIKTDEDYFVLEL
OsLAZY1     379 CC-TNGAFGASSPG-GNAEMNGNKSGHWIKTDADYLVLEL
TaLAZY1-Un  340 CCCTKRSFNASPVDDGGEELNGDKSGHWIKTDADYLVLEL
TaLAZY1-B   350 CCCTKRSFSASPVDDGGEELNGDKSGHWIKTDADYLVLEL
TaLAZY1-D   340 CCCTKRSFSASPVDDVGEELNGDKSGHWIKTDADYLVLEL
AtLAZY2     264 LKSEEEE-----TS---ERRSSSDGYKWVKTDSDFIVLEI
AtLAZY4     260 LKNEEE----------EGRSSNDGGKWVKTDSDFIVLEI
OsDRO1      220 EINECLE-----DA---LRDLDDDGAKWVKTDSEYIVLEM
OsqSOR1     262 MQREHLH-----DDED-DDENAEDIFKWDKTDSDFIVLEM
TaDRO1-A    220 EINECLE-----DA---LRDLDDDGAKWVKTDSDFIVLEM
TaDRO1-B    219 EINECLE-----DA---LRDLDDDGAKWVKTDSDFIVLEM
TaDRO1-D    220 EINECLE-----DA---LRDLDDDGAKWVKTDSDFIVLEM
TaqSOR1-A   248 IQMDGHH-----DE-E-ELDYGEDVFKWDKTDSDFIVLEV
TaqSOR1-B   243 IQMDGRH-----DEDE-ELDYGEDVFKWDKTDSDFIVLEV
TaqSOR1-D   247 IQMDGRH-----DEEEELDYNDEDIFKWDKTDSDFIVLEV
```

Figure 4.1: Protein alignment of Arabidopsis, rice wheat *LAZY* gene sequences.

Protein sequences (EnsemblPlants) aligned and shaded with T-Coffee and Boxshade. Black shading shows 100% conservation and grey shading shows weak conservation. Gene IDs can be found in Table 4.1. Gene nomenclature for Arabidopsis *LAZY* genes from Yoshihara and Spalding (2017), rice and wheat *LAZY1*, *DRO1* and *qSOR1* genes from Kitomi et al. (2020), Rasool et al. (2023). Blue lines and roman numerals indicate *LAZY* conserved domains and orange line indicates extended domain III (D3X) (Binns, 2022).
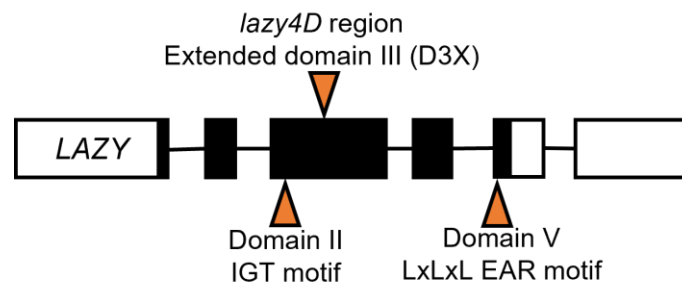
Figure 4.2: Typical *LAZY* gene structure with locations of annotated features.

White squares show 5' and 3' UTRs, black lines show introns and black rectangles show exons. Orange arrows show the approximate locations of three motifs.

Another characteristic of the *LAZY* gene family is the intron-exon structure and the first two codons (the 'ATGAAG' nucleotide sequence) of each gene (Figure 4.2) (Dardick et al., 2013). These characteristics are present in all wheat *LAZY* homoeologs, though the second codon is not 'AAG' in all homoeologs (Fig. 4.1). The gene annotation of *TaDRO1-A* contained an additional 96 amino acids prior to conserved domain I, which is likely to be a misannotation and so these amino acids were not included in the alignment (Fig. 4.1).

Table 4.2: Arabidopsis, rice and wheat *LAZY* genes.

Gene IDs and sequences obtained from EnsemblPlants. Arabidopsis = *Arabidopsis thaliana* 'Col-0', Rice = *Oryza sativa ssp. Japonica* 'Nipponbare', Wheat = *Triticum aestivum* 'Chinese Spring'. "Un" = Unknown chromosome, "-" indicates the region or motif is not present, "*" represents a stop codon, "D3X" = extended domain III.

Species	Gene name	Gene ID	Amino acid sequence		
			IGT motif (Domain II)	*lazy4D* region (D3X)	EAR-like motif (Domain V)
Arabidopsis	*AtLAZY1*	AT5G14090	GLLTIGTLG	-	LVLEL*
Rice	*OsLAZY1*	Os11g0490600	GLLTIGTLG	-	LVLEL*
Wheat	*TaLAZY1-Un*	TraesCSU02G083100	GLLTIGTLG	-	LVLEL*
	TaLAZY1-B	TraesCS6B02G461400	GLLTIGTLG	-	LVLEL*
	TaLAZY1-D	TraesCS6D02G396500	GLLTIGTLG	-	LVLEL*
Arabidopsis	*AtLAZY2*	AT1G17400	ALLAIGTFG	LEVDRR	IVLEI*
Arabidopsis	*AtLAZY4*	AT1G72490	GLLAIGTFG	LEVDRR	IVLEI*
Rice	*OsDRO1*	Os09g0439800	SLLAIGTFG	-	IVLEM*
Rice	*OsqSOR1*	Os07g0614400	HLLSIGTLG	LEVDRR	IVLEM*
Wheat	*TaDRO1-A*	TraesCS5A02G213300	SLLAIGTFG	KEVDES	IVLEM*
	TaDRO1-B	TraesCS5B02G210500	SLLAIGTFG	KNVDES	IVLEM*
	TaDRO1-D	TraesCS5D02G218700	SLLAIGTFG	KDVDES	IVLEM*
Wheat	*TaqSOR1-A*	TraesCS2A02G169900	SIGTIGTIG	LEVDRR	IVLEV*
	TaqSOR1-B	TraesCS2B02G196200	SMLSIGTLG	LEVDRR	IVLEV*
	TaqSOR1-D	TraesCS2D02G177400	SMLSIGTLG	LEVDRR	IVLEV*

Domain V is well conserved across all wheat *LAZY* homoeologs which contain EAR-like motifs, although only *TaLAZY1* homoeologs have the exact LxLxL EAR motif sequence (Table 4.2) (Kagale and Rozwadowski, 2011). The domain V WxxTD motif identified previously in the *TaDRO1* homoeologs (Ashraf et al., 2019) was also highly conserved in *TaLAZY1* and *TaqSOR1* homoeologs (Fig. 4.1).

4.2.2 Introducing steeper rooting into wheat with the *lazy4D* mutation

Steeper rooting has great potential to improve modern wheat cultivars as a more vertical root system can increase drought tolerance and crop yields in water-limited conditions (Uga et al., 2013). The Arabidopsis *lazy4D* mutant has a steeper lateral root phenotype due to a point mutation in the extended domain III (D3X) of *AtLAZY4* (Fig. 4.3) (Binns, 2022). Analysis of the wheat *LAZY* family found that the *lazy4D* region in D3X was not present in *TaLAZY1* and poorly conserved in *TaDRO1* homoeologs, but highly conserved in all *TaqSOR1* homoeologs (Table 4.2). This established that *TaqSOR1* homoeologs would be

good candidates for targeting to introduce the *lazy4D* mutation via wheat transformation.
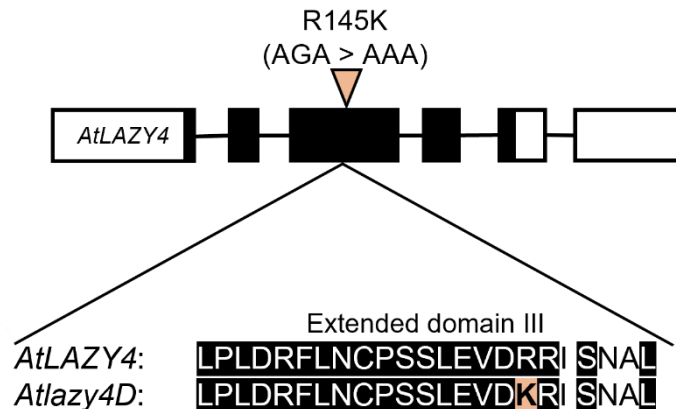
Figure 4.3: The Arabidopsis *lazy4D* steeper rooting mutant has a point mutation in *AtLAZY4* extended domain III.

Location of SNP in *Atlazy4D* EMS mutant: *R145K* substitution due to an AGA > AAA base change within extended domain III (Binns, 2022).

Wheat *LAZY* expression analysis was performed to identify the best *TaqSOR1* homoeolog to introduce the *lazy4D* mutation. Previous studies have looked at *TaDRO1* homoeolog expression in specific tissues including crown roots, root tips, basal shoot and spikelets of two Pakistani wheat cultivars, with highest expression in root tip tissue (Ashraf et al., 2019). Wheat *LAZY* family expression has also been investigated in whole roots and shoots of a further two wheat varieties originating from Pakistan, which found highest *TaqSOR1* (*TaDRO2*) expression in roots (Rasool et al., 2023). Arabidopsis *LAZY* genes have unique patterns of expression with important functions in root and shoot statocytes (Taniguchi et al., 2017, Nishimura et al., 2023), and *LAZY* gene expression is highest in root tip and shoot hypocotyl tissues of young seedlings (Yoshihara and Spalding, 2017). *LAZY* genes have differing functions and patterns of expression in lateral and primary roots, so wheat *LAZY* expression was investigated in seminal root tips, lateral root tips and young shoot tissue (Fig. 4.4).

LAZY1, *DRO1* and *qSOR1* homoeolog expression was examined in wheat cv. 'Fielder' root and shoot samples. Fielder was used as Fielder is the cultivar widely used for wheat transformation. *TaLAZY1* expression was only seen in wheat shoot tissue and no *TaLAZY1* expression was found in seminal or lateral root tips

(Fig. 4.4). The *TaDRO1* homoeologs had strong root and shoot expression in comparison to the *TaqSOR1* homoeologs which were weakly expressed in shoots (Fig. 4.4). The three *TaqSOR1* homoeologs have high sequence homology (Rasool et al., 2023) and had similar expression levels within each tissue type (Fig. 4.4). This meant that there was not a clear homoeolog candidate to use for future mutagenesis or gene editing to generate a *lazy4D* construct for wheat transformation. As there was not an obvious candidate, the *TaqSOR1-A* homoeolog was chosen to create the native promoter constructs as *TaqSOR1-A* had slightly higher expression in wheat lateral roots (Fig. 4.4). The *lazy4D* R > K mutation (R145K) was introduced into the wildtype *TaqSOR1-A* gene sequence to generate a wheat *lazy4D* construct (R136K) (Fig. 4.5b). Two approaches were used to create the transformed wheat lines; *qSOR1-A* with the *lazy4D* mutation was fused to the native *qSOR1* promoter, or *lazy4D* expressed under the control of the constitutive maize ubiquitin-1 (*ZmUbi*) overexpression promoter. The *lazy4D ZmUbi* overexpression construct used for wheat transformation had been constructed prior to this work using a *lazy4D* R > A mutation of the *TaqSOR1-D* homoeolog (R135A) and so could not be changed (Fig. 4.5c). Due to differences in homoeolog sequences the *lazy4D* mutation site was *R136* in *TaqSOR1-A* whereas the site was located at *R135* in *TaqSOR1-D.* The use of these native and constitutive promoters would enable investigation into the effects of different levels of *lazy4D* expression in wheat. Overexpression of wildtype *LAZY* genes can induce steeper rooting in Arabidopsis (Guseman et al., 2017), so wildtype *qSOR1* under the control of the native *qSOR1* promoter was also transformed into wheat as a control. These constructs were transformed into wheat cv. Fielder by the Crop Transformation group at the John Innes Centre (Norwich). Gene editing of the *qSOR1* homoeologs to introduce the *lazy4D* mutation into Fielder wheat was also attempted in collaboration with the Crop Transformation group, however, it was unsuccessful within this project.
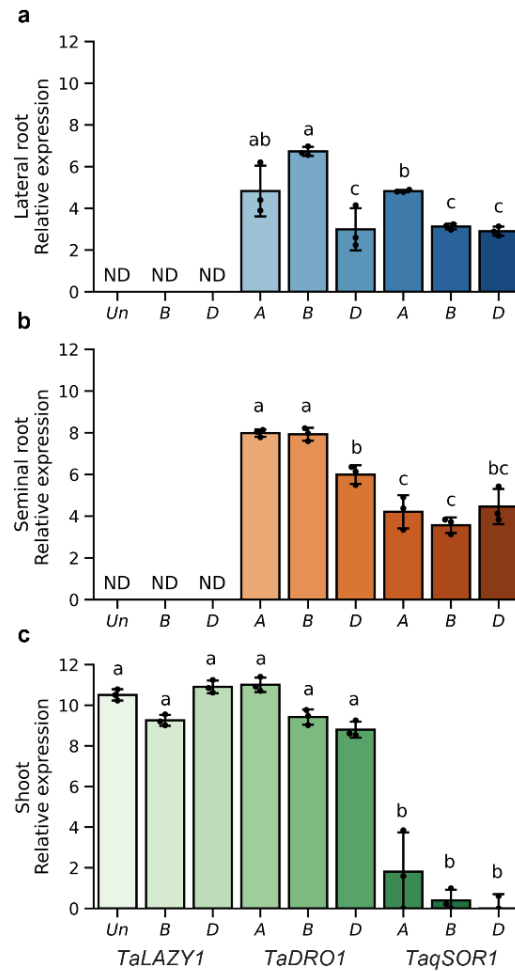
Figure 4.4: Wheat *LAZY* gene expression in wheat root and shoot samples.

Relative expression (normalised to *ACTIN* and *ELONGATION FACTOR*) of wheat *LAZY1*, *DRO1* and *qSOR1* A, B and D homoeologs in wheat cv. 'Fielder' (a) lateral roots, (b) seminal roots and (c) shoot samples, 3 independent biological replicates, with three technical replicates for each. Error bars show standard deviation, statistical analysis performed with one-way ANOVA and Tukey's post-hoc tests, $p < 0.05$, 'ND' = not detected, 'Un' = unknown chromosome.
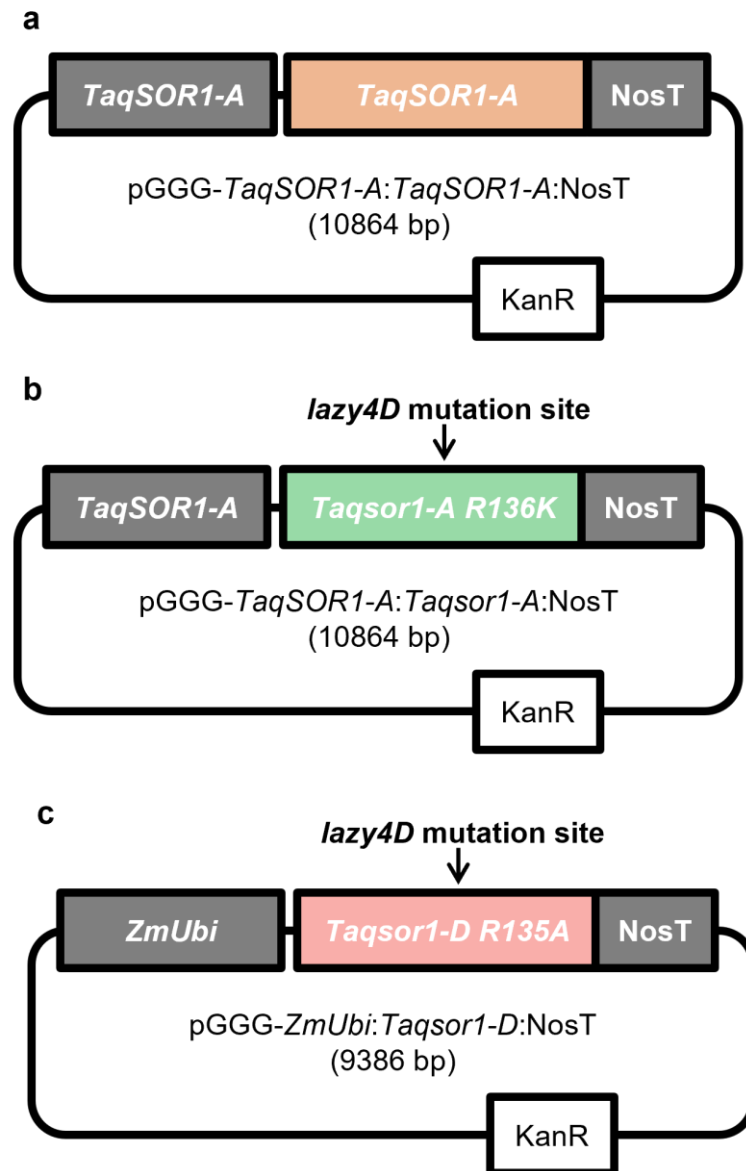
Figure 4.5: Generating wheat *qSOR1* constructs with the *lazy4D* mutation for transformation into Fielder.

(a) WT native promoter construct: wildtype A homoeolog *TaqSOR1* promoter fused to *TaqSOR1-A* (gDNA). (b) *lazy4D* native promoter construct: wildtype *TaqSOR1-A* promoter fused to *Taqsor1-A* containing the *lazy4D* mutation (*R136K*). (c) Overexpression *lazy4D* construct: *Maize ubiquitin-1 (ZmUbi)* constitutive promoter fused to *Taqsor1-D* (CDS) containing the *lazy4D* mutation (*R135A)*. All gene constructs assembled into an adapted pGGG vector (Smedley et al., 2021).

4.2.3 Root system architecture analysis of *lazy4D* transformed wheat lines

Expression of the *qSOR1-A:qSOR1-A* construct did not cause a change in lateral root growth angle compared to Fielder, the untransformed background (Fig. 4.6). There was a possibility that expressing this construct in wheat could have altered the root phenotype as overexpression of wildtype *LAZY* genes can induce steeper rooting in Arabidopsis (Guseman et al., 2017). The wheat lines expressing constructs with *lazy4D* mutations; *qSOR1-A:qsor1-A* (*R136K*) and *ZmUbi:qsor1-D* (R135A), also did not show any significant differences in root growth angle phenotype (Fig. 4.6). This shows there may be differences in *LAZY* D3X function in wheat and Arabidopsis lateral roots, as mutating the equivalent arginine residue in Arabidopsis *LAZY2* and *LAZY4* results in a more vertical lateral root phenotype (Binns, 2022).
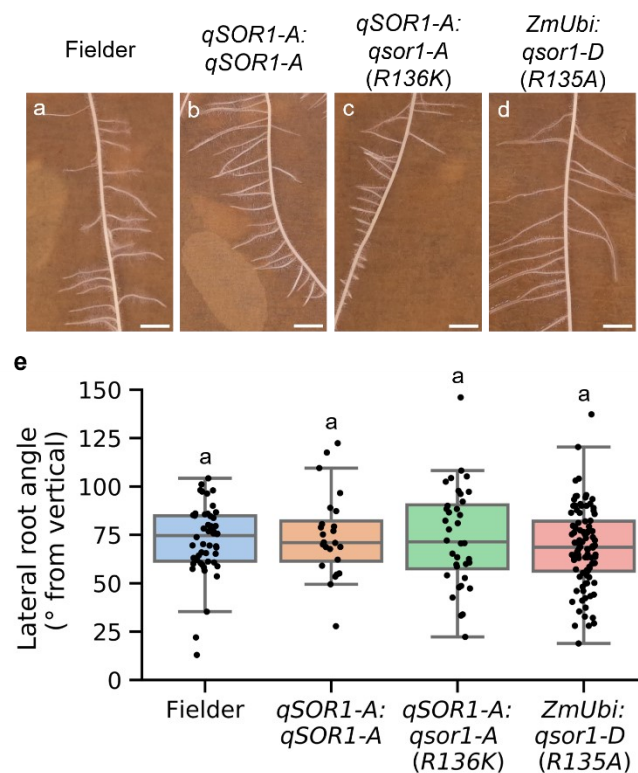
Figure 4.6: Lateral root angle analysis of transformed wheat lines.

(a – d) Example images of lateral roots branching from primary seminal roots of 9-day old wheat plants (a) Fielder (b) *qSOR1-A:qSOR1-A* (c) *qSOR1-A:qsor1-A* and (d) *ZmUbi:qsor1-D*, scale bars = 5 mm. (e) Lateral root angle from vertical measured 0.5 – 1 mm at the site of lateral root emergence from the primary seminal root. Statistical analysis was performed with Shapiro-Wilk and Kruskal-Wallis tests: H = 2.246, p = 0.523, n = 24 – 96 roots per genotype.

Analysis of root system traits was conducted to investigate any effects of the *lazy4D* mutation on the overall root system architecture of the transformed wheat lines (Fig. 4.7). The *lazy4D* overexpression lines (*ZmUbi:qsor1-D*) had on average 10.71 mm longer seminal roots compared to *qSOR1-A:qsor1-A* plants expressing the *lazy4D* mutation under the control of the native *qSOR1* promoter (*p* = 0.0001) (Fig. 4.7h). This resulted in the *ZmUbi:qsor1-D* lines having a larger convex hull area than the *qSOR1-A:qsor1-A* root systems (*p* = 0.0108) (Fig. 4.7g). There were no differences in seminal root emergence or tip angles between *ZmUbi:qsor1-D* and *qSOR1-A:qsor1-A* (Fig. 4.7i, j). A slight increase in seminal tip angle verticality was present in *qSOR1-A:qSOR1-A* plants compared to Fielder (*p* = 0.0396), although this was not seen in root emergence angle (Fig. 4.7i, j). Plant root gravitropic setpoint angles including in wheat and Arabidopsis roots are known to become more vertical over time (Fig. 3.7) (Mullen and Hangarter, 2003). A possible explanation for the increase in seminal tip angle verticality could be due to a faster change in GSA in the *qSOR1-A:qSOR1-A* lines.

Finally, further analysis of the transformed wheat lines was performed to explore any effects of construct copy number. No effect of copy number was seen in *qSOR1-A:qSOR1-A* or *qSOR1-A:qsor1-A* lines and there were no significant differences in lateral root growth angle in *ZmUbi:qsor1-D* lines (Fig. 4.8a – f). However, the highest copy number overexpression line (copy number = 9) had a more vertical seminal root phenotype compared to the single copy number line, as shown by a significantly lower root system width/depth ratio by 0.34 on average (*p* = 0.029) (Fig. 4.8g - l). This indicates that exceptionally high expression of the *lazy4D* mutation is required to affect seminal root growth angle in wheat.
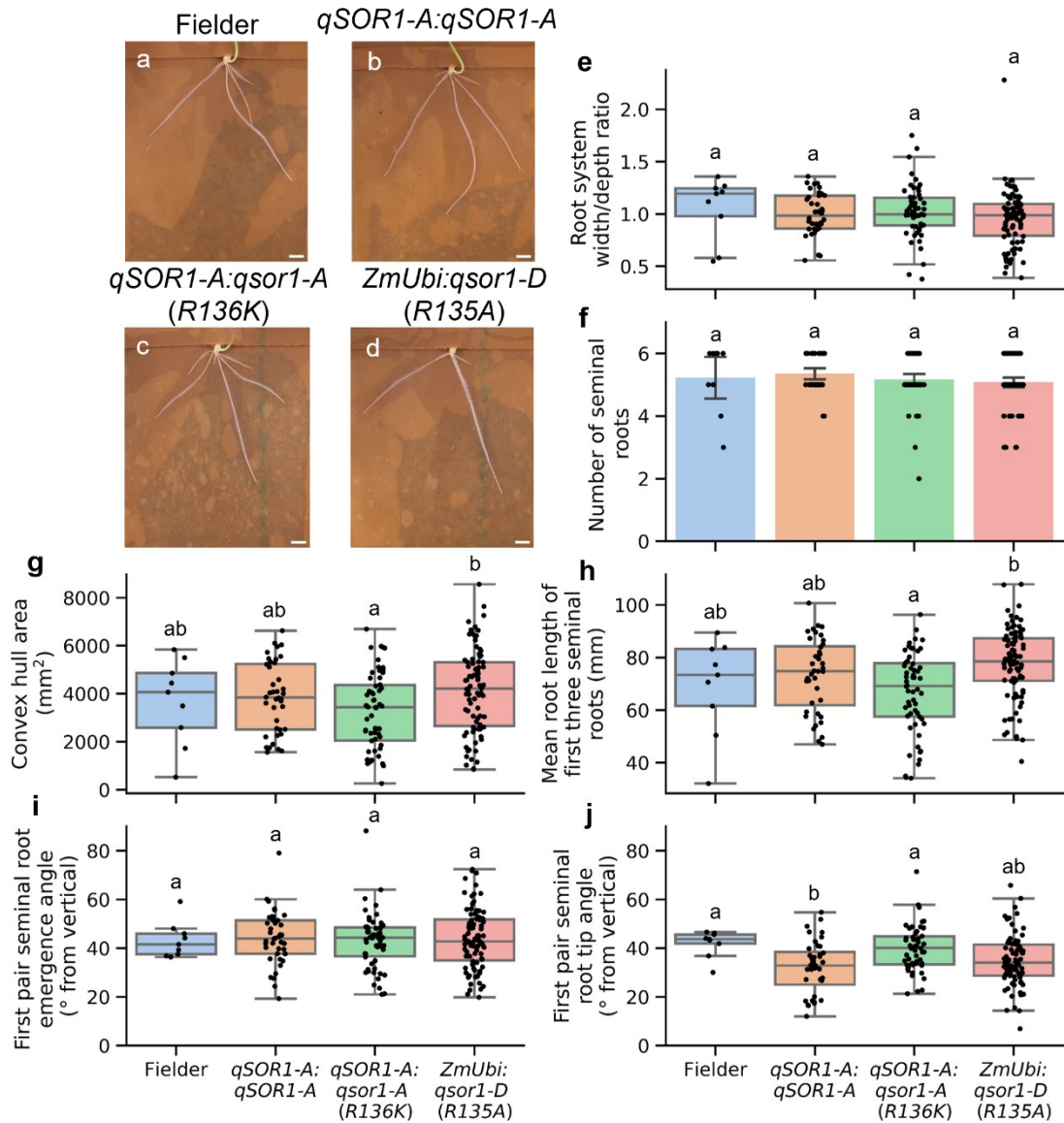
Figure 4.7: Phenotyping wheat lines transformed with the *lazy4D* mutation.

Example images of the 4 different genotypes (a - d), chosen as the plant with the median root system width/depth ratio. (a) Fielder, n = 9 plants (b) *qSOR1-A:qSOR1-A*, n = 40 plants (c) *qSOR1-A:qsor1-A* (*R136K*), n = 58 plants (d) *ZmUbi:qsor1-D* (*R135A*), n = 87 plants. (e) Root system width/depth ratio, H = 4.326, p = 0.228. (f) Number of seminal roots, H = 4.140, p = 0.247, error bars = 95% confidence interval (g) Convex hull area, F = 3.3009, p = 0.0215 (h) Mean root length of the first three seminal roots, F = 6.5766, p = 0.0003 (i) first pair seminal root emergence angle, F = 0.0763, p = 0.973 (j) first pair seminal root tip angle, F = 6.3758, p = 0.0004. Scale bars = 10 mm. Statistical analysis performed with Shapiro-Wilk, one-way ANOVA (g – j) and Tukey's post hoc tests (g, h, j), and Kruskal-Wallis tests (e, f), letters denote statistical significance, p < 0.05.
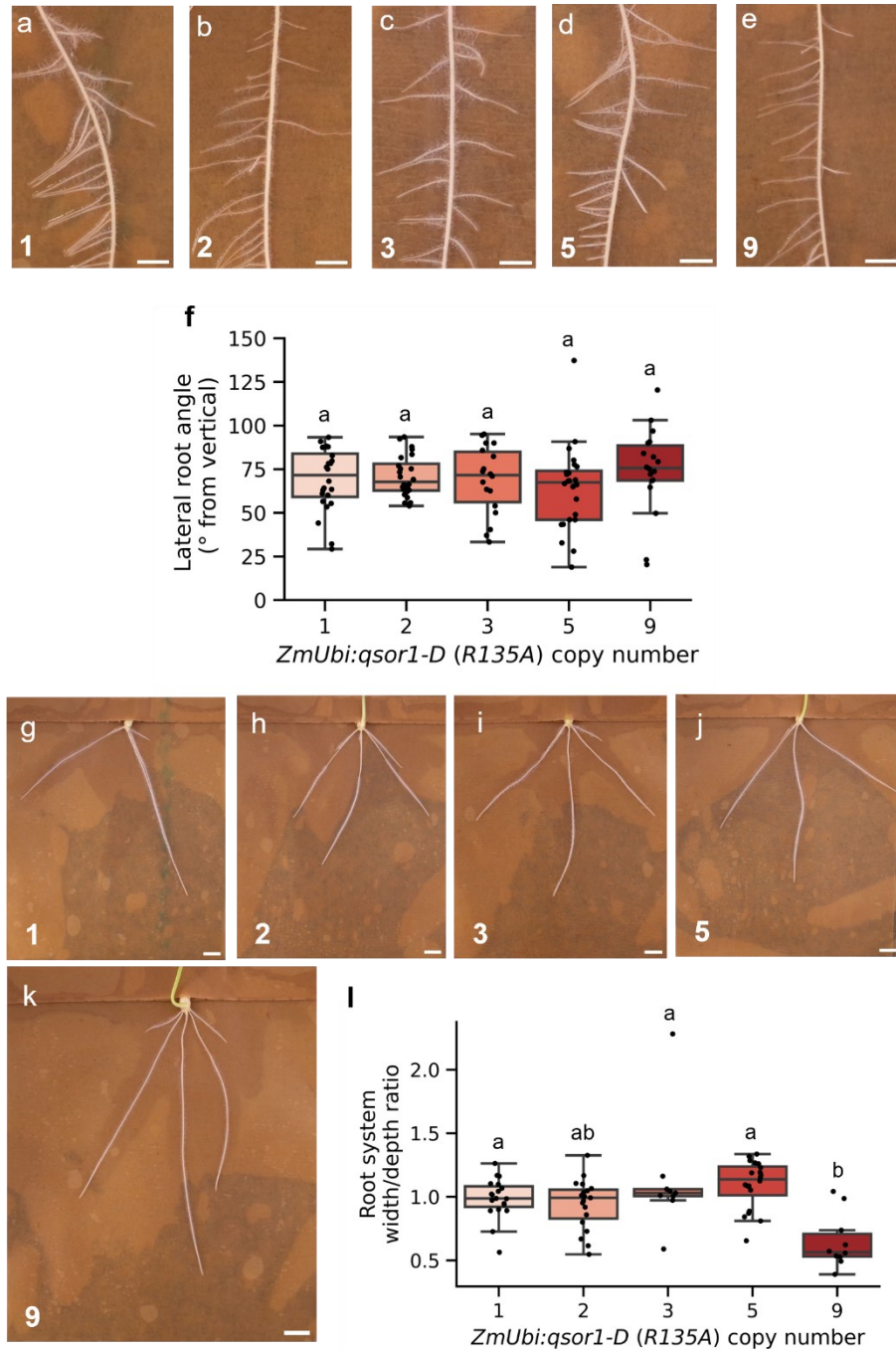
Figure 4.8: A high copy number overexpression line carrying a *qsor1* mutation has a steeper seminal root phenotype.

(a - e) 9-day lateral root images of *ZmUbi:qsor1-D* lines; (a) construct copy number 1, (b) 2, (c) 3, (d) 5 and (e) 9, scale bars = 5 mm. (f) lateral root angle analysis of *qsor1-D* overexpression lines separated by copy number. Lateral root angle from vertical measured 0.5 – 1 mm at the site of lateral root emergence from the seminal root in 9-day old wheat plants, n = 18 – 24 roots. Statistical analysis was performed with Shapiro-Wilk and one-way ANOVA tests: $F = 0.753$, $p = 0.558$. (g – k) Example 5-day old wheat seedling seminal root images of lines (g) copy number 1, (h) 2, (i) 3 (j) 5 and (k) 9, scale bars = 10 mm. (l) Root system width/depth ratio of *ZmUbi:qsor1-D* (*R135A*) overexpression lines split by copy number, n = 9 – 20 plants per *ZmUbi:qsor1-D* copy number. Statistical analysis was performed with Shapiro-Wilk, Kruskal-Wallis and Dunn's post-hoc tests, $H = 22.19$, $p = 0.0002$.

4.3 Discussion

4.3.1 The wheat *LAZY* gene family

Sequence alignment and domain analysis identified nine wheat *LAZY* family homoeologs which have since been published as the *LAZY1*, *DRO1* and *qSOR1* A, B and D homoeologs (Fig. 4.1) (Kitomi et al., 2020, Rasool et al., 2023). The Arabidopsis *LAZY* gene family have been reported under different names including *NGR*, *DRO1* and *LZY* (Yoshihara et al., 2013) so a consensus on wheat *LAZY* naming is needed to avoid this issue developing in wheat *LAZY* literature. The names used in this chapter (Table 4.1) are based on the first reported names while keeping within the wheat gene nomenclature guidelines (Boden et al., 2023). The *LAZY* domains I, II, IV and V are present and conserved in the wheat *LAZY1*, *DRO1* and *qSOR1* homoeologs (Fig. 4.1). The presence of domain V in these genes confirms their inclusion as *LAZY* genes, as the *TAC1* genes lack domain V within the IGT family (Yoshihara and Spalding, 2017). The *TaTAC1* homoeologs have now been identified (Rasool et al., 2023), but this chapter focuses on the wheat genes within the *LAZY* family. All wheat *LAZY* homoeologs contained the IGT motif in domain II including a conserved leucine residue two amino acids away from the IGT motif. These residues are important for Arabidopsis *LAZY* function as introducing a construct with mutations in this residue and the isoleucine in the *AtLAZY1* IGT motif (*L92A/I94A*) into *lazy1* plants caused a more severe downwards shoot phenotype, showing that this domain is crucial for shoot gravitropism (Yoshihara and Spalding, 2020).

Extended domain III (D3X) is not conserved in *TaLAZY1* similar to Arabidopsis *LAZY1*, but D3X is present in *qSOR1* and partially present in *DRO1* (Table 4.2). Sequence analysis showed that the *DRO1* and *qSOR1* sequences are similar to Arabidopsis *LAZY2* and *LAZY4*, although these Arabidopsis genes both contain D3X. This domain is not present in Arabidopsis *LAZY3* (Yoshihara and Spalding, 2020) so wheat *DRO1* homoeologs may have a similar function to *AtLAZY3*. Arabidopsis *LAZY3* has strong expression only in the root tip of Arabidopsis seedlings and is thought to function in primary root gravitropism (Yoshihara and Spalding, 2017). *DRO1* homoeologs are expressed in wheat roots and were found to interact with TOPLESS (TPL) repressor proteins via the domain V EAR motif (Ashraf et al., 2019). Therefore, wheat *DRO1* is likely to have an important

role in root growth angle control differing to the role of *qSOR1* homoeologs as D3X is not present.

Establishing wheat *LAZY* homoeolog expression patterns in Fielder is important for further wheat *LAZY* research, as Fielder is the wheat cultivar most used for transformation and gene editing (Sato et al., 2021). The wheat *LAZY* genes had different expression patterns in Fielder root and shoot tissue, but expression was consistent within each homoeolog triad (Fig. 4.4). The A, B and D gene copies constitute a wheat homoeolog triad, and approximately 70% of homoeolog triads identified in the wheat genome have balanced expression (Ramírez-González et al., 2018). The expression of *DRO1* homoeologs was observed in both root and shoot tissues, which is consistent with previous studies (Rasool et al., 2023). Together with *qSOR1* expression in both seminal and lateral roots, it could be hypothesised that wheat *DRO1* and *qSOR1* may function in root growth angle control.

The shoot-specific expression of wheat *LAZY1* homoeologs supports the hypothesis that the *TaLAZY1* homoeologs have a role in gravity signalling during shoot gravitropism as reported in Arabidopsis, rice and other species (Li et al., 2007, Yoshihara et al., 2013). Similar to *TaLAZY1* expression, rice *LAZY1* is undetectable in roots but strongly expressed in young leaves, shoot vasculature and etiolated coleoptiles (Li et al., 2007). Arabidopsis *LAZY1* is also primarily shoot expressed (Yoshihara and Spalding, 2017). A previous study found low levels of wheat *LAZY1* in shoots (Rasool et al., 2023), which highlights the potential variation in *LAZY* family gene expression between wheat cultivars. Broadly, the wheat *LAZY* gene family share similar patterns of expression to Arabidopsis and rice which could suggest that the wheat genes have similar roles in gravitropism.

4.3.2 Effect of the *lazy4D* mutation on wheat root system architecture

The steeper rooting *lazy4D* mutant is unusual within Arabidopsis *lazy* mutants as the mutation is dominant and gain-of-function, and causes a steeper lateral root phenotype (Binns, 2022) unlike the shallower lateral rooting *lazy* knock-out mutants (Taniguchi et al., 2017). The dominance of *lazy4D* in Arabidopsis makes the mutation a good candidate for introduction into wheat via transformation as removal of wildtype *LAZY* expression within hexaploid wheat would be

challenging. The wheat root system solely consists of non-vertical roots unlike the Arabidopsis vertical taproot system, so it was hypothesised that the *lazy4D* mutation may regulate root growth angle of all root types in the fibrous wheat root system. The *lazy4D* mutation was introduced into wheat *qSOR1* as the *qSOR1* homoeologs are the only homoeologs to contain a fully conserved extended domain III. Overexpression of wildtype *AtLAZY4* (*AtDRO1*) can result in a steeper rooting phenotype (Guseman et al., 2017), so two wheat lines were created expressing *qSOR1* and *qsor1* (*R136K*) under the native *qSOR1* promoter as well as a *qsor1* overexpression line. The overexpression construct used an alanine substitution strategy as it was created prior to this work, whereas the native promoter constructs were constructed using the original lysine substitution. This should not affect the impact of the mutation as previous work has found that it is the loss of the arginine residue rather than the specific change to a lysine residue that causes the Arabidopsis steeper lateral root phenotype (Binns, 2022).

High copy number lines are usually less desirable due to susceptibility to transgene silencing in later generations (Sivamani et al., 2015, Mieog et al., 2013). However, the highest *qsor1* overexpression line (copy number of 9) had a more vertical seminal root phenotype compared to the single copy number line, but no differences in lateral root angle (Fig. 4.8). This indicates that introducing the *lazy4D* mutation into *qSOR1* does not disrupt wheat lateral root growth angle control unlike in Arabidopsis (Binns, 2022), but may have an effect in seminal roots. This is intriguing as similar levels of *qSOR1* homoeolog expression are seen in both seminal and lateral roots (Fig. 4.4). Analysis of *ZmUbi:qsor1-D* construct expression within lateral and seminal root tips could help understand the phenomenon of a seminal root angle phenotype but no lateral phenotype. An overexpression line of wildtype *qSOR1* would be required to confirm if the root angle phenotype is due to the overexpression of *qSOR1* or specifically due to the *R135A* mutation. Finally, further work to determine the root growth angle phenotype of this line at later growth stages in crown roots may uncover whether the phenotype seen in the seminal roots correlates with the mature root system phenotype.

The absence of any consistent root angle differences in the native promoter lines and the phenotypes seen in the overexpression lines may mean that wheat

requires higher levels of *lazy4D* expression to induce a root angle phenotype than in Arabidopsis. The three *qSOR1* gene copies present in the hexaploid bread wheat genome means that there would be higher wildtype transcript levels present in the background of the transformed wheat lines in comparison to diploid Arabidopsis transformed with the *lazy4D* mutation. These wildtype *qSOR1* homoeologs within the transformed wheat lines may prevent the expression of the introduced construct influencing root growth angle control. Due to these ploidy effects, a very high expression of this mutation in wheat may be needed to induce the steeper rooting phenotype, despite the mutation being a dominant gain-of-function mutation in Arabidopsis (Binns, 2022). Gene editing of *qSOR1* homoeologs in wheat to introduce the *lazy4D* mutation would enable understanding of wheat *qSOR1* function and the effects of the *lazy4D* mutation. The *qSOR1* homoeolog sequences are highly conserved so the *lazy4D* arginine residue in D3X could be targeted in each of the A, B and D homoeologs.

The lack of lateral root phenotypes in any of the lines including the steeper seminal rooting *ZmUbi:qsor1-D* line may show that *qSOR1* functions in seminal root growth angle control but not in lateral roots as in Arabidopsis. There are known lateral root developmental differences between wheat and Arabidopsis as wheat lateral roots originate from pericycle or endodermis cells opposite phloem poles, whereas Arabidopsis laterals emerge from pericycle cells opposite protoxylem cells (Orman-Ligeza et al., 2013). Cereal root types also have differences in development and root type-specific gravitropic pathways, as some cereal root mutants specifically affect lateral root or crown root phenotypes (Zhu et al., 2012, Smith and De Smet, 2012).

This work discovered differences in wheat *LAZY* gene function in root systems with *qSOR1* potentially acting mainly in seminal roots. There was no evidence that *qSOR1* functions in lateral roots, however, the *qSOR1* homoeologs may be important for root growth angle control in different root types. Other *LAZY* family genes also have great potential for generating crop varieties with improved root system architecture. A steeper seminal root angle phenotype could translate into steeper root system architecture, as the growth angles of seminal roots have been found to determine the mature root system angle phenotype in cereals (Nakamoto, 1994, Manschadi et al., 2008). Further investigation in the wheat

LAZY family will enable optimisation of crop root systems, for example, characterisation of *LAZY* gene functions in crown roots and DRO1 homoeolog functions in lateral root growth angle control. The wheat *LAZY* genes are good potential candidates to achieve the 'steep, cheap and deep' ideotype proposed to increase water and nitrogen uptake in drought environments (Lynch, 2013).

Chapter 5

Exploring the functions of the *qSOR1* genes in wheat root system architecture

Chapter 5: Exploring the functions of *qSOR1* genes in wheat root system architecture

5.1 Introduction

Root system architecture (RSA) describes the spatial arrangement of roots within soil, which is important for determining the uptake efficiency of non-uniformly distributed water and nutrients in soil (de Dorlodot et al., 2007). Wheat has a fibrous root system consisting of early forming seminal roots which are later replaced by a network of post-embryonic crown and lateral roots. These root types develop at non-vertical angles which contrasts with the vertical primary taproot system of the dicot Arabidopsis (Smith and De Smet, 2012). As discussed previously, non-vertical roots which include Arabidopsis lateral roots are maintained at specific angles known as gravitropic setpoint angles due to a balance between root gravitropism and an auxin-dependent antigravitropic offset mechanism (Roychoudhry et al., 2023). Wheat seminal roots (Kaye, 2018) and lateral roots (Chapter 3) are also capable of GSA maintenance showing that understanding the molecular basis of GSA maintenance and root gravitropism in wheat is important to be able to modify root system architecture traits.

Root system architecture is thought to have been neglected in comparison to aboveground traits during crop breeding programmes due to the difficulties of root phenotyping, and so there is great potential for optimisation to improve crop performance (Maqbool et al., 2022). However, screening for root system traits in a soil environment is difficult as extracting plants can damage the root system architecture. Seedling phenotyping or growing plants in controlled environmental conditions does not always reflect field conditions, so a combination of strategies is required for accurate root system architecture analysis. The hexaploid wheat cv. Cadenza (*Triticum aestivum*) and the tetraploid wheat cv. Kronos (*Triticum durum*) TILLING (targeted induced local lesions in genomes) populations are valuable genetic resources that can be used to screen for root traits (Krasileva et al., 2017). These populations consist of over 2,500 EMS mutagenized and sequenced wheat lines which can be screened to find beneficial traits and investigate genes of interest (Krasileva et al., 2017). The tetraploid Kronos population is a useful as only one cross is needed to generate a knockout mutant in both genomes whereas the hexaploid Cadenza population requires two

crosses to generate mutations in all three genomes. However, Cadenza lines are more relevant for commercial crop breeding as most wheat grown is hexaploid bread wheat (Krasileva et al., 2017). Each line in these TILLING populations contains a high level of background mutations with an average of 2,705 (Kronos) or 5,351 (Cadenza) mutations so backcrossing is required to reduce the background mutation load and allow comparison of the mutation of interest in equivalent mutation backgrounds (Krasileva et al., 2017). TILLING populations have been used to identify root angle mutants such as the steeper rooting barley *egt2* (*enhanced gravitropism 2*) mutant identified from a mutagenized barley population. *EGT2* was found to control seminal and lateral root growth angle in barley and wheat (Kirschner et al., 2021).

There is potential for root system architecture optimisation to improve crop yields in water scarce or nutrient-limited environments. The "steep, cheap and deep" root system architecture ideotype has been proposed to increase uptake of water and nitrogen soil resources as the roots can access sources deeper underground (Lynch, 2013). Reported advantages of this ideotype include drought avoidance and improved yields in water-limited conditions as shown by rice plants with more vertical and deeper roots due to *DEEPER ROOTING 1* (*DRO1*) overexpression (Uga et al., 2013). Mutations in *qSOR1* (*quantitative trait locus for SOIL SURFACE ROOTING 1*), a homolog of *DRO1*, causes increased soil surface rooting and a shallower root system which shows that *qSOR1* is involved in root growth angle control (Kitomi et al., 2020). Loss-of-function *qsor1* mutants may have improved performance in saline or phosphorus limited growth environments as a shallower root system is predicted to be optimal for these environments (Kitomi et al., 2020).

An early study of root growth angle in wheat found that the gravitropic responses of roots are primarily controlled by genetic factors with influence from the environment (Oyanagi et al., 1993a). The *LAZY* gene family have important roles in gravitropism and are conserved in many plant species (Li et al., 2007, Guseman et al., 2017, Dardick et al., 2013, Yoshihara and Spalding, 2017). Within the *LAZY* family, Arabidopsis *LAZY2* and *LAZY4* are predominantly associated with root gravitropism and *lazy2* and *lazy4* loss-of-function mutants have more horizontal lateral root phenotypes (Yoshihara and Spalding, 2017). There are five conserved domains present in the *LAZY* gene family with domains

II and V documented to be important in *LAZY* function (Dardick et al., 2013, Furutani et al., 2020). A similarity between *AtLAZY2* and *AtLAZY4* is that both genes contain a conserved domain named as extended domain III (D3X) which is important for non-vertical root growth angle control as shown by the steeper lateral rooting Arabidopsis *lazy4D* mutant (Binns, 2022). Translating the *lazy4D* steeper rooting phenotype into cereals could help create the "steep, cheap and deep" ideotype proposed to improve crop yields under drought and low nitrate environmental conditions.

The *LAZY* gene family in wheat has now been identified within this work and more recently (Rasool et al., 2023), but the role of wheat *LAZY* genes in root growth angle control is not yet known. The wheat *qSOR1* homoeologs are the only wheat *LAZY* genes to contain extended domain III which is known to be important in lateral root angle regulation in Arabidopsis. This suggests that the wheat *qSOR1* genes may have roles in wheat root gravitropism and non-vertical root growth angle control. In the previous chapter the *lazy4D* extended domain III mutation was introduced into wheat via transformation, however, no effects of this mutation on lateral root phenotype were observed. The main aim of this chapter was to investigate the functions of *LAZY* extended domain III (D3X) in wheat root growth angle control by screening wheat lines with *TaqSOR1* D3X mutations.

The objectives of this chapter were to:

1. Perform root system architecture phenotyping of wheat TILLING lines with *qSOR1* D3X mutations.
2. Create transformed Arabidopsis lines with mutations introduced from a *qSOR1* extended domain III mutant; Cadenza1761.
3. Generate backcrossed Cadenza1761 BC_2F_2 plants and perform root growth angle analysis.

5.2 Results

5.2.1 Screening wheat TILLING lines with mutations in *LAZY* extended domain III

The Arabidopsis *lazy4D* mutant was identified from an EMS screen and found to have a more vertical lateral root phenotype due to a dominant point mutation within extended domain III (D3X) of *AtLAZY4* (Binns, 2022). To determine whether this steeper rooting trait could be translated into wheat, root system phenotyping was performed of wheat TILLING lines with mutations in D3X of *qSOR1* homoeologs for a number of traits. The *qSOR1* homoeologs are the only wheat *LAZY* genes to contain a fully conserved extended domain III and have high amino acid sequence similarity to Arabidopsis *LAZY2* and *LAZY4,* so the *qSOR1* genes were predicted to have functions in wheat root growth angle control. Two lines with *TaqSOR1* D3X mutations both in the *TaqSOR1-B* homoeolog were found in the Cadenza TILLING population: Cadenza0220 and Cadenza1761.

The Cadenza0220 and Cadenza1761 had substitution mutations located within four amino acids of the original *lazy4D* mutation site. These missense mutations (*E128K*) and (*R132W*) had SIFT scores of 0.01 and 0 respectively which predicted that both mutations affect protein function (Martin et al., 2022). Root system phenotyping of these TILLING lines found that Cadenza0220 had a similar width/depth ratio phenotype to the EMS mutant background cultivar Cadenza. Cadenza1761 had a significantly steeper root system phenotype than Cadenza ($p < 0.0001$) as shown by a lower root system width/depth ratio (Figure 5.1). The Cadenza1761 mutation is caused by a C > T transition base change, a common occurrence in EMS mutagenesis (Lethin et al., 2020), which resulted in a CGG to TGG amino acid codon change. Additionally, the Cadenza1761 mutation was closest to the original *lazy4D* mutation site, so Cadenza1761 was selected for further root system architecture and root growth angle analysis.
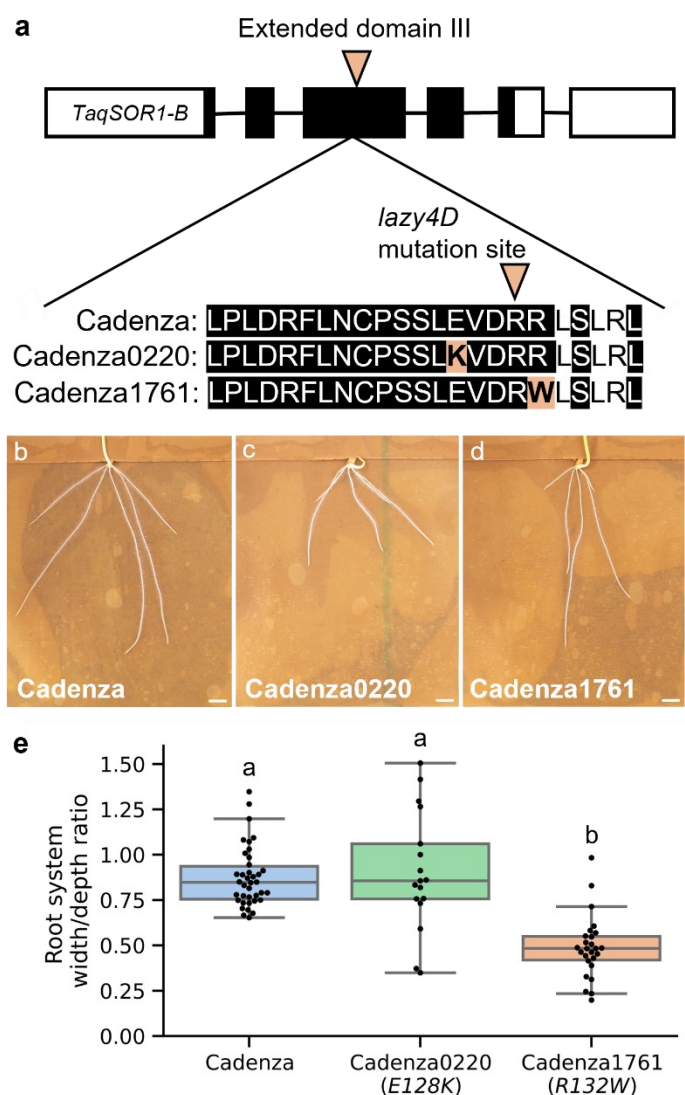
Figure 5.1: Screening wheat TILLING lines with *qSOR1* mutations in extended domain III.

(a) Diagram of *TaqSOR1-B* showing location of extended domain III (D3X) with sequence alignment of Cadenza and EMS TILLING mutants Cadenza0220 and Cadenza1761 with substitution mutations in D3X (*E128K* and *R132W* respectively). (b – d) Example images of (b) Cadenza, (c) Cadenza0220 and (d) Cadenza1761, scale bars = 10 mm. (e) Root system width/depth ratio analysis, n = 17 – 38. Statistical analysis performed with Shapiro-Wilk, Kruskal-Wallis and Dunn's post-hoc tests, *H* = 37.590, *p* = 6.879 x 10^{-9}**.**

A high throughput strategy was developed for genotyping large numbers of plants to screen for the presence of the Cadenza1761 SNP. The KASP (kompetitive allele-specific PCR) assay was initially trialled for the SNP genotyping, however, the two alleles could not be distinguished for the Cadenza1761 *TaqSOR1-B* SNP (Appendix 7.1). This lack of functionality could be due to the high homology between the *qSOR1* homoeolog sequences, particularity within the conserved

domains. The Cadenza1761 *Taqsor1-B* SNP sequence created a BshTI (AgeI) restriction site (Fig. 5.2a) so a restriction digest method could be used for genotyping. A *TaqSOR1-B* DNA fragment was amplified and digested with BshTI, resulting in two bands for Cadenza1761 (Fig. 5.2b, c). Sanger sequencing was used to confirm the reliability of this method (Fig. 5.2d).

Detailed root system architecture and root growth angle analysis of Cadenza1761 was performed, which showed Cadenza1761 had a shorter seminal root length than wildtype Cadenza plants although there were no differences in the number of seminal roots between the lines (Fig. 5.3b, d). The shorter seminal root length resulted in a decrease in overall area covered by the root system, as reflected in the convex hull area (Fig. 5.3c). Non-vertical root gravitropic setpoint angles can become more vertical with age (Mullen and Hangarter, 2003), so root growth angle analysis was performed at the same distance from seminal root emergence to account for any differences in seminal root length. Cadenza1761 had a significantly steeper seminal root phenotype at all intervals analysed (Fig. 5.3a) which supported the initial findings of a lower width/depth ratio and a steeper root system. There were no differences in lateral root growth angle between Cadenza1761 and Cadenza (Fig. 5.3e – g), indicating that *TaqSOR1* may have different functions in seminal and lateral roots.
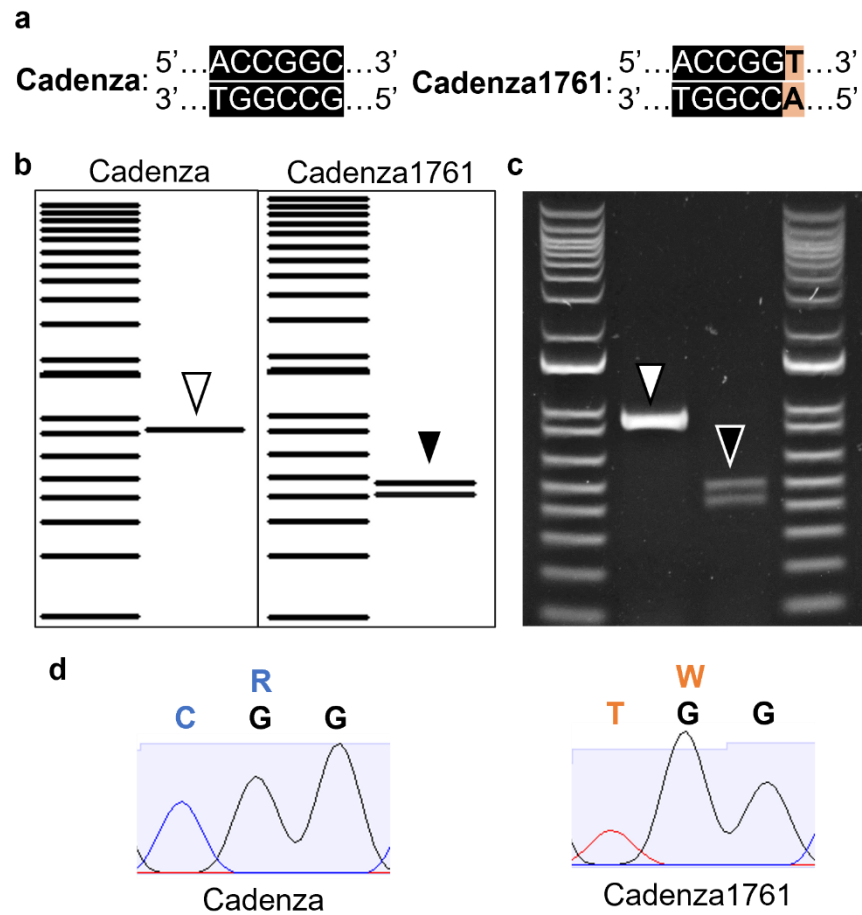
Figure 5.2: Strategies for Cadenza1761 genotyping.

(a) The C > T SNP responsible for the R > W substitution mutation in *TaqSOR1-B* of Cadenza1761 creates a BshTI (AgeI) restriction site that is not present in Cadenza *TaqSOR1-B*. (b) Predicted agarose gel electrophoresis result for an 879 bp amplicon amplified from Cadenza and Cadenza1761 gDNA and digested with BshTI, 1 x 467 bp and 1 x 412 bp fragment present for Cadenza1761. (c) Result of agarose gel electrophoresis of digested Cadenza and Cadenza *TaqSOR1-B* fragments, ladder = ThermoFisher 1kb+ DNA ladder. (d) Confirmation of restriction digest results via Sanger sequencing of the 879 bp *TaqSOR1-B* fragment amplified from Cadenza and Cadenza1761 gDNA, R = arginine, W = tryptophan.
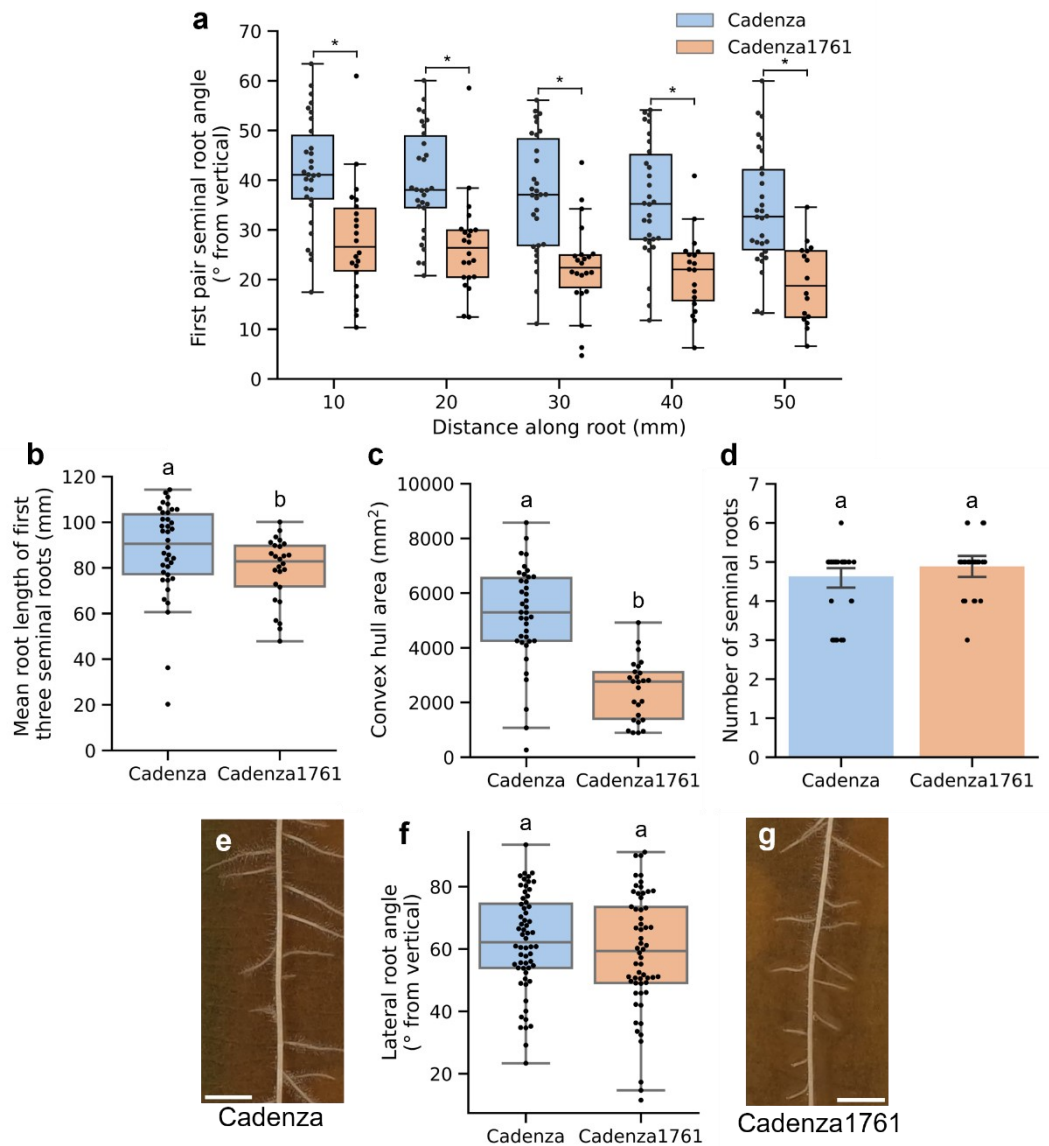
Figure 5.3: Cadenza1761 has a steeper seminal root phenotype.

Plants grown in germination pouches for 5 days (a - d) or 10 days (e - g). (a) Angle analysis of Cadenza and Cadenza1761 at 10 mm intervals along the first pair of seminal roots, * = p < 0.05, n = 16 – 30. (b - d) n = 26 – 38. (b) Mean root length of first three seminal roots, U = 659, p = 0.0245. (c) Convex hull area, t = 6.838, p = 4.103 x 10^{-9}. (d) Number of seminal roots, error bars = 95% confidence interval, U = 429.5, p = 0.286. (f) lateral root angle measured 0.5 – 1 mm from lateral root emergence from seminal root, n = 58 – 60 roots, t = 1.0428, p = 0.309. Example images of (e) Cadenza and (g) Cadenza1761 lateral roots, scale bars = 5 mm. Statistical analysis performed with Shapiro-Wilk and (a, c, f) t-tests or (b, d) Mann-Whitney U tests.

5.2.2 Transforming the Cadenza1761 mutation into Arabidopsis

The Cadenza1761 mutation was introduced into Arabidopsis *LAZY2* (*R144W*) to further confirm if this wheat mutation can influence root growth angle in other species (Fig. 5.4). *LAZY2* was chosen for this experiment as *LAZY2* has columella-specific expression in Arabidopsis and the columella cells are the site of root gravity sensing (Taniguchi et al., 2017). Additionally, previous work found that introducing the *lazy4D* mutation into *LAZY2* gives a more vertical Arabidopsis lateral root phenotype showing that *LAZY2* D3X is involved in root growth angle control (Binns, 2022). The mutation was introduced into Col-0 and a *lazy2* loss-of-function mutant which has a more horizontal lateral root phenotype.
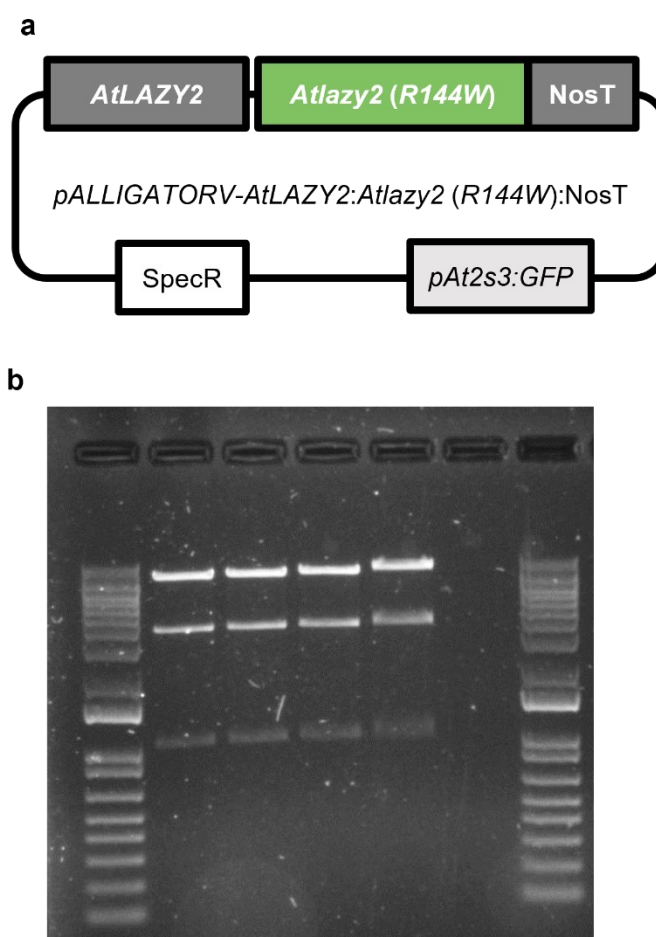
Figure 5.4: Introducing the Cadenza1761 *TaqSOR1-B* mutation into Arabidopsis *LAZY2*.

(a) Construct generated containing the Cadenza1761 mutation (R > W) introduced into *AtLAZY2.1* via site-directed mutagenesis. SpecR = spectinomycin resistance, *pAt2s3:GFP* = seed coat fluorescence reporter. (b) Agarose gel electrophoresis of assembled *lazy2* (*R144W*) construct double digested with PmeI and KpnI restriction enzymes, ladder = ThermoFisher 1kb+ ladder.

The lateral root phenotypes of *lazy2 R144W* were analysed at Stage III (0.5 – 1 mm) and Stage IV (2.5 – 3 mm), along with *lazy2D* (*lazy2 R143A*) and *LAZY2:LAZY2* lateral roots for comparison (Fig. 5.5). The expression of the *lazy2 R144W* construct induced a more vertical lateral root phenotype in both Col-0 and *lazy2* (Fig. 5.5), but was not significantly different from the *lazy2D* steeper lateral root angle phenotype (Binns, 2022). Lateral root growth angle was steeper at Stage IV in both Col-0 and *lazy2* backgrounds (Fig. 5.5f, l). This was expected as non-vertical root growth setpoint angle is known to become more vertical during root development (Mullen and Hangarter, 2003), so older Stage IV roots are likely to be steeper than younger Stage III roots. The *LAZY2:LAZY2* lines had a slightly steeper lateral root angle at Stage III in both Col-0 and *lazy2* backgrounds (Fig. 5.5e, k), which confirms previous studies that found *LAZY* overexpression can increase lateral root verticality (Guseman et al., 2017). *LAZY2:LAZY2* lines did not have significantly steeper lateral root angles compared to the background at Stage IV in both Col-0 and *lazy2* backgrounds (Fig. 5.5f, l).

The results of this experiment show that mutating other residues in extended domain III in addition to the *lazy4D* mutation site can influence lateral root angle. The mutated arginine's in *lazy2D* (*R145*) and *lazy2 R144W* were altered to different amino acids; alanine and tryptophan respectively, which shows that it is the loss of the arginine within D3X rather than the specific substituted residue that is important for *LAZY2* functions in growth angle control. These findings show that the *lazy2 R144W* mutation affects root angle in Arabidopsis and that more than one residue in D3X is essential for the function of this domain in root growth angle control. This supports the hypothesis that the steeper seminal root phenotype of Cadenza1761 is due to the *TaqSOR1-B R144W* mutation.
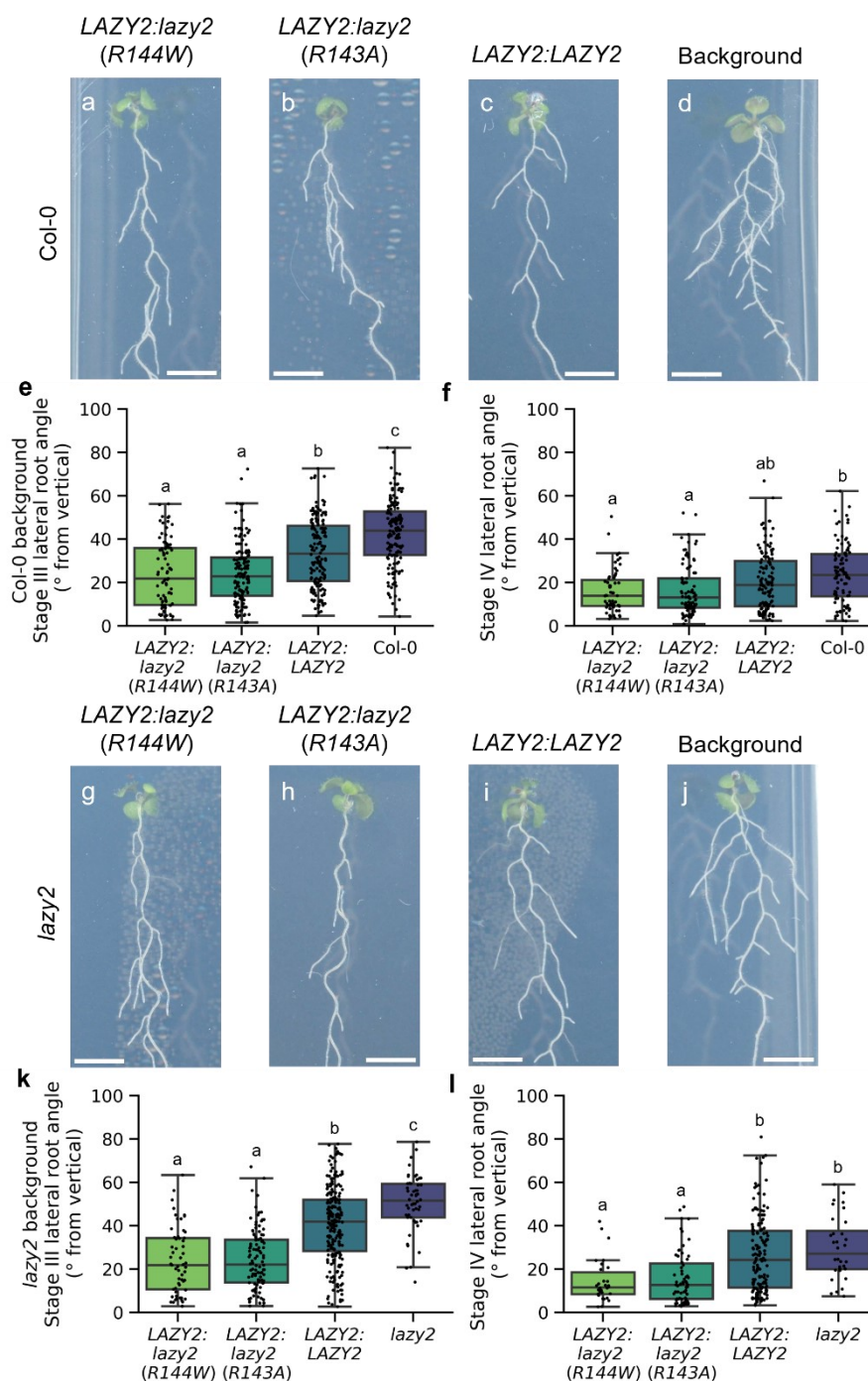
Figure 5.5: The Cadenza1761 *Taqsor1-B* mutation induces a steeper lateral root angle in Arabidopsis.

(a - d, g - j) Representative images of 9-day old Arabidopsis lateral root phenotypes transformed with (a, g) *LAZY2:lazy2* (*R144W*)*,* (b, h) *LAZY2:lazy2* (R143A), (c, i) *LAZY2:LAZY2* with a Col-0 background (a – c) or *lazy2* background (g – i), plants grown to T3. (d) Col-0 and (j) *lazy2* T-DNA insertion mutant used as lines for transformation, scale bars = 5 mm. (e, k) Stage III (0.5 – 1 mm) and (f, l) Stage IV (3.5 – 4 mm) lateral root angle analysis of transformed Arabidopsis lines in a (e, f) Col-0 or (k, l) *lazy2* background, n = 30 – 228 roots. Statistical analysis performed with Shapiro-Wilk, Kruskal-Wallis and Dunn's post-hoc tests. (e) Stage III Col-0; H = 105.660, p = 9.425 x 10^{-23}, (f) Stage IV Col-0 H = 22.017, p = 6.471 x 10^{-5}, (k) Stage III *lazy2*; H = 119.373, p = 1.053 x 10^{-25}, (l) Stage IV *lazy2*; H = 38.772, p = 1.940 x 10^{-8}.

5.2.3 Shoot and root phenotyping of the Cadenza1761 BC$_2$F$_2$ generation

Cadenza1761 backcrossing was performed to confirm that the observed Cadenza1761 root angle phenotypes were not due to background mutations. The Cadenza1761 mutant was backcrossed to Cadenza twice to reduce the background mutation load, and then selfed to generate BC$_2$F$_2$ plants with the Cadenza allele (*R132*) or the Cadenza1761 allele (*R132W*) (Fig. 5.6a). It is recommended to cross TILLING mutants back to the non-mutagenized parent line for at least two generations as the Cadenza TILLING population has an average of 5,351 mutations per line (Krasileva et al., 2017). Backcrossing reduces the level of mutations present and generates lines with and without the mutation of interest for comparison in the same mutation background (Krasileva et al., 2017). From the initial backcrosses, three independent heterozygous BC$_1$F$_1$ plants were identified and further backcrossed to Cadenza (Fig. 5.6b). Five heterozygous BC$_2$F$_1$ lines (Fig. 5.6c) were grown to obtain the BC$_2$F$_2$ generation.
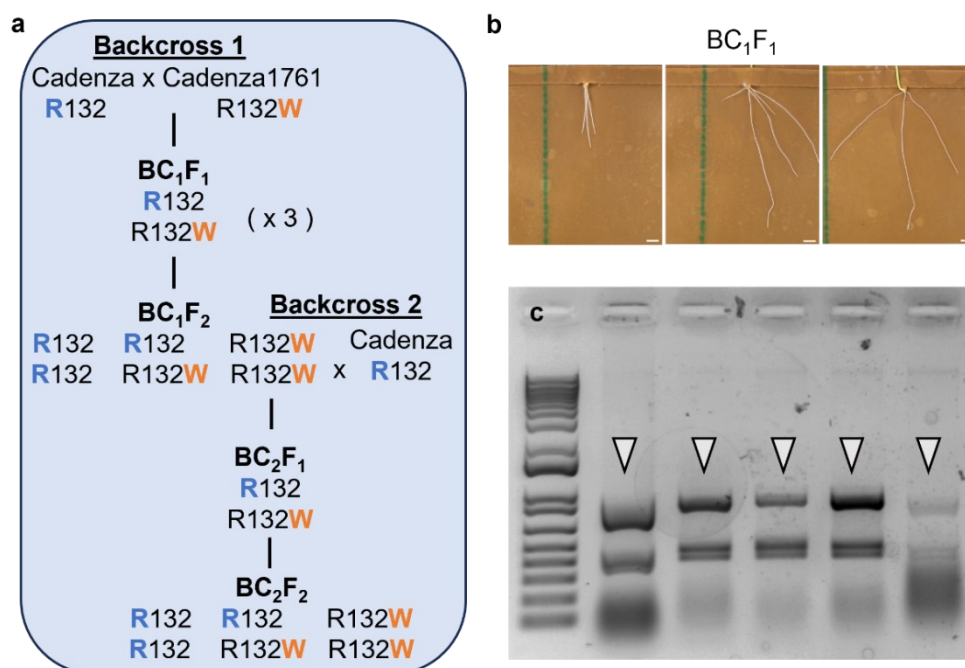
Figure 5.6: Backcrossing scheme to generate Cadenza1761 BC$_2$F$_2$ plants.

(a) Backcross scheme for generating BC$_2$F$_2$ plants, Cadenza 1761 *Taqsor1-B* mutation represented by *R132W*. Three independent BC$_1$F$_1$ backcrosses were selfed to create BC$_1$F$_2$ plants. BC$_1$F$_2$ homozygous *R132W* plants were backcrossed to Cadenza to produce the BC$_2$F$_1$ generation. (b) 5-day images of the root system phenotypes of the three independent BC$_1$F$_1$ backcrosses using in this crossing scheme, scale bars = 10 mm. (c) BshTI restriction digest of the five heterozygous BC$_2$F$_1$ plants selfed to produce BC$_2$F$_2$ plants, grey arrows indicate heterozygous *R132W$^{+/-}$* genotype with three DNA fragments of 412 bp, 467 bp and 879 bp, ladder = ThermoFisher 1 kb+ ladder.

Wheat shoot traits were analysed at 16 weeks to determine if any differing shoot phenotypes were present between the genotypes due to the *Taqsor1-B R132W* mutation or other background mutations. No differences in the number of tillers, tiller height or number of spikelets were seen between Cadenza and Cadenza1761 (Fig. 5.7). In the BC_1F_2 generation, plants containing the *R132W* SNP had shorter tillers and a reduced number of spikelets per spike (Fig. 5.6b, c). This indicates that the *R132W* SNP or other mutations present in Cadenza1761 may influence spikelet number and tiller height, potentially related to the shorter seminal root phenotype seen in Cadenza1761 seedlings (Fig. 5.3b).

Root phenotyping was performed for homozygous *R132*, heterozygous *R132W+/-* and homozygous *R132W* BC_2F_2 plants (Fig. 5.8). Whole root system phenotyping of 5-day old plants revealed the shorter seminal root phenotype in Cadenza1761 was not present in *R132W* plants, and there were no differences in convex hull area between the three BC_2F_2 genotypes (Fig. 5.8f, g). The lines each had a mean of 4 – 5 seminal roots (Fig. 5.8e) which matched the average root numbers seen in Cadenza and Cadenza1761 (Fig. 5.3d). There were no differences in seminal root emergence angle between the genotypes, however, seminal root tip angle was more vertical in *R132W* plants (Fig. 5.8h, i). This shows that the seminal roots initially emerge at the same angle, and then the GSA of BC_2F_2 *R132W* seminal roots may become more vertical at a faster rate than in plants without the *R132W* SNP. The root system width/depth ratio was significantly lower in *R132W* plants compared to *R132* and *R132W^{+/-}* (Fig. 5.8d), which together with the steeper seminal root tip angle results shows that the *R132W* plants have a steeper root system. Finally, root angle analysis was performed to investigate differences in root growth angle in seminal and lateral roots, and in mature plants in compost (Fig. 5.9, 5.10).
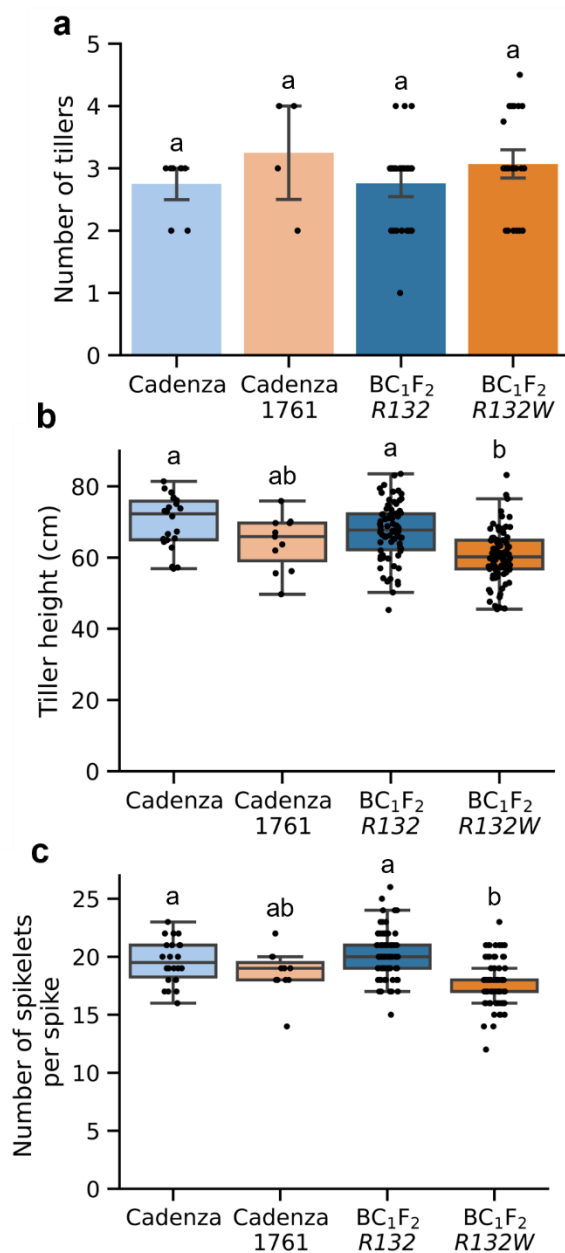
Figure 5.7: Shoot phenotyping of Cadenza, Cadenza1761 and BC$_1$F$_2$ lines.

Shoot measurements of mature wheat plants at 16 weeks. (a) Number of tillers, H = 4.444, p = 0.217, n = 4 – 33 plants per genotype (b) Tiller height, F = 15.113, p = 7.410 x 10^{-9}, n = 11 – 85 tillers (c) Number of spikelets per spike, H = 53.447, p = 1.472 x 10^{-11}, n = 11 – 85 spikes. (a – c) Statistical analysis performed with Shapiro-Wilk, and (b) one-way ANOVA and Tukey's post-hoc tests or (a, c) Kruskal-Wallis and Dunn's post-hoc tests, letters show statistical significance, p < 0.05.
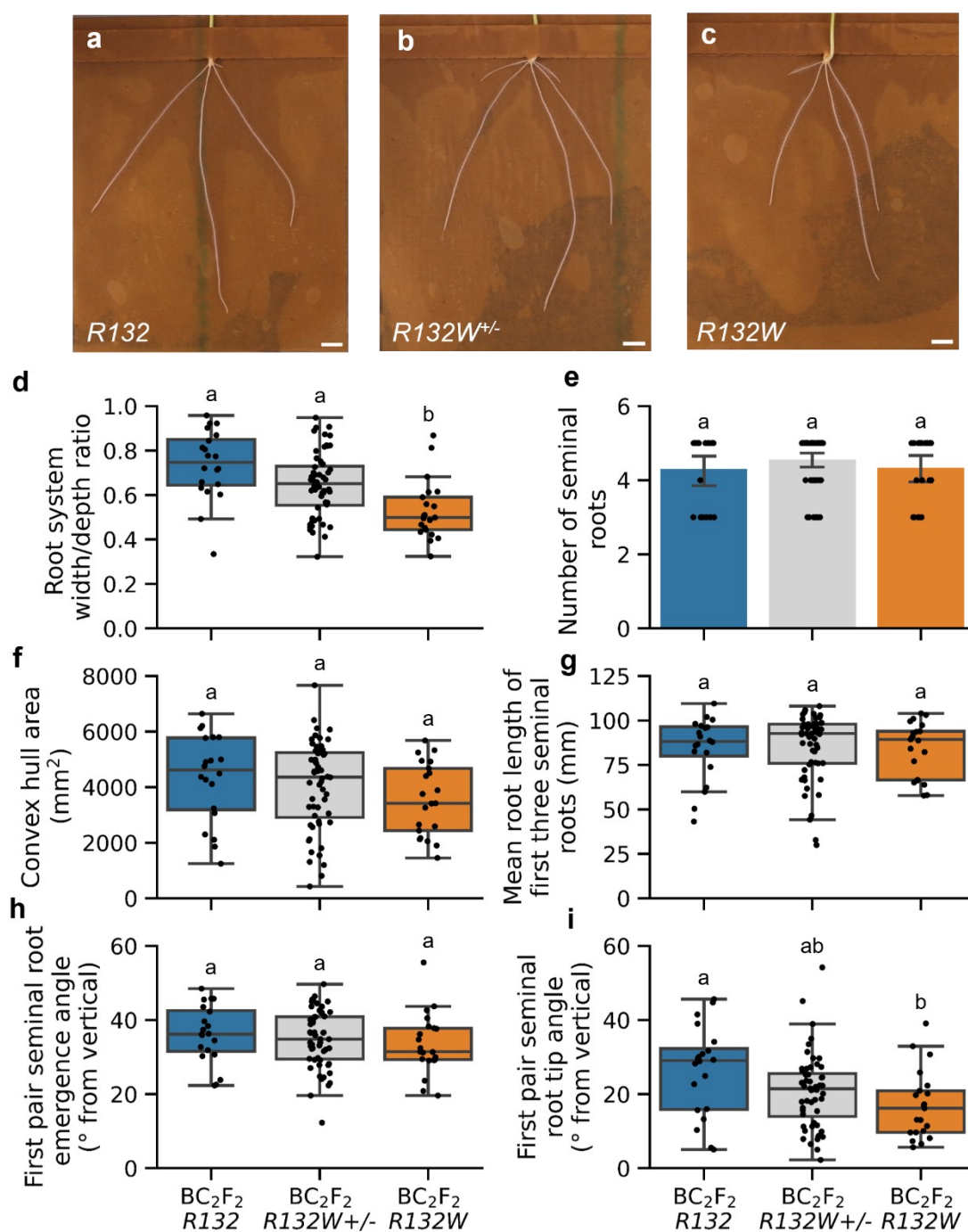
Figure 5.8: Root system architecture analysis of BC$_2$F$_2$ plants.

(a - c) Example images of BC$_2$F$_2$ plants with (a) homozygous *R132*, (b) heterozygous *R132W$^{+/-}$* and (c) homozygous *R132W* alleles in *TaqSOR1-B*, scale bars = 10 mm. (d) Root system width/depth ratio, *F* = 10.526, *p* = 7.497 x 10^{-5} (e) Number of seminal roots, *H* = 1.574, *p* = 0.455, error bars = 95% confidence interval (f) Convex hull area, *F* = 1.432, *p* = 0.244 (g) Mean root length of first three seminal roots, *H* = 0.716, *p* = 0.699 (h) First pair seminal root emergence angle, *F* = 0.580, *p* = 0.562 (i) First pair seminal root tip angle, *H* = 8.734, *p* = 0.0127. Statistical analysis performed with Shapiro-Wilk, one-way ANOVA and Tukey's post-hoc tests (d, f, h) or Kruskal-Wallis and Dunn's post-hoc tests (e, g, i). letters show statistical significance, p < 0.05, n = 20 – 56 plants per genotype.

The BC₂F₂ *R132W* plants had a more vertical seminal root angle than *R132* but no differences in lateral root angle (Fig. 5.9), matching with the seminal and lateral phenotypes seen in Cadenza and Cadenza1761 (Fig. 5.3). The plants heterozygous for the *R132W* allele (*R132W⁺ᐟ⁻*) had an intermediate phenotype between *R132* and *R132W*, consistent with the phenotype being semi-dominant in wheat (Fig. 5.9). No differences were observed in lateral root growth angle between *R132* and *R132W*, which further confirms that this *TaqSOR1-B* mutation does not affect lateral root angles and may indicate that *TaqSOR1* does not have a major function in wheat lateral roots.
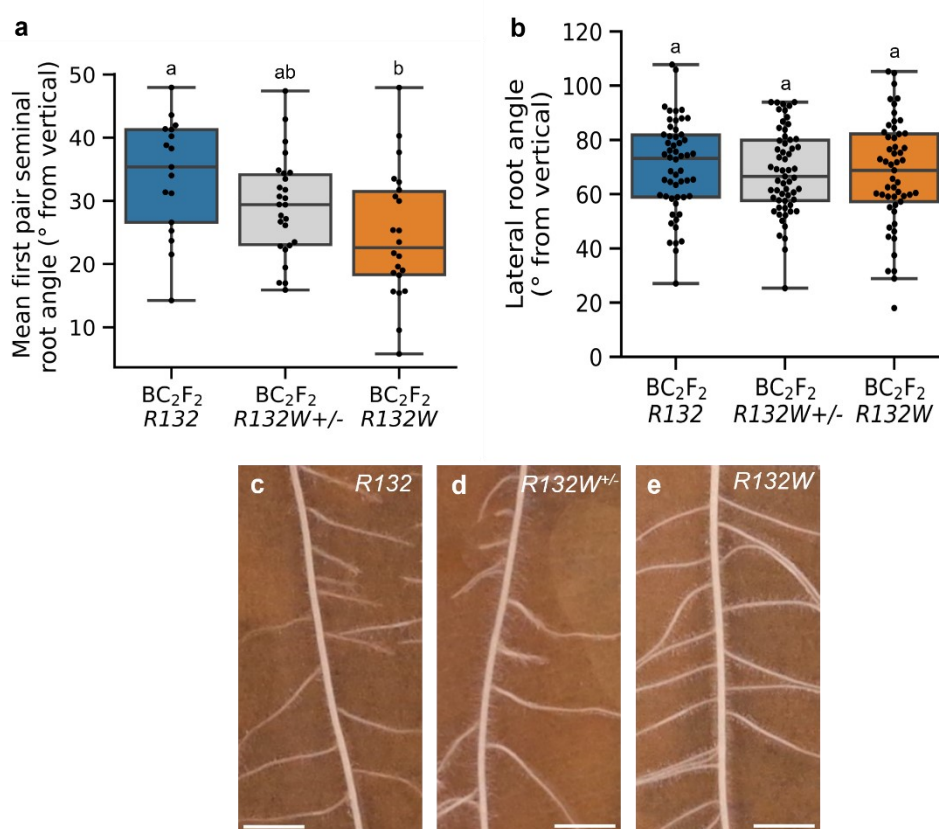
Figure 5.9: Seminal and lateral root angle analysis of BC₂F₂ plants.
(a) Mean first pair seminal root angle analysis, n = 17 – 26 plants, $F = 5.164$, $p = 0.00843$. (b) Lateral root angle measured in degrees from vertical 0.5 – 1 mm from lateral root emergence, n = 53 - 59 lateral roots, $t = 0.305$, $p = 0.737$. (c – e) Example lateral root images of (c) homozygous *R132*, (d) heterozygous *R132W⁺ᐟ⁻* and (e) homozygous *R132W* plants, scale bars = 5 mm.

Wheat seminal root growth angles at the seedling stage have been found to correlate with the architecture of the mature wheat root system (Manschadi et al., 2008, Oyanagi, 1994). Root growth angle of mature wheat root systems can be quantified using soil coring methods in the field (Wasson et al., 2014), but root

system angle analysis is difficult in a controlled growth environment. One pot-based method for root angle analysis involves growing plants in mesh baskets or colanders placed in soil-filled pots, where the angle that roots emerge from the colander holes can be calculated (Uga et al., 2011, Oyanagi et al., 1993b). This method has been successfully used to quantify the effect of the *DRO1* allele on rice root system architecture (Uga et al., 2013). Plants were grown to maturity in colanders within compost-filled pots for root angle analysis to understand whether the steeper root growth angle phenotype at the seedling stage was still present in mature plants (Fig. 5.10). The distribution of roots at different angles down the compost profile was visualised using counts of roots emerging from each layer of colander holes (Fig. 5.10c). The root angle profile was similar in both *R132* and *R132W* plants, although there may be an increased percentage of shallower roots above 50° from vertical in *R132* plants as shown by the non-overlapping 95% confidence interval (Fig. 5.10c).

The deep rooting ratio metric was used to quantify the differences in root growth angle, this metric was originally developed for analysis of rice root growth angle (Uga et al., 2009). The deep rooting ratio has been successfully used to distinguish between shallow and deep rooting rice cultivars (Uga et al., 2013). The deep rooting ratio was calculated by dividing the number of steep roots by the total number of roots, with root angles between 40° and 0° from vertical defined as steep root growth angles based on previous research (Uga et al., 2011, Uga et al., 2013). There was greater variation in deep rooting ratio for *R132* compared to *R132W*, but there was no significant difference between the two genotypes (Fig. 5.10d). This finding indicates that the Cadenza1761 seminal root growth angle trait may not translate into a mature wheat root system phenotype, however, the limited number of plants and uncontrolled soil moisture reduces the reliability of this experiment and repetition of this experiment would be needed to confirm the results.
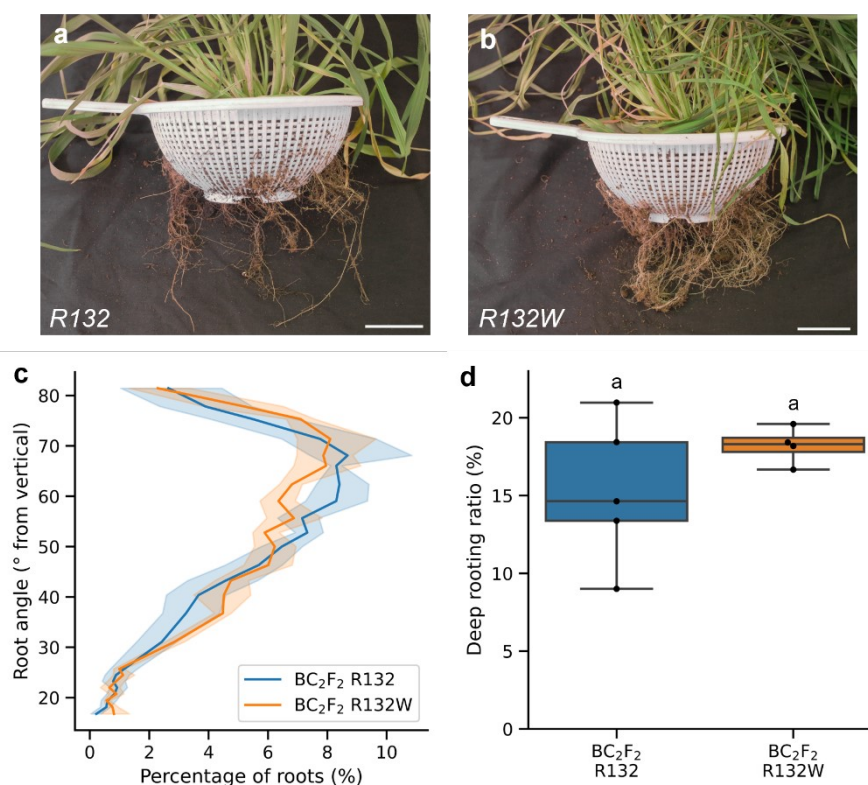
Figure 5.10: Root growth angle characterisation in a compost environment.

(a, b) Example images of BC_2F_2 homozygous *R132* and *R132W* root systems grown in colanders in compost-filled pots, scale bars = 50 mm. (c) Distribution plot of the angle of roots emerging from the colander holes, shading shows the 95% confidence interval. (d) Deep rooting ratio calculated as the number of roots emerging at $0 - 40°$ from vertical divided by the total number of roots, t = 1.483, p = 0.263. Statistical analysis performed with Shapiro-Wilk test and t-test, n = 4 – 5 plants per genotype.

5.3 Discussion

5.3.1 *LAZY* extended domain III mutations in wheat

Wheat TILLING populations are important genetic resources that were used in this work to identify wheat lines with mutations in *LAZY* extended domain III (D3X). The wheat TILLING populations contain an average of 23 – 24 missense mutations or truncations per gene and each line in the Cadenza TILLING population contains an average of 5,351 mutations (Krasileva et al., 2017). Two Cadenza TILLING lines were identified as containing D3X missense mutations, both in the *TaqSOR1-B* homoeolog (Fig. 5.1). *TaqSOR1-B* is one of three *qSOR1* homoeologs in the wheat *LAZY* gene family, which are the only wheat genes to contain extended domain III. Of the two identified mutants, the Cadenza1761 line was selected for further analysis due to the presence of a steeper seminal root phenotype (Fig. 5.3). Cadenza1761 has a *Taqsor1-B R132W* point mutation in the adjacent arginine residue to the *lazy4D* mutation site. The effects of single gene mutations in wheat are often hidden by the functional redundancy of the other gene homoeologs (Uauy et al., 2009). However, the Arabidopsis *lazy4D* D3X mutation is a dominant gain-of-function mutation (Binns, 2022) so there was a possibility that the Cadenza1761 *Taqsor1-B* mutation was also dominant.

D3X is an important *LAZY* gene domain required for lateral root growth angle control in Arabidopsis as shown by the steeper rooting *lazy4D* mutant (Binns, 2022). Cadenza1761 was found to have a steeper seminal root growth angle phenotype at the seedling stage, however, no lateral root phenotype was seen (Fig. 5.3). This is an intriguing result which indicates that the *TaqSOR1* homoeolog D3X is not involved in wheat lateral root angle control even though D3X is required for Arabidopsis lateral root angle regulation and the *qSOR1* homoeologs are expressed in wheat lateral roots. In the previous chapter, the same steeper seminal root and wildtype lateral root phenotype was seen in wheat plants transformed with a high copy number *ZmUbi:qsor1-A* (*R136K*) overexpression line. These findings suggest that wheat seminal and lateral root growth angle regulation may be controlled by different mechanisms with *TaqSOR1* acting in seminal roots.

5.3.2 Translating the Cadenza1761 *LAZY* mutation into Arabidopsis

Arabidopsis LAZY proteins function within the root and shoot gravitropic sensing and response pathways. LAZY proteins have recently been shown to localise on amyloplasts following gravistimulation and relocate to the lower side of the columella cells to trigger auxin redistribution and root differential growth (Chen et al., 2023). Despite these recent insights into the role of LAZY proteins in gravitropism, the functions of *LAZY* domain III and the extended domain III present in *LAZY2* and *LAZY4* are still unknown. The steeper lateral root phenotype of the Arabidopsis *lazy2D* and *lazy4D* mutants shows that *LAZY2* and *LAZY4* extended domain III is required for lateral root angle control (Binns, 2022).

Transforming the Cadenza1761 mutation into Arabidopsis induced a more vertical lateral root phenotype in both Col-0 and *lazy2* (Fig. 5.5), which supports the hypothesis that the *R132W Taqsor1-B* mutation is responsible for the Cadenza1761 steeper seminal root phenotype. The mutation was generated in *AtLAZY2* so the impact of the mutation acting in the columella could be seen, as *LAZY2* has a columella-specific expression pattern whereas *LAZY4* has root wide expression in Arabidopsis (Yoshihara and Spalding, 2017). Mutating the adjacent arginine to the *lazy4D* site increased lateral root verticality which shows that additional residues in *LAZY* domain III are required for *LAZY* function as well as the *lazy4D* site.

5.3.3 Achieving steeper and deeper rooting in mature wheat root systems

The Cadenza1761 seminal root phenotype could not be definitively assigned to the *TaqSOR1-B* missense mutation as the Cadenza TILLING mutants contain an average of 5,351 EMS-type mutations per line (Krasileva et al., 2017). The BC_2F_2 Cadenza1761 x Cadenza *R132* and *R132W* lines generated for phenotypic analysis of the *R132W* SNP allowed the effects of the SNP to be seen in equivalent backgrounds. Highly penetrant traits can be seen when comparing the TILLING line and the parent, however, at least two generations of backcrossing are usually recommended prior to analysis due to the level of background mutations (Krasileva et al., 2017). Root angle analysis in 5-day old plants found that the homozygous *R132W* plants had more vertical seminal roots than homozygous *R132* plants, but no difference between the lateral root angle

phenotypes (Fig. 5.9). The heterozygous *R132W*^{+/-} seminal root angle was not significantly different to either *R132* or *R132W*, so there is a possibility that the mutation is semi-dominant. The wildtype qSOR1-A and qSOR1-D proteins are still present which may reduce seminal root angle verticality and mask the effects of the *R132W* mutation. Introducing the *qsor1 R132W* mutation into a triple knock out *qsor1* wheat mutant would allow the effects of the mutation to be seen without the presence of wildtype *qSOR1*.

A shorter plant height and reduced number of spikelets was seen in *R132W* plants in the BC$_1$F$_2$ generation (Fig. 5.7). *qSOR1* homoeolog expression was not found in wheat shoot tissue, so this phenotype is not thought to be due to the *Taqsor1-B R132W* mutation. The shorter *R132W* tiller height may be explained by additional mutations present in the *R132W* lines. Recently, Cadenza1761 was found to contain a *HB-A2* (*HOMEOBOX DOMAIN*) mutation in an miRNA165/166 binding site and documented as having a paired spikelet phenotype (Dixon et al., 2022) and reduced plant height (Jiang et al., 2023), although root phenotypes were not investigated. Screening the BC$_2$F$_2$ lines for the presence of the *HB-A2 G194R* SNP would confirm whether this mutation may be responsible for the shorter plant height phenotype.

The steeper seminal root and narrower root system traits were still present in the BC$_2$F$_2$ *R132W* plants at 5 days, so these lines were grown in pots within compost-filled colanders to understand whether these traits were maintained in mature root systems. This colander experiment to investigate root system growth angles in mature root systems found no differences between the *R132* and *R132W* lines, although there can be limited conclusions from this due to the low numbers of plants analysed for this experiment (Fig. 5.10). Variation in soil moisture was noted upon recovering the root systems for analysis. Controlling soil moisture would have improved the reliability of this experiment, as hydrotropism can modify root growth in response to a soil water gradient (Dietrich, 2018). A further improvement would be to use more plants, as Uga et al. (2013) analysed the 20 plant root systems of 3 lines whereas this experiment used 1 plant for 5 lines of each genotype. Measuring root growth angles with colanders or mesh baskets has been successfully used for analysis of shallow and deep rooting rice cultivars (Uga et al., 2013), durum wheat (El Hassouni et al., 2018) and winter wheat seedlings (Oyanagi et al., 1993b). The root growth angle of seminal roots in wheat

cultivar seedlings has been shown to have a positive correlation with the vertical root distribution of plants in the field (Oyanagi et al., 1993b) and they proposed that seedling seminal root angle is a useful predictor of later root growth angles. However, other research found that seminal root growth angle did not directly correlate with mature root angles in durum wheat (El Hassouni et al., 2018). Further analysis of *R132W* mature root system angles and *qSOR1* expression in wheat crown roots would help to confirm the hypothesis that seminal and crown root phenotypes are correlated. Base editing to introduce the *R132W* mutation into the wheat *qSOR1* homoeologs would confirm whether this point mutation is responsible for the Cadenza1761 steeper rooting phenotype. Introducing the Cadenza1761 D3X point mutation into Arabidopsis resulted in a more vertical lateral root phenotype, however, lateral root growth angles were not affected in wheat. This indicates that wheat *qSOR1* may not function in lateral root growth angle control and that seminal and lateral roots are potentially regulated via different mechanisms in wheat. The conclusions of this chapter are that the Cadenza1761 *Taqsor1-B R132W* D3X mutation can induce steeper rooting in wheat seminal roots but *qSOR1* may not regulate root growth angle in lateral or crown roots.

Chapter 6

General Discussion

Chapter 6: General Discussion

6.1 Cereal root system architecture

The results of this work demonstrate new discoveries in cereal root system architecture and gravitropism research. In Chapter 3, the diversity and effects of growth medium on root system architecture root traits in wheat were investigated. Growing three wheat varieties in germination paper, agar or compost mediums yielded relative differences in the root angle traits of the three varieties (Fig. 3.2). These experiments have similarities with a previous study which found significant differences in the root length of dwarf wheat cultivars when wheat plants were grown in gel chambers for 10 days, but no differences were seen after 26 days of growth in soil (Wojciechowski et al., 2009, Gregory et al., 2009). Differing environmental influences of the three growth methods could influence the observed root system phenotypes including agar plate exposure to light or heterogeneously distributed soil water and nutrient resources. Root growth is thought to be determined by gravitropism and then adjusted by tropic responses to other environmental factors such as the interaction of hydrotropism and gravitropism (Dietrich, 2018). This work and previous research show the added complication of genotype-environment interactions and highlight the importance of root system phenotyping at a range of growth stages and growth environments for accurate assessment of root system architecture traits.

One proposed pipeline for crop improvement involves phenotyping root growth in agar, followed by hydroponic culture and pot-based soil experiments before selection for field trials (McGrail et al., 2020). This pipeline could be improved with the addition of X-ray computed tomography (X-ray CT) which is a 3D root phenotyping method that allows visualization of soil-grown plant root systems (Atkinson et al., 2019). X-ray CT has been successfully used to image a range of crop species, and may become an important method for future plant phenotyping and crop breeding although it is currently a low throughput method (Mooney et al., 2012, Atkinson et al., 2019).

The root phenotyping of the wheat landrace panel discovered the diversity and range in seedling root system architecture of 285 globally distributed wheat lines (Fig. 3.4). With the knowledge of the effect of growth environment on wheat root system traits, phenotyping of these lines using different growth methods would

allow investigation of phenotype maintenance in a soil environment and the potential usefulness in crop breeding. Integration of landrace root traits into modern cultivars could reintroduce important traits lost during breeding programmes, for example, the root biomass of green revolution wheat cultivars was found to be reduced by two-thirds compared to wheat landraces (Waines and Ehdaie, 2007). A wheat landrace screen for yield performance under drought conditions selected landraces with drought-adaptive traits such as improved deep soil water extraction for incorporation into a drought breeding programme (Reynolds et al., 2006). Plant breeding is thought to indirectly select for advantageous root traits when breeding for high crop yields, however, the beneficial landrace traits lacking in modern cultivars show that direct breeding for root traits is needed (Wasson et al., 2012).

6.2 Gravitropic setpoint angles in cereals

Detailed studies of gravitropic responses and auxin signalling in cereal roots were performed to investigate the processes underlying cereal root system architecture traits. Gravitropic setpoint angle (GSA) is a crucial concept in gravitropism research (Roychoudhry et al., 2013, Digby and Firn, 1995). The results of the cereal GSA reorientation experiments suggest that mechanisms of gravitropic setpoint angle maintenance may have differences between wheat and rice plants. This hypothesis is supported by the horizontal nature of rice lateral roots and slower reorientation responses over 2 days compared to relatively steeper wheat lateral roots which regained their original GSA 12 hours post-reorientation (Fig. 3.9). Lateral roots have important roles in soil resource capture as lateral roots form most of the root length in many plants (Postma et al., 2014). The differences in lateral root GSAs of wheat and rice may reflect adaptation to the different environmental conditions during the growth of these plants.

The lowland rice variety 'Nipponbare' was used for lateral root GSA analysis and lowland varieties are grown with deep water irrigation and are reported to have shallow, thin roots (Song et al., 2020), as was found in this work. Further progress in cereal GSA research could target investigation of lateral root GSA maintenance in an upland rice variety. Upland varieties are typically grown in field conditions comparable to wheat, and so may have a steeper GSA similar to wheat lateral roots (Li et al., 2011). Characterization of lateral root GSA in upland rice varieties

could allow further discoveries in the molecular mechanisms of lateral root GSA within rice and other cereals.

Auxin is known to be important for root growth angle regulation as demonstrated by the identification of *large root angle 1* (*lra1*), a rice shallow root angle mutant with a premature stop codon in rice auxin efflux transporter *OsPIN2* (Wang et al., 2017). Differences in auxin fluxes and polar auxin transport could potentially be the cause of the observed differences in lateral root GSA between wheat and rice. The variation in root gravitropic responses between these two monocots shows the importance of species-specific research for root system architecture optimisation. Future work could investigate post-embryonic crown or nodal root GSA in cereal species as these root types make up a large proportion of the mature root system (Hochholdinger et al., 2004). These experiments would be technically challenging due to the larger scale of the root systems required for analysis; however, it is important not to generalise the embryonic root GSA findings to crown roots as there are likely to be root type differences. For example, a study of maize root water uptake discovered a higher axial conductivity and uptake of water in crown roots compared to seminal roots (Ahmed et al., 2018).

6.3 Progressing auxin research with the wheat DII-VENUS auxin reporter

The wheat DII-VENUS reporter generated is the first known auxin reporter to be developed in wheat and lattice light-sheet imaging of wheat DII-VENUS seminal roots was successfully trialled in this work (Fig. 3.15). Light-sheet fluorescence microscopy is proposed as a useful technology for crop research and investigation of root performance, although imaging large samples such as cereal roots can be difficult (Ovečka et al., 2018). Wheat DII-VENUS was found to have strong signal in root cap and epidermis indicating low levels of auxin in these root tissues and auxin application reduced DII-VENUS expression consistent with Arabidopsis DII-VENUS (Fig. 3.16), showing the functionality of the reporter (Brunoud et al., 2012). However, imaging DII-VENUS fluorescence in the wheat seminal root centre tissues was challenging. This was due to the thickness of the seminal root tissue, although limited DII-VENUS expression may be a contributing factor. The same low fluorescence pattern in the root centre was seen in DII-VENUS and mDII-VENUS wheat lines which rules out the presence

of auxin degrading the DII-VENUS signal in the root centre. Brunoud et al. (2012) suggested that DII-VENUS fluorescence may be impacted in the root epidermis and cortex due to higher activity of the 35S promoter. Lower TIR1/AFB co-receptor expression in the root cap may also cause lower auxin sensitivity and resulting in auxin level underestimation (Brunoud et al., 2012). If these complications also occur in wheat, then this could be one explanation for the high wheat DII-VENUS epidermis and root cap fluorescence. Analysis of maize ubiquitin-1 promoter expression and auxin co-receptor activity in wheat could provide a solution.

A previous study using a DII-VENUS auxin reporter in rice successfully showed lateral root emergence and root tip DII-VENUS signal in outer cell layers, although there was limited signal in the quiescent centre or root vasculature and the reporter was described not to work well in specific root tissues (Yang et al., 2017). Imaging of rice root centres could be achieved with longitudinal sectioning (Yang et al., 2017), which may be a solution to wheat DII-VENUS root imaging although this would not allow for live imaging of auxin distribution. Two-photon or multiphoton microscopy allows deep live tissue imaging at greater depths than can be achieved with confocal microscopy and can be used with ClearSee clearing treatment as was trialled in this work (Kurihara et al., 2015, Mizuta, 2021).

Two-photon microscopy could be an important technique to improve wheat DII-VENUS imaging. DII-VENUS expression may be improved by using an alternative promoter as the maize ubiquitin-1 promoter may have limited expression in root tissues; or by replacing the domain II fragment with a species-specific DII (Yang et al., 2017). The maize ubiquitin-1 promoter has been shown with GUS fusion to have strong constitutive expression in young rice roots and rice lateral roots, but expression did decrease with root age (Cornejo et al., 1993). 3-day old wheat DII-VENUS roots were imaged for the experiments in this work, so theoretically there should have been high DII-VENUS expression levels. However, variability in maize ubiquitin expression between transformed wheat lines has been reported (Rooke et al., 2000), so future wheat auxin reporters could investigate promoter options for optimal constitutive root expression.

Future research into wheat auxin signalling and root gravitropism could involve crossing wheat DII-VENUS with wheat gravitropism mutants such as the wheat lines with *qSOR1* mutations generated in this work, or the *EGT1* and *EGT2* wheat root angle mutants (Kirschner et al., 2021, Fusi et al., 2022). This experiment could show any involvement of these wheat genes in auxin localisation as crossing an Arabidopsis *lazy4* (*dro1*) mutant with DII-VENUS resulted in impairment of polar auxin gradient formation following gravistimulation (Waite et al., 2020). A next step could be to generate R2D2 (ratiometric version of 2 D2s) in wheat which would improve quantitative analysis of auxin distribution. R2D2 consists of DII-VENUS and mDII-ntdTomato fused together to allow direct comparison of DII and mDII signal in the same plant (Liao et al., 2015). Creating a wheat DR5v2 reporter would enable the detection of auxin response and maxima sites, and DR5v2 and R2D2 have even been combined into a single auxin reporter for visualisation of auxin input and output in Arabidopsis (Liao et al., 2015).

6.4 The wheat *LAZY* gene family

The *LAZY* genes in wheat have previously been identified though comparison with rice LAZY gene sequences but not fully characterised (Li et al., 2007, Kitomi et al., 2020). Investigation of the wheat *LAZY* genes in this work has helped further wheat *LAZY* research, and this identification was consistent with the recently published wheat IGT family which included the wheat *LAZY* and *TAC1* genes (Rasool et al., 2023). Similarities between Arabidopsis and wheat *LAZY* expression patterns were discovered in this work with *TaDRO1* and *TaqSOR1* homoeologs expressed in both root and shoot tissues similar to *AtLAZY2* and *AtLAZY4* (Fig. 4.4). Rasool et al. (2023) reported varying *LAZY* expression patterns in root and shoot tissues under drought conditions which did not match the results in this study. One explanation for this inconsistency may be genetic differences between wheat cv. Fielder and the wheat cultivars used by Rasool et al. (2023). Analysis of crown root *LAZY* family expression in wheat would be an important further experiment to perform as crown roots are a large component of cereal root systems (Hochholdinger et al., 2004).

Wheat *LAZY1* homoeologs were shoot expressed (Fig. 4.4), which matched the Arabidopsis *LAZY1* predominantly shoot-specific functions and lack of root

statocyte expression (Taniguchi et al., 2017). An important area of further research for wheat gravitropism would be the functions of wheat *LAZY1*. BREVIS RADIX (BRX) genes have been demonstrated to regulate tiller angle and shoot gravitropism in rice by interacting with LAZY1 at the plasma membrane to facilitate nuclear localisation (Li et al., 2019). BRX-LAZY1 interaction at the plasma membrane also controls shoot gravitropism in Arabidopsis with BRXL4 (BRX-LIKE 4) found to negatively regulate LAZY1 function and promote nuclear accumulation (Che et al., 2023). Studying the interaction of the recently identified wheat BRXL genes (Tiwari et al., 2023) with the *TaLAZY1* homoeologs could lead to new discoveries in wheat gravitropism.

Extended domain III (D3X) was first characterised due to the Arabidopsis *lazy4D* steeper lateral root angle mutant with a dominant gain-of-function point mutation in *AtLAZY4* D3X (Binns, 2022). This work was the first report of the presence of D3X in the three wheat *qSOR1* homoeologs, however, introducing the *lazy4D* mutation into wheat by expressing a mutated *qSOR1-D* construct did not result in a steeper lateral root phenotype, although a high overexpression line had a more vertical seminal root phenotype (Figs. 4.6, 4.8). This was an intriguing finding as D3X is known to be important for lateral root growth angle control in Arabidopsis (Binns, 2022), and the wheat *qSOR1* homoeologs are expressed in lateral root tips. It is possible that higher levels of mutated D3X LAZY protein are required for a steeper root angle phenotype in wheat due to the presence of wildtype homoeologs in the transformed wheat background. This hypothesis could be investigated with genome editing of the wheat *qSOR1* homoeologs to introduce the *lazy4D* mutation.

The identification of wheat TILLING lines with D3X mutations discovered Cadenza1761 (*Taqsor1-B R132W*); a line with a steeper seminal root phenotype but no angle effect in lateral roots (Fig. 5.3). TILLING lines are important genetic resources in wheat research; however, they have limitations due to the high number of mutations present in each line with an average of 5,351 mutations in the Cadenza TILLING population lines (Krasileva et al., 2017). The presence of background mutations is the greatest disadvantage of TILLING populations due to the potential for multiple phenotypic effects (Szurman-Zubrzycka et al., 2023). Recent publications showing that Cadenza1761 contains a *HB-A2* (*HOMEOBOX DOMAIN*) mutation which can cause shoot phenotypes (Dixon et al., 2022, Jiang

et al., 2023). This demonstrates that TILLING phenotypes cannot be definitively assigned to one mutation out of the many mutations present in the background of a line. Two generations of Cadenza1761 backcrossing to allow analysis of the Cadenza1761 *R132W* SNP in equivalent backgrounds (*R132W* or *R132*) saw maintenance of the seminal angle phenotype in plants containing the Cadenza1761 SNP (Fig. 5.9). It was unclear whether this steeper phenotype was present in mature compost grown root systems, partly due to the difficulty in performing root angle analyses with soil-based methods (Fig. 5.10). Specific root growth angle analysis of crown roots and soil phenotyping methods including X-ray CT imaging and field trials would help determine the mature root system phenotype of the backcrossed *Taqsor1-B* (*R132W*) lines.

The *lazy4D* D3X mutation is known to be dominant in Arabidopsis but analysis of the heterozygous *R132W*^{+/-} lines suggested that the mutation is semi-dominant in wheat, although there may be added complexity due to the hexaploid nature of wheat. There were no *qSOR1* D3X mutations identified in the A or D homoeologs so generating lines with mutations in D3X of these homoeologs could allow any additional functions of these homoeologs in root angle maintenance to be seen. The Cadenza1761 D3X mutation did induce a more vertical lateral root phenotype when transformed into Arabidopsis (Fig. 5.5), which supports the hypothesis that the Cadenza1761 D3X SNP could affect root growth angle control and that this SNP is the causal mutation of the steeper seminal root phenotype. Additionally, this experiment showed that another residue in Arabidopsis D3X is crucial for lateral root growth angle control. The *lazy4D* D3X mutation was hypothesised to increase LAZY stability or affinity to statoliths in lateral root gravitropism (Binns, 2022), and this work showed that the adjacent arginine residue to the D3X *lazy4D* site could also be involved.

6.5 Questions arising from this work

6.5.1 What are the roles of the wheat *qSOR1* homoeologs?

The differences in wheat seminal and lateral root phenotypes in plants containing *qSOR1* D3X mutations via transformation or from a TILLING background (Figs. 4.8, 5.9), raises the possibility that wheat lateral and seminal roots are regulated by different control mechanisms. Due to the lack of lateral root angle phenotype seen in *qsor1* transformed or TILLING lines, it could be hypothesised that the

qSOR1 homoeologs do not have roles in lateral root angle regulation. This is despite the finding that *qSOR1* homoeologs are expressed in lateral root tips, as root tip columella cells are known to be the site of gravity sensing and angle control regulation. Alternatively, the level of *qsor1 R132W* expression may not be high enough to induce a steeper lateral root phenotype. Quantitative gene expression analysis of the *qSOR1* homoeologs in these mutated or transformed lines would show whether the mutations were causing differences in gene expression or the level of transformed construct expression. The wheat transformation experiments were performed using the A and D *qSOR1* homoeologs and Cadenza1761 *qSOR1* mutation is situated in the B homoeolog, so it is possible that none of the three *qSOR1* homoeologs function in lateral root growth angle control. There is potential that the wildtype *qSOR1* homoeolog expression in the transformed or TILLING wheat lines would mask the effect of the *lazy4D* mutation as there is known to be a masking effect of redundant homoeologs in single genome knockouts (Krasileva et al., 2017).

The presence of multiple genome copies in hexaploid wheat is a limitation of expressing mutated constructs in a wildtype background, and a solution could be expressing the *qSOR1* D3X mutation in a *qsor1* knock out background. The investigation of D3X in wheat was focussed on in this work to understand the role of D3X in root growth angle control, but generation of a *qsor1* triple knock out line would be an important next step to understand any masked effects of *qSOR1.* Expression of fluorescent protein-tagged LAZYs has been performed in Arabidopsis and would allow visualisation of wheat LAZY protein localisation (Chen et al., 2023). Additionally, generating wheat lines with mutations in the other *LAZY* domains of *qSOR1* would show whether a different domain regulates root growth angle control such as domain V as has been suggested in rice (Kitomi et al., 2020). Recent discoveries are improving crop transformation efficiencies such as expression of GRF4-GIF1 (GROWTH REGULATION FACTOR 4 – GRF-INTERACTING FACTOR 1) found to enhance transformation in cereal species, although the process is still more involved with a longer timeframe than Arabidopsis (Debernardi et al., 2020, Chen et al., 2022b). Performing additional transformation experiments and use of genome editing will help to further research into functions of wheat *qSOR1* genes and the *LAZY* family in root growth angle control and gravitropism.

6.5.2 How is root growth angle controlled in the root types of wheat?

The results of this work suggest that wheat *qSOR1* and extended domain III function in seminal root angle control due to the steeper seminal root phenotype seen in wheat lines with *qSOR1* D3X mutations due to transformation or a TILLING background (Figs. 4.8, 5.9). The lateral root growth angle analysis of these lines revealed that the *qSOR1 R132W* mutation did not impact lateral root growth angle control in wheat. This could be due to the absence of D3X involvement, unlike in Arabidopsis, or increased *R132W* expression might be required to induce a steeper lateral phenotype. Further analysis of crown root growth angle control in wheat would need to be performed to be able to draw any conclusions on *LAZY* regulation of crown roots. These findings lead onto the question of which wheat genes do function in lateral angle regulation. The *TaDRO1* homoeologs were originally discounted as they do not contain a well conserved D3X, however, there is a possibility that this domain is not required for angle control in wheat and so the *DRO1* genes could be candidates for lateral root angle regulation. These wheat *DRO1* homoeologs were originally designated as *TaANDRO1-like*, *TaBNDRO1-like* and *TaDNDRO1-like* (Ashraf et al., 2019) and were later renamed to *TaDRO1* (Kitomi et al., 2020). Characterization of these genes has included identification of AuxRE motifs in the promoter sequences and Domain V shown to interact with the TOPLESS auxin co-repressor (Ashraf et al., 2019).

Wheat *DRO1* functions in root growth angle control have not been investigated, however, evidence that *TaDRO1* is likely to be involved in root angle regulation includes the fact that rice *DRO1* overexpression causes a steeper root system phenotype even though D3X is not conserved in *OsDRO1* (Uga et al., 2013). Additionally, increased expression of *DRO1* orthologs in *Triticum turgidum* has been found to correlate with a steeper seedling root angle (Loarce et al., 2022). Alternatively, a different *LAZY* domain such as Domain V in the *qSOR1* or *DRO1* homoeologs may work in wheat to regulate root growth angle. This shows there are likely to be differences in gene function and root growth angle regulation between Arabidopsis and cereal species. In rice, it has been shown that *qSOR1* and *DRO1* independently control root growth angle and have different roles in root gravitropism, so it is important to understand the functions of each *LAZY* family gene (Kitomi et al., 2020). Investigation of the angle phenotypes of lateral,

seminal and crown roots in complete *dro1* and *qsor1* mutants would give clarity to the functions of these homoeologs in wheat root growth angle control and gravitropism.

6.5.3 What is the potential of the *LAZY* gene family in crop breeding?

Multiple genes are suggested to be involved in the genetic variation of root growth angle (Kitomi et al., 2020) and some genes can control the root angle of several root classes, such as the *EGT1* and *EGT2* genes which control root growth angle in both seminal and lateral roots of barley and durum wheat (Kirschner et al., 2021, Fusi et al., 2022). Genes such as wheat *qSOR1* have great potential as breeding targets, as *LAZY* mutations can be dominant and *LAZY* expression is often restricted to gravity sensing cells and not expressed ubiquitously. Further work will be important to understand whether mutating other amino acid residues within the D3X domain can alter root growth angle for modification of root system architecture. Wheat *qSOR1* variants could be deployed in combination with other genes such as the *EGT* genes, as *OsDRO1* and *OsqSOR1* have been shown to do in rice (Kitomi et al., 2020). Barley *EGT2* was found to regulate genes in the root elongation zone suggesting that *EGT2* is involved in regulation of root gravitropic bending and acts in the gravitropic pathway after gravity perception (Guo et al., 2023). Genes differentially expressed in the *egt2* barley mutant following gravistimulation included downregulation of the *AtLAZY2* and *AtLAZY4* barley orthologs in root cap cells indicating that *EGT* and *LAZY* genes may interact (Guo et al., 2023).

LAZY family genes are proposed to be attractive targets for root architecture optimisation to enable plants to avoid stresses such as drought, salt and flooding (Kitomi et al., 2020). The findings of this work in relation to wheat *LAZY* functions in root growth angle regulation show there is potential for these genes to be used in wheat breeding. It is important to perform wheat *LAZY* research so the *LAZY* discoveries in other species such as the rice *DRO1* and *qSOR1* phenotypes can be trialled in wheat for crop improvement, although it will be crucial to determine that discoveries can be translated between species. The best approach for future wheat *LAZY* gene functional root angle studies may be utilising the complementary approaches of TILLING and gene editing (Szurman-Zubrzycka et al., 2023). An important consideration for crop studies is to ensure phenotypes

are tested in multisite, multiyear field trials with correct planting density and yield analysis (Khaipho-Burch et al., 2023). Interdisciplinary strategies between research and crop breeding are thought to optimise crop research for the needs of plant breeders to produce new cultivars for improved, more resilient crop production (Kusmec et al., 2021). Additionally, incorporating the perspectives and needs of the end users into developing new varieties is important for the generation of adapted varieties suitable for the local environmental conditions and climate challenges (Morris and Bellon, 2004, Colley et al., 2021). These considerations should be implemented if wheat *LAZY* mutant varieties are incorporated into breeding programmes to ensure any root system architecture modifications are truly beneficial for improving crop yields.

6.6 Conclusions

Resilient root system architecture capable of accessing topsoil and deep soil resources is projected to combat the challenges facing global agriculture (Lynch, 2022). Different root ideotypes will be optimal for different environmental conditions and high or low input systems, with steeper and deeper rooting advantageous for water and nitrogen uptake, carbon sequestration and drought avoidance (Lynch, 2013, Lynch, 2022). The cereal lateral root gravitropic setpoint angle work has provided new insights into cereal root gravitropism and highlighted the species-specific differences in root growth angle regulatory mechanisms between Arabidopsis and cereals. The investigation of the wheat *LAZY* family in this project has started to explore the functional significance of *LAZY* genes in wheat, with comparison to Arabidopsis, rice and other crop species (Jiao et al., 2021). This work has raised many further questions such as understanding the differences in gravitropic setpoint angle maintenance between wheat and rice or the root specific functions of wheat *LAZY* genes.

Overall, this work has documented the creation of the first wheat DII-VENUS auxin reporter and discovered that wheat and rice lateral roots can maintain gravitropic setpoint angles. The investigation into the roles of gravitropism and the *LAZY* genes in shaping cereal root system architecture have provided a basis for wheat *qSOR1* research and improved the understanding of cereal root system architecture for future crop development.

Appendix
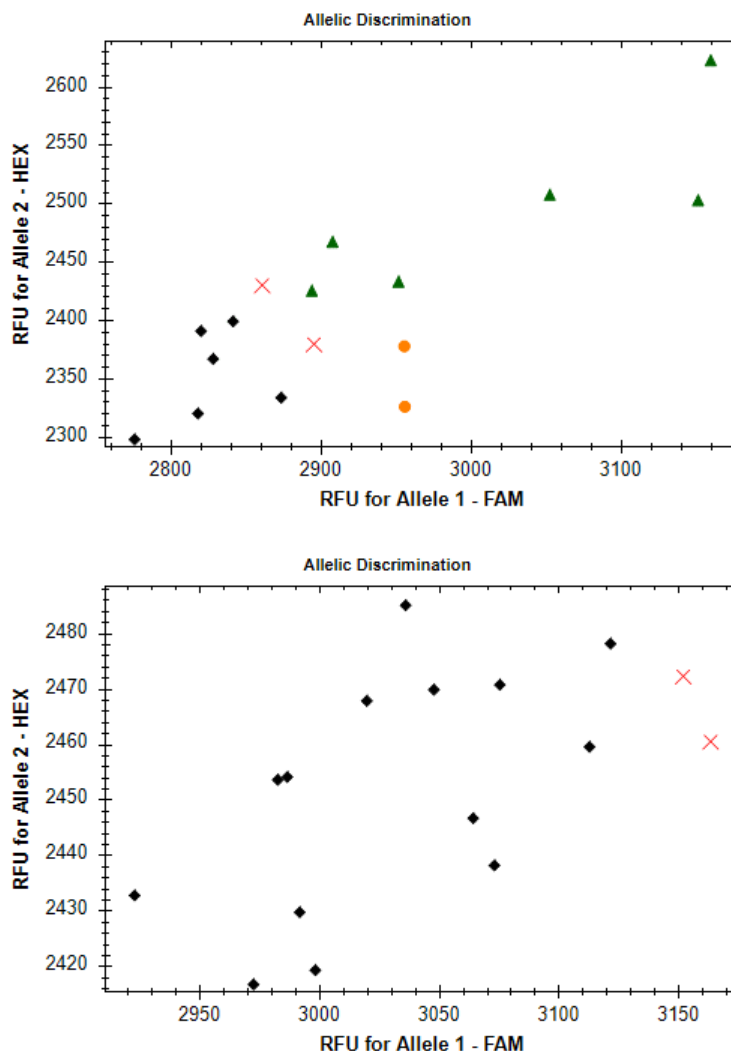
Appendix 1: Example of KASP assay results.

Two examples of kompetitive allele specific PCR (KASP) assay results obtained with PACE Genotyping Master Mix for allele-specific PCR. The assay was used with wheat leaf genomic DNA and should distinguish between the *TaqSOR1-B R132*, *R132W* and heterozygous *R132W^{+/-}* genotypes. The samples did not cluster into separate genotypes, so this method was replaced with restriction digest and Sanger sequencing to determine sample genotypes.
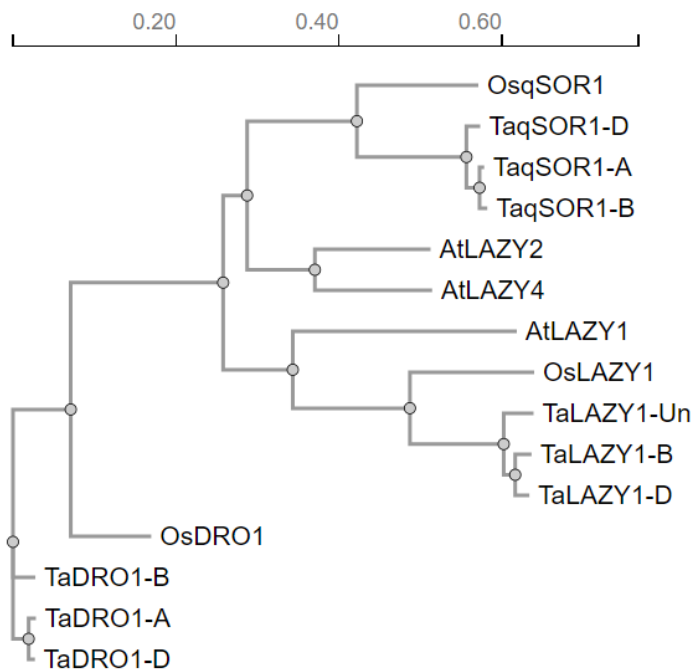
Appendix 2: Phylogenetic tree of Arabidopsis, rice and wheat *LAZY* genes.

Gene IDs and sequences obtained from EnsemblPlants. Arabidopsis = Arabidopsis thaliana 'Col-0', Rice = Oryza sativa ssp. Japonica 'Nipponbare', Wheat = Triticum aestivum 'Chinese Spring'. "Un" = unknown chromosome, diagram created with Clustal Omega Multiple Sequence Alignment tool.

List of References

ADAMOWSKI, M. & FRIML, J. 2015. PIN-Dependent Auxin Transport: Action, Regulation, and Evolution. *The Plant Cell,* 27**,** 20-32.

ADELEKE, E., MILLAS, R., MCNEAL, W., FARIS, J. & TAHERI, A. 2020. Variation Analysis of Root System Development in Wheat Seedlings Using Root Phenotyping System. *Agronomy,* 10**,** 206.

AHMED, M. A., ZAREBANADKOUKI, M., MEUNIER, F., JAVAUX, M., KAESTNER, A. & CARMINATI, A. 2018. Root type matters: measurement of water uptake by seminal, crown, and lateral roots in maize. *Journal of Experimental Botany,* 69**,** 1199-1206.

ALAHMAD, S., EL HASSOUNI, K., BASSI, F. M., DINGLASAN, E., YOUSSEF, C., QUARRY, G., AKSOY, A., MAZZUCOTELLI, E., JUHÁSZ, A., ABLE, J. A., CHRISTOPHER, J., VOSS-FELS, K. P. & HICKEY, L. T. 2019. A Major Root Architecture QTL Responding to Water Limitation in Durum Wheat. *Frontiers in Plant Science,* 10**,** 436.

ASHRAF, A., REHMAN, O. U., MUZAMMIL, S., LÉON, J., NAZ, A. A., RASOOL, F., ALI, G. M., ZAFAR, Y. & KHAN, M. R. 2019. Evolution of *Deeper Rooting 1-like* homoeologs in wheat entails the C-terminus mutations as well as gain and loss of auxin response elements. *PLOS ONE,* 14.

ASSENG, S., FOSTER, I. & TURNER, N. C. 2011. The impact of temperature variability on wheat yields. *Global Change Biology,* 17**,** 997-1012.

ATKINSON, J. A., POUND, M. P., BENNETT, M. J. & WELLS, D. M. 2019. Uncovering the hidden half of plants using new advances in root phenotyping. *Current Opinion in Biotechnology,* 55**,** 1-8.

ATKINSON, J. A., RASMUSSEN, A., TRAINI, R., VOSS, U., STURROCK, C., MOONEY, S. J., WELLS, D. M. & BENNETT, M. J. 2014. Branching Out in Roots: Uncovering Form, Function, and Regulation. *Plant Physiology,* 166**,** 538-550.

BAILEY-SERRES, J., FUKAO, T., RONALD, P., ISMAIL, A., HEUER, S. & MACKILL, D. 2010. Submergence Tolerant Rice: *SUB1*'s Journey from Landrace to Modern Cultivar. *Rice,* 3**,** 138-147.

BAILEY-SERRES, J., PARKER, J. E., AINSWORTH, E. A., OLDROYD, G. E. D. & SCHROEDER, J. I. 2019. Genetic strategies for improving crop yields. *Nature,* 575**,** 109-118.

BALZAN, S., JOHAL, G. S. & CARRARO, N. 2014. The role of auxin transporters in monocots development. *Frontiers in Plant Science,* 5.

BAND, L. R., WELLS, D. M., LARRIEU, A., SUN, J., MIDDLETON, A. M., FRENCH, A. P., BRUNOUD, G., SATO, E. M., WILSON, M. H., PERET, B., OLIVA, M., SWARUP, R., SAIRANEN, I., PARRY, G., LJUNG, K., BEECKMAN, T., GARIBALDI, J. M., ESTELLE, M., OWEN, M. R., VISSENBERG, K., HODGMAN, T. C., PRIDMORE, T. P., KING, J. R., VERNOUX, T. & BENNETT, M. J. 2012. Root gravitropism is regulated by a transient lateral auxin gradient controlled by a tipping-point mechanism. *Proceedings of the National Academy of Sciences,* 109**,** 4668-4673.

BARRATT, L. J., HE, Z., FELLGETT, A., WANG, L., MASON, S. M., BANCROFT, I. & HARPER, A. L. 2023. Co-expression network analysis of diverse wheat landraces reveals markers of early thermotolerance and a candidate master regulator of thermotolerance genes. *The Plant Journal,* 115**,** 614-626.

BENSMIHEN, S., TO, A., LAMBERT, G., KROJ, T., GIRAUDAT, J. & PARCY, F. 2004. Analysis of an activated *ABI5* allele using a new selection method for transgenic *Arabidopsis* seeds. *FEBS Letters,* 561**,** 127-131.

BINNS, A., J. 2022. *The role of LAZY proteins and columella-specific auxin response in root growth angle control.* Doctor of Philosophy, The University of Leeds.

BODEN, S. A., MCINTOSH, R. A., UAUY, C., KRATTINGER, S. G., DUBCOVSKY, J., ROGERS, W. J., XIA, X. C., BADAEVA, E. D., BENTLEY, A. R., BROWN-GUEDIRA, G., CACCAMO, M., CATTIVELLI, L., CHHUNEJA, P., COCKRAM, J., CONTRERAS-MOREIRA, B., DREISIGACKER, S., EDWARDS, D., GONZÁLEZ, F. G., GUZMÁN, C., IKEDA, T. M., KARSAI, I., NASUDA, S., POZNIAK, C., PRINS, R., SEN, T. Z., SILVA, P., SIMKOVA, H., ZHANG, Y. & THE WHEAT, I. 2023. Updated guidelines for gene nomenclature in wheat. *Theoretical and Applied Genetics,* 136**,** 72.

BOONJUNG, H. & FUKAI, S. 1996. Effects of soil water deficit at different growth stages on rice growth and yield under upland conditions. 2. Phenology, biomass production and yield. *Field Crops Research,* 48**,** 47-55.

BRUNNER, S., HURNI, S., HERREN, G., KALININA, O., VON BURG, S., ZELLER, S. L., SCHMID, B., WINZELER, M. & KELLER, B. 2011. Transgenic *Pm3b* wheat lines show resistance to powdery mildew in the field. *Plant Biotechnology Journal,* 9**,** 897-910.

BRUNOUD, G., WELLS, D. M., OLIVA, M., LARRIEU, A., MIRABET, V., BURROW, A. H., BEECKMAN, T., KEPINSKI, S., TRAAS, J., BENNETT, M. J. & VERNOUX, T. 2012. A novel sensor to map auxin response and distribution at high spatio-temporal resolution. *Nature,* 482**,** 103-106.

CAO, R., JIA, X., HUANG, L., ZHU, Y., WU, L. & SHAO, M. A. 2018. Deep soil water storage varies with vegetation type and rainfall amount in the Loess Plateau of China. *Scientific Reports,* 8**,** 12346.

CASAÑAS, F., SIMÓ, J., CASALS, J. & PROHENS, J. 2017. Toward an Evolved Concept of Landrace. *Frontiers in Plant Science,* 8.

CHE, X., SPLITT, B. L., ECKHOLM, M. T., MILLER, N. D. & SPALDING, E. P. 2023. BRXL4-LAZY1 interaction at the plasma membrane controls Arabidopsis branch angle and gravitropism. *The Plant Journal,* 113**,** 211-224.

CHEN, B.-C., LEGANT, W. R., WANG, K., SHAO, L., MILKIE, D. E., DAVIDSON, M. W., JANETOPOULOS, C., WU, X. S., HAMMER, J. A., LIU, Z., ENGLISH, B. P., MIMORI-KIYOSUE, Y., ROMERO, D. P., RITTER, A. T., LIPPINCOTT-SCHWARTZ, J., FRITZ-LAYLIN, L., MULLINS, R. D., MITCHELL, D. M., BEMBENEK, J. N., REYMANN, A.-C., BÖHME, R., GRILL, S. W., WANG, J. T., SEYDOUX, G., TULU, U. S., KIEHART, D. P. & BETZIG, E. 2014. Lattice light-sheet microscopy: Imaging molecules to embryos at high spatiotemporal resolution. *Science,* 346**,** 1257998.

CHEN, J., YU, R., LI, N., DENG, Z., ZHANG, X., ZHAO, Y., QU, C., YUAN, Y., PAN, Z., ZHOU, Y., LI, K., WANG, J., CHEN, Z., WANG, X., WANG, X., HE, S.-N.,

DONG, J., DENG, X. W. & CHEN, H. 2023. Amyloplast sedimentation repolarizes LAZYs to achieve gravity sensing in plants. *Cell,* 186**,** 4788-4802.e15.

CHEN, S., HUANG, Y., HAN, J., ZHANG, S., YANG, Q., LI, Z., ZHANG, Y., MAO, R., FAN, L., LIU, Y., CHEN, Y. & XIE, X. 2022a. Blocking Rice Shoot Gravitropism by Altering One Amino Acid in LAZY1. *International Journal of Molecular Sciences,* 23**,** 9452.

CHEN, Z., DEBERNARDI, J. M., DUBCOVSKY, J. & GALLAVOTTI, A. 2022b. Recent advances in crop transformation technologies. *Nature Plants,* 8**,** 1343-1351.

CHOW, V., KIRZINGER, M. W. & KAGALE, S. 2023. Lend Me Your EARs: A Systematic Review of the Broad Functions of EAR Motif-Containing Transcriptional Repressors in Plants. *Genes,* 14**,** 270.

CLOUGH, S. J. & BENT, A. F. 1998. Floral dip: a simplified method for Agrobacterium-mediated transformation of *Arabidopsis thaliana*. *The Plant Journal,* 16**,** 735-743.

COLLEY, M. R., DAWSON, J. C., MCCLUSKEY, C., MYERS, J. R., TRACY, W. F. & LAMMERTS VAN BUEREN, E. T. 2021. Exploring the emergence of participatory plant breeding in countries of the Global North – a review. *The Journal of Agricultural Science,* 159**,** 320-338.

CORNEJO, M.-J., LUTH, D., BLANKENSHIP, K. M., ANDERSON, O. D. & BLECHL, A. E. 1993. Activity of a maize ubiquitin promoter in transgenic rice. *Plant Molecular Biology,* 23**,** 567-581.

COURTOIS, B., AUDEBERT, A., DARDOU, A., ROQUES, S., GHNEIM- HERRERA, T., DROC, G., FROUIN, J., ROUAN, L., GOZÉ, E., KILIAN, A., AHMADI, N. & DINGKUHN, M. 2013. Genome-Wide Association Mapping of Root Traits in a Japonica Rice Panel. *PLOS ONE,* 8**,** e78037.

CSEH, A., POCZAI, P., KISS, T., BALLA, K., BERKI, Z., HORVÁTH, Á., KUTI, C. & KARSAI, I. 2021. Exploring the legacy of Central European historical winter wheat landraces. *Scientific Reports,* 11**,** 23915.

DAO, T. Q., DRAPEK, C., JONES, A. & LEIBOFF, S. 2023. Comparing hormone dynamics in cereal crops via transient expression of hormone sensors. *bioRxiv***,** 2023.11.14.567063.

DARDICK, C., CALLAHAN, A., HORN, R., RUIZ, K. B., ZHEBENTYAYEVA, T., HOLLENDER, C., WHITAKER, M., ABBOTT, A. & SCORZA, R. 2013. *PpeTAC1* promotes the horizontal growth of branches in peach trees and is a member of a functionally conserved gene family found in diverse plant species. *The Plant Journal,* 75**,** 618-630.

DE DORLODOT, S., FORSTER, B., PAGÈS, L., PRICE, A., TUBEROSA, R. & DRAYE, X. 2007. Root system architecture: opportunities and constraints for genetic improvement of crops. *Trends in Plant Science,* 12**,** 474-481.

DEBERNARDI, J. M., TRICOLI, D. M., ERCOLI, M. F., HAYTA, S., RONALD, P., PALATNIK, J. F. & DUBCOVSKY, J. 2020. A GRF–GIF chimeric protein improves the regeneration efficiency of transgenic plants. *Nature Biotechnology,* 38**,** 1274-1279.

DIETRICH, D. 2018. Hydrotropism: how roots search for water. *Journal of Experimental Botany,* 69**,** 2759-2771.

DIGBY, J. & FIRN, R. D. 1995. The gravitropic set-point angle (GSA): the identification of an important developmentally controlled variable governing plant architecture. *Plant, Cell and Environment,* 18**,** 1434-1440.

DIXON, L. E., PASQUARIELLO, M., BADGAMI, R., LEVIN, K. A., POSCHET, G., NG, P. Q., ORFORD, S., CHAYUT, N., ADAMSKI, N. M., BRINTON, J., SIMMONDS, J., STEUERNAGEL, B., SEARLE, I. R., UAUY, C. & BODEN, S. A. 2022. MicroRNA-resistant alleles of *HOMEOBOX DOMAIN-2* modify inflorescence branching and increase grain protein content of wheat. *Science Advances,* 8**,** eabn5907.

DONG, Z., JIANG, C., CHEN, X., ZHANG, T., DING, L., SONG, W., LUO, H., LAI, J., CHEN, H., LIU, R., ZHANG, X. & JIN, W. 2013. Maize LAZY1 Mediates Shoot Gravitropism and Inflorescence Development through Regulating Auxin Transport, Auxin Signaling, and Light Response. *Plant Physiology,* 163**,** 1306-1322.

DWIVEDI, S. L., CECCARELLI, S., BLAIR, M. W., UPADHYAYA, H. D., ARE, A. K. & ORTIZ, R. 2016. Landrace Germplasm for Improving Yield and Abiotic Stress Adaptation. *Trends in Plant Science,* 21**,** 31-42.

DYACHOK, J., PAEZ-GARCIA, A., YOO, C.-M., PALANICHELVAM, K. & BLANCAFLOR, E. B. 2016. Fluorescence Imaging of the Cytoskeleton in Plant Roots. Springer New York.

EL HASSOUNI, K., ALAHMAD, S., BELKADI, B., FILALI-MALTOUF, A., HICKEY, L. T. & BASSI, F. M. 2018. Root System Architecture and Its Association with Yield under Different Water Regimes in Durum Wheat. *Crop Science,* 58**,** 2331-2346.

EVANS, J. R. & LAWSON, T. 2020. From green to gold: agricultural revolution for food security. *Journal of Experimental Botany,* 71**,** 2211-2215.

FEIKE, D., KOROLEV, A. V., SOUMPOUROU, E., MURAKAMI, E., REID, D., BREAKSPEAR, A., ROGERS, C., RADUTOIU, S., STOUGAARD, J., HARWOOD, W. A. & OLDROYD, G. E. D. 2019. Characterizing standard genetic parts and establishing common principles for engineering legume and cereal roots. *Plant Biotechnology Journal,* 17**,** 2234-2245.

FERNÁNDEZ-GÓMEZ, J., TALLE, B., TIDY, A. C. & WILSON, Z. A. 2020. Accurate staging of reproduction development in Cadenza wheat by non-destructive spike analysis. *Journal of Experimental Botany,* 71**,** 3475-3484.

FIORANI, F. & SCHURR, U. 2013. Future Scenarios for Plant Phenotyping. *Annual Review of Plant Biology,* 64**,** 267-291.

FUKUOKA, S. & OKUNO, K. 2001. QTL analysis and mapping of *pi21*, a recessive gene for field resistance to rice blast in Japanese upland rice. *Theoretical and Applied Genetics,* 103**,** 185-190.

FURUTANI, M., HIRANO, Y., NISHIMURA, T., NAKAMURA, M., TANIGUCHI, M., SUZUKI, K., OSHIDA, R., KONDO, C., SUN, S., KATO, K., FUKAO, Y., HAKOSHIMA, T. & MORITA, M. T. 2020. Polar recruitment of RLD by LAZY1-like protein during gravity signaling in root branch angle control. *Nature Communications,* 11.

FUSI, R., ROSIGNOLI, S., LOU, H., SANGIORGI, G., BOVINA, R., PATTEM, J. K., BORKAR, A. N., LOMBARDI, M., FORESTAN, C., MILNER, S. G., DAVIS, J. L., LALE, A., KIRSCHNER, G. K., SWARUP, R., TASSINARI, A., PANDEY, B. K., YORK, L. M., ATKINSON, B. S., STURROCK, C. J., MOONEY, S. J., HOCHHOLDINGER, F., TUCKER, M. R., HIMMELBACH, A., STEIN, N., MASCHER, M., NAGEL, K. A., DE GARA, L., SIMMONDS, J., UAUY, C., TUBEROSA, R., LYNCH, J. P., YAKUBOV, G. E., BENNETT, M. J., BHOSALE, R. & SALVI, S. 2022. Root angle is controlled by *EGT1* in cereal crops employing an antigravitropic mechanism. *Proceedings of the National Academy of Sciences,* 119**,** e2201350119.

GAMUYAO, R., CHIN, J. H., PARIASCA-TANAKA, J., PESARESI, P., CATAUSAN, S., DALID, C., SLAMET-LOEDIN, I., TECSON-MENDOZA, E. M., WISSUWA, M. & HEUER, S. 2012. The protein kinase Pstol1 from traditional rice confers tolerance of phosphorus deficiency. *Nature,* 488**,** 535-539.

GAO, C. 2021. Genome engineering for crop improvement and future agriculture. *Cell,* 184**,** 1621-1635.

GE, L. & CHEN, R. 2016. Negative gravitropism in plant roots. *Nature Plants,* 2**,** 1-4.

GE, L. & CHEN, R. 2019. Negative gravitropic response of roots directs auxin flow to control root gravitropism. *Plant, Cell & Environment,* 42**,** 2372-2383.

GOMIERO, T., PIMENTEL, D. & PAOLETTI, M. G. 2011. Environmental Impact of Different Agricultural Management Practices: Conventional vs. Organic Agriculture. *Critical Reviews in Plant Sciences,* 30**,** 95-124.

GREGORY, P. J., BENGOUGH, A. G., GRINEV, D., SCHMIDT, S., THOMAS, W. T. B., WOJCIECHOWSKI, T. & YOUNG, I. M. 2009. Root phenomics of crops: opportunities and challenges. *Functional Plant Biology,* 36**,** 922-929.

GUO, L., KLAUS, A., BAER, M., KIRSCHNER, G. K., SALVI, S. & HOCHHOLDINGER, F. 2023. ENHANCED GRAVITROPISM 2 coordinates molecular adaptations to gravistimulation in the elongation zone of barley roots. *New Phytologist,* 237**,** 2196-2209.

GUSEMAN, J. M., WEBB, K., SRINIVASAN, C. & DARDICK, C. 2017. *DRO1* influences root system architecture in Arabidopsis and Prunus species. *The Plant Journal,* 89**,** 1093-1105.

HAGEN, G. & GUILFOYLE, T. 2002. Auxin-responsive gene expression: genes, promoters and regulatory factors. *Plant Molecular Biology,* 49**,** 373-385.

HAYTA, S., SMEDLEY, M. A., CLARKE, M., FORNER, M. & HARWOOD, W. A. 2021. An Efficient Agrobacterium-Mediated Transformation Protocol for Hexaploid and Tetraploid Wheat. *Current Protocols,* 1**,** e58.

HENRY, A.-M., MANICACCI, D., FALQUE, M. & DAMERVAL, C. 2005. Molecular Evolution of the Opaque-2 Gene in Zea mays L. *Journal of Molecular Evolution,* 61**,** 551-558.

HOAGLAND, D. & SNYDER, W. 1933. Nutrition of strawberry plant under controlled conditions: (a) effects of deficiencies of boron and certain other elements, (b) susceptibility to injury from sodium salts. *Proc. Amer Soc. Hort. Sci,* 30.

HOCHHOLDINGER, F., PARK, W. J., SAUER, M. & WOLL, K. 2004. From weeds to crops: genetic analysis of root development in cereals. *Trends in Plant Science,* 9**,** 42-48.

HOLLENDER, C. A., HILL, J. L., WAITE, J. & DARDICK, C. 2020. Opposing influences of TAC1 and LAZY1 on Lateral Shoot Orientation in Arabidopsis. *Scientific Reports,* 10**,** 6051.

HOLME, I. B., GREGERSEN, P. L. & BRINCH-PEDERSEN, H. 2019. Induced Genetic Variation in Crop Plants by Random or Targeted Mutagenesis: Convergence and Differences. *Frontiers in Plant Science,* 10.

HUND, A. 2010. Genetic variation in the gravitropic response of maize roots to low temperatures. *Plant Root,* 4**,** 22-30.

HUNTER, M. C., SMITH, R. G., SCHIPANSKI, M. E., ATWOOD, L. W. & MORTENSEN, D. A. 2017. Agriculture in 2050: Recalibrating Targets for Sustainable Intensification. *BioScience,* 67**,** 386-391.

IINO, M., TARUI, Y. & UEMATSU, C. 1996. Gravitropism of maize and rice coleoptiles: dependence on the stimulation angle. *Plant, Cell & Environment,* 19**,** 1160-1168.

IQUEBAL, M. A., SHARMA, P., JASROTIA, R. S., JAISWAL, S., KAUR, A., SAROHA, M., ANGADI, U. B., SHEORAN, S., SINGH, R., SINGH, G. P., RAI, A., TIWARI, R. & KUMAR, D. 2019. RNAseq analysis reveals drought-responsive molecular pathways with candidate genes and putative molecular markers in root tissue of wheat. *Scientific Reports,* 9**,** 1-8.

IYER-PASCUZZI, A. S., SYMONOVA, O., MILEYKO, Y., HAO, Y., BELCHER, H., HARER, J., WEITZ, J. S. & BENFEY, P. N. 2010. Imaging and Analysis Platform for Automatic Phenotyping and Trait Ranking of Plant Root Systems. *Plant Physiology,* 152**,** 1148-1157.

JEDLIČKOVÁ, V., EBRAHIMI NAGHANI, S. & ROBERT, H. S. 2022. On the trail of auxin: Reporters and sensors. *The Plant Cell,* 34**,** 3200-3213.

JIANG, D., HUA, L., ZHANG, C., LI, H., WANG, Z., LI, J., WANG, G., SONG, R., SHEN, T., LI, H., BAI, S., LIU, Y., WANG, J., LI, H., DUBCOVSKY, J. & CHEN, S. 2023. Mutations in the miRNA165/166 binding site of the *HB2* gene result in pleiotropic effects on morphological traits in wheat. *The Crop Journal,* 11**,** 9-20.

JIAO, Z., DU, H., CHEN, S., HUANG, W. & GE, L. 2021. LAZY Gene Family in Plant Gravitropism. *Frontiers in Plant Science,* 11.

JOBSON, E. M., JOHNSTON, R. E., OIESTAD, A. J., MARTIN, J. M. & GIROUX, M. J. 2019. The Impact of the Wheat *Rht-B1b* Semi-Dwarfing Allele on Photosynthesis and Seed Development Under Field Conditions. *Frontiers in Plant Science,* 10.

JULIN, D. A. 2018. Blue/White Selection. *In:* WELLS, R. D., BOND, J. S., KLINMAN, J. & MASTERS, B. S. S. (eds.) *Molecular Life Sciences: An Encyclopedic Reference.* New York, NY: Springer New York.

KAGALE, S. & ROZWADOWSKI, K. 2011. EAR motif-mediated transcriptional repression in plants. *Epigenetics,* 6**,** 141-146.

KAYE, R. 2018. *The Mechanisms of Gravity-Dependent Non-Vertical Growth in Higher Plants.* Doctor of Philosophy, University of Leeds.

KELL, D. B. 2011. Breeding crop plants with deep roots: their role in sustainable carbon, nutrient and water sequestration. *Annals of Botany,* 108**,** 407-418.

KELL, D. B. 2012. Large-scale sequestration of atmospheric carbon via plant roots in natural and agricultural ecosystems: why and how. *Philosophical Transactions of the Royal Society B: Biological Sciences,* 367**,** 1589-1597.

KEPINSKI, S. & LEYSER, O. 2005. The Arabidopsis F-box protein TIR1 is an auxin receptor. *Nature,* 435**,** 446-451.

KHAIPHO-BURCH, M., COOPER, M., CROSSA, J., DE LEON, N., HOLLAND, J., LEWIS, R., MCCOUCH, S., MURRAY, S. C., RABBI, I. & RONALD, P. 2023. Genetic modification can improve crop yields - but stop overselling it. Nature Publishing Group.

KIRSCHNER, G. K., ROSIGNOLI, S., GUO, L., VARDANEGA, I., IMANI, J., ALTMÜLLER, J., MILNER, S. G., BALZANO, R., NAGEL, K. A., PFLUGFELDER, D., FORESTAN, C., BOVINA, R., KOLLER, R., STÖCKER, T. G., MASCHER, M., SIMMONDS, J., UAUY, C., SCHOOF, H., TUBEROSA, R., SALVI, S. & HOCHHOLDINGER, F. 2021. *ENHANCED GRAVITROPISM 2* encodes a STERILE ALPHA MOTIF-containing protein that controls root growth angle in barley and wheat. *Proceedings of the National Academy of Sciences,* 118**,** e2101526118.

KITOMI, Y., HANZAWA, E., KUYA, N., INOUE, H., HARA, N., KAWAI, S., KANNO, N., ENDO, M., SUGIMOTO, K., YAMAZAKI, T., SAKAMOTO, S., SENTOKU, N., WU, J., KANNO, H., MITSUDA, N., TORIYAMA, K., SATO, T. & UGA, Y. 2020. Root angle modifications by the *DRO1* homolog improve rice yields in saline paddy fields. *Proceedings of the National Academy of Sciences,* 117**,** 21242-21250.

KLEINE-VEHN, J., DING, Z., JONES, A. R., TASAKA, M., MORITA, M. T. & FRIML, J. 2010. Gravity-induced PIN transcytosis for polarization of auxin fluxes in gravity-sensing root cells. *Proceedings of the National Academy of Sciences,* 107**,** 22344-22349.

KRASILEVA, K. V., VASQUEZ-GROSS, H. A., HOWELL, T., BAILEY, P., PARAISO, F., CLISSOLD, L., SIMMONDS, J., RAMIREZ-GONZALEZ, R. H., WANG, X., BORRILL, P., FOSKER, C., AYLING, S., PHILLIPS, A. L., UAUY, C. & DUBCOVSKY, J. 2017. Uncovering hidden variation in polyploid wheat. *Proceedings of the National Academy of Sciences,* 114**,** E913-E921.

KURIHARA, D., MIZUTA, Y., SATO, Y. & HIGASHIYAMA, T. 2015. ClearSee: a rapid optical clearing reagent for whole-plant fluorescence imaging. *Development,* 142**,** 4168-4179.

KUROWSKA, M., DASZKOWSKA-GOLEC, A., GRUSZKA, D., MARZEC, M., SZURMAN, M., SZAREJKO, I. & MALUSZYNSKI, M. 2011. TILLING - a shortcut in functional genomics. *Journal of Applied Genetics,* 52**,** 371-390.

KUSMEC, A., ZHENG, Z., ARCHONTOULIS, S., GANAPATHYSUBRAMANIAN, B., HU, G., WANG, L., YU, J. & SCHNABLE, P. S. 2021. Interdisciplinary strategies to enable data-driven plant breeding in a changing climate. *One Earth,* 4**,** 372-383.

LESK, C., ROWHANI, P. & RAMANKUTTY, N. 2016. Influence of extreme weather disasters on global crop production. *Nature,* 529**,** 84-87.

LETHIN, J., SHAKIL, S. S. M., HASSAN, S., SIRIJOVSKI, N., TÖPEL, M., OLSSON, O. & ARONSSON, H. 2020. Development and characterization of an EMS-mutagenized wheat population and identification of salt-tolerant wheat lines. *BMC Plant Biology,* 20**,** 18.

LI, J., WANG, D., XIE, Y., ZHANG, H., HU, G., LI, J., DAI, A., LIU, L. & LI, Z. 2011. Development of upland rice introgression lines and identification of QTLs for basal root thickness under different water regimes. *Journal of Genetics and Genomics,* 38**,** 547-556.

LI, P., WANG, Y., QIAN, Q., FU, Z., WANG, M., ZENG, D., LI, B., WANG, X. & LI, J. 2007. LAZY1 controls rice shoot gravitropism through regulating polar auxin transport. *Cell Research,* 17**,** 402-410.

LI, X., ZENG, R. & LIAO, H. 2016. Improving crop nutrient efficiency through root architecture modifications. *Journal of Integrative Plant Biology,* 58**,** 193-202.

LI, Z., LIANG, Y., YUAN, Y., WANG, L., MENG, X., XIONG, G., ZHOU, J., CAI, Y., HAN, N., HUA, L., LIU, G., LI, J. & WANG, Y. 2019. OsBRXL4 Regulates Shoot Gravitropism and Rice Tiller Angle through Affecting LAZY1 Nuclear Localization. *Molecular Plant,* 12**,** 1143-1156.

LIAO, C.-Y., SMET, W., BRUNOUD, G., YOSHIDA, S., VERNOUX, T. & WEIJERS, D. 2015. Reporters for sensitive and quantitative measurement of auxin response. *Nature Methods,* 12**,** 207-210.

LIN, Q., ZONG, Y., XUE, C., WANG, S., JIN, S., ZHU, Z., WANG, Y., ANZALONE, A. V., RAGURAM, A., DOMAN, J. L., LIU, D. R. & GAO, C. 2020. Prime genome editing in rice and wheat. *Nature Biotechnology,* 38**,** 582-585.

LOARCE, Y., CABEZA, A., CAÑAS, R. & GONZÁLEZ, J. M. 2022. Isolation and Molecular Characterisation of *TtDro1A* and *TtDro1B* Genes from *Triticum turgidum* Subspecies *durum* and *turgidum*, Study of Their Influences on Seedling Root Angles. *Plants,* 11**,** 821.

LOBELL, D. B. & GOURDJI, S. M. 2012. The Influence of Climate Change on Global Crop Productivity. *Plant Physiology,* 160**,** 1686-1697.

LOBET, G., DRAYE, X. & PÉRILLEUX, C. 2013. An online database for plant image analysis software tools. *Plant Methods,* 9**,** 38.

LOBET, G., KOEVOETS, I. T., NOLL, M., MEYER, P. E., TOCQUIN, P., PAGÈS, L. & PÉRILLEUX, C. 2017. Using a Structural Root System Model to Evaluate and Improve the Accuracy of Root Image Analysis Pipelines. *Frontiers in Plant Science,* 8.

LOBET, G., POUND, M. P., DIENER, J., PRADAL, C., DRAYE, X., GODIN, C., JAVAUX, M., LEITNER, D., MEUNIER, F., NACRY, P., PRIDMORE, T. P. & SCHNEPF, A. 2015. Root System Markup Language: Toward a Unified Root Architecture Description Language. *Plant Physiology,* 167**,** 617-627.

LÓPEZ-ARREDONDO, D. L., LEYVA-GONZÁLEZ, M. A., GONZÁLEZ-MORALES, S. I., LÓPEZ-BUCIO, J. & HERRERA-ESTRELLA, L. 2014. Phosphate Nutrition:

Improving Low-Phosphate Tolerance in Crops. *Annual Review of Plant Biology,* 65**,** 95-123.

LUO, L., XIA, H. & LU, B.-R. 2019. Editorial: Crop Breeding for Drought Resistance. *Frontiers in Plant Science,* 10.

LYNCH, J. P. 2007. Roots of the Second Green Revolution. *Australian Journal of Botany,* 55**,** 493-512.

LYNCH, J. P. 2013. Steep, cheap and deep: an ideotype to optimize water and N acquisition by maize root systems. *Annals of Botany,* 112**,** 347-357.

LYNCH, J. P. 2022. Harnessing root architecture to address global challenges. *The Plant Journal,* 109**,** 415-431.

MANCUSO, S., BARLOW, P. W., VOLKMANN, D. & BALUŠKA, F. 2006. Actin Turnover-Mediated Gravity Response in Maize Root Apices. *Plant Signaling & Behavior,* 1**,** 52-58.

MANSCHADI, A. M., CHRISTOPHER, J. T., HAMMER, G. L. & DEVOIL, P. 2010. Experimental and modelling studies of drought-adaptive root architectural traits in wheat (*Triticum aestivum* L.). *Plant Biosystems - An International Journal Dealing with all Aspects of Plant Biology,* 144**,** 458-462.

MANSCHADI, A. M., HAMMER, G. L., CHRISTOPHER, J. T. & DEVOIL, P. 2008. Genotypic variation in seedling root architectural traits and implications for drought adaptation in wheat (*Triticum aestivum* L.). *Plant and Soil,* 303**,** 115-129.

MAQBOOL, S., HASSAN, M. A., XIA, X., YORK, L. M., RASHEED, A. & HE, Z. 2022. Root system architecture in cereals: progress, challenges and perspective. *The Plant Journal,* 110**,** 23-42.

MARASCHIN, F. S., MEMELINK, J. & OFFRINGA, R. 2009. Auxin-induced, SCF TIR1-mediated poly-ubiquitination marks AUX/IAA proteins for degradation. *The Plant Journal,* 59**,** 100-109.

MARTIN, F. J., AMODE, M. R., ANEJA, A., AUSTINE-ORIMOLOYE, O., AZOV, ANDREY G., BARNES, I., BECKER, A., BENNETT, R., BERRY, A., BHAI, J., BHURJI, SIMARPREET K., BIGNELL, A., BODDU, S., BRANCO LINS, P. R., BROOKS, L., RAMARAJU, S. B., CHARKHCHI, M., COCKBURN, A., DA RIN FIORRETTO, L., DAVIDSON, C., DODIYA, K., DONALDSON, S., EL HOUDAIGUI, B., EL NABOULSI, T., FATIMA, R., GIRON, C. G., GENEZ, T., GHATTAORAYA, G. S., MARTINEZ, J. G., GUIJARRO, C., HARDY, M., HOLLIS, Z., HOURLIER, T., HUNT, T., KAY, M., KAYKALA, V., LE, T., LEMOS, D., MARQUES-COELHO, D., MARUGÁN, J. C., MERINO, GABRIELA A., MIRABUENO, LOUISSE P., MUSHTAQ, A., HOSSAIN, SYED N., OGEH, D. N., SAKTHIVEL, M. P., PARKER, A., PERRY, M., PILIŽOTA, I., PROSOVETSKAIA, I., PÉREZ-SILVA, J. G., SALAM, AHAMED IMRAN A., SARAIVA-AGOSTINHO, N., SCHUILENBURG, H., SHEPPARD, D., SINHA, S., SIPOS, B., STARK, W., STEED, E., SUKUMARAN, R., SUMATHIPALA, D., SUNER, M.-M., SURAPANENI, L., SUTINEN, K., SZPAK, M., TRICOMI, FRANCESCA F., URBINA-GÓMEZ, D., VEIDENBERG, A., WALSH, THOMAS A., WALTS, B., WASS, E., WILLHOFT, N., ALLEN, J., ALVAREZ-JARRETA, J., CHAKIACHVILI, M., FLINT, B., GIORGETTI, S., HAGGERTY, L., ILSLEY, GARTH R., LOVELAND, JANE E., MOORE, B., MUDGE,

JONATHAN M., TATE, J., THYBERT, D., TREVANION, STEPHEN J., WINTERBOTTOM, A., FRANKISH, A., HUNT, S. E., RUFFIER, M., CUNNINGHAM, F., DYER, S., FINN, ROBERT D., HOWE, KEVIN L., HARRISON, P. W., YATES, A. D. & FLICEK, P. 2022. Ensembl 2023. *Nucleic Acids Research,* 51**,** D933-D941.

MATHEW, I. & SHIMELIS, H. 2022. Genetic analyses of root traits: Implications for environmental adaptation and new variety development: A review. *Plant Breeding,* 141**,** 695-718.

MCGRAIL, R. K., VAN SANFORD, D. A. & MCNEAR, D. H. 2020. Trait-Based Root Phenotyping as a Necessary Tool for Crop Selection and Improvement. *Agronomy,* 10**,** 1328.

MELLOR, N. L., VOß, U., JANES, G., BENNETT, M. J., WELLS, D. M. & BAND, L. R. 2020. Auxin fluxes through plasmodesmata modify root-tip auxin distribution. *Development,* 147.

MIEOG, J. C., HOWITT, C. A. & RAL, J.-P. 2013. Fast-tracking development of homozygous transgenic cereal lines using a simple and highly flexible real-time PCR assay. *BMC Plant Biology,* 13**,** 71.

MIGUEL, M. A., POSTMA, J. A. & LYNCH, J. P. 2015. Phene Synergism between Root Hair Length and Basal Root Growth Angle for Phosphorus Acquisition. *Plant Physiology,* 167**,** 1430-1439.

MILANI, P., TORRES-AGUILAR, P., HAMAKER, B., MANARY, M., ABUSHAMMA, S., LAAR, A., STEINER, R., EHSANI, M., DE LA PARRA, J., SKAVEN-RUBEN, D., DE KOCK, H., HAWKES, C., COVIC, N., MITCHELL, C. & TAYLOR, J. 2022. The whole grain manifesto: From Green Revolution to Grain Evolution. *Global Food Security,* 34**,** 100649.

MIR, R., ARANDA, L. Z., BIAOCCHI, T., LUO, A., SYLVESTER, A. W. & RASMUSSEN, C. G. 2017. A DII Domain-Based Auxin Reporter Uncovers Low Auxin Signaling during Telophase and Early G1. *Plant Physiology,* 173**,** 863-871.

MIZUTA, Y. 2021. Advances in Two-Photon Imaging in Plants. *Plant and Cell Physiology,* 62**,** 1224-1230.

MOCKAITIS, K. & ESTELLE, M. 2008. Auxin Receptors and Plant Development: A New Signaling Paradigm. *Annual Review of Cell and Developmental Biology,* 24**,** 55-80.

MOLLA, K. A., SRETENOVIC, S., BANSAL, K. C. & QI, Y. 2021. Precise plant genome editing using base editors and prime editors. *Nature Plants,* 7**,** 1166-1187.

MOONEY, S. J., PRIDMORE, T. P., HELLIWELL, J. & BENNETT, M. J. 2012. Developing X-ray Computed Tomography to non-invasively image 3-D root systems architecture in soil. *Plant and Soil,* 352**,** 1-22.

MORRIS, E. C., GRIFFITHS, M., GOLEBIOWSKA, A., MAIRHOFER, S., BURR-HERSEY, J., GOH, T., VON WANGENHEIM, D., ATKINSON, B., STURROCK, C. J. & LYNCH, J. P. 2017. Shaping 3D root system architecture. *Current Biology,* 27**,** R919-R930.

MORRIS, M. L. & BELLON, M. R. 2004. Participatory plant breeding research: Opportunities and challenges for the international crop improvement system. *Euphytica,* 136**,** 21-35.

MULLEN, J. L. & HANGARTER, R. P. 2003. Genetic analysis of the gravitropic set-point angle in lateral roots of Arabidopsis. *Advances in Space Research,* 31**,** 2229-2236.

NAKAMOTO, T. 1994. The Direction of Growth of Seminal Roots of *Triticum aestivum* L. and Experimental Modification Thereof. *Annals of Botany,* 73**,** 363-367.

NAKAMURA, M., NISHIMURA, T. & MORITA, M. T. 2019. Gravity sensing and signal conversion in plant gravitropism. *Journal of Experimental Botany,* 70**,** 3495-3506.

NERKAR, G., DEVARUMATH, S., PURANKAR, M., KUMAR, A., VALARMATHI, R., DEVARUMATH, R. & APPUNU, C. 2022. Advances in Crop Breeding Through Precision Genome Editing. *Frontiers in Genetics,* 13.

NEWTON, A. C., AKAR, T., BARESEL, J. P., BEBELI, P. J., BETTENCOURT, E., BLADENOPOULOS, K. V., CZEMBOR, J. H., FASOULA, D. A., KATSIOTIS, A., KOUTIS, K., KOUTSIKA-SOTIRIOU, M., KOVACS, G., LARSSON, H., DE CARVALHO, M. A. A. P., RUBIALES, D., RUSSELL, J., SANTOS, T. M. M. D. & PATTO, M. C. V. 2011. Cereal Landraces for Sustainable Agriculture. *In:* LICHTFOUSE, E., HAMELIN, M., NAVARRETE, M. & DEBAEKE, P. (eds.) *Sustainable Agriculture Volume 2.* Dordrecht: Springer Netherlands.

NISHIMURA, T., MORI, S., SHIKATA, H., NAKAMURA, M., HASHIGUCHI, Y., ABE, Y., HAGIHARA, T., YOSHIKAWA, H. Y., TOYOTA, M., HIGAKI, T. & MORITA, M. T. 2023. Cell polarity linked to gravity sensing is generated by LZY translocation from statoliths to the plasma membrane. *Science,* 381**,** 1006-1010.

OBER, E. S., ALAHMAD, S., COCKRAM, J., FORESTAN, C., HICKEY, L. T., KANT, J., MACCAFERRI, M., MARR, E., MILNER, M., PINTO, F., RAMBLA, C., REYNOLDS, M., SALVI, S., SCIARA, G., SNOWDON, R. J., THOMELIN, P., TUBEROSA, R., UAUY, C., VOSS-FELS, K. P., WALLINGTON, E. & WATT, M. 2021. Wheat root systems as a breeding target for climate resilience. *Theoretical and Applied Genetics,* 134**,** 1645-1662.

ORMAN-LIGEZA, B., PARIZOT, B., GANTET, P. P., BEECKMAN, T., BENNETT, M. J. & DRAYE, X. 2013. Post-embryonic root organogenesis in cereals: branching out from model plants. *Trends in Plant Science,* 18**,** 459-467.

ORTIZ, R., TRETHOWAN, R., FERRARA, G. O., IWANAGA, M., DODDS, J. H., CROUCH, J. H., CROSSA, J. & BRAUN, H.-J. 2007. High yield potential, shuttle breeding, genetic diversity, and a new international wheat improvement strategy. *Euphytica,* 157**,** 365-384.

OUYANG, W., YIN, X., YANG, J. & STRUIK, P. C. 2020. Comparisons with wheat reveal root anatomical and histochemical constraints of rice under water-deficit stress. *Plant and Soil,* 452**,** 547-568.

OVEČKA, M., VON WANGENHEIM, D., TOMANČÁK, P., ŠAMAJOVÁ, O., KOMIS, G. & ŠAMAJ, J. 2018. Multiscale imaging of plant development by light-sheet fluorescence microscopy. *Nature Plants,* 4**,** 639-650.

OYANAGI, A. 1994. Gravitropic response growth angle and vertical distribution of roots of wheat (*Triticum aestivum* L.). *Plant and Soil,* 165**,** 323-326.

OYANAGI, A., NAKAMOTO, T. & MORITA, S. 1993a. The gravitropic response of roots and the shaping of the root system in cereal plants. *Environmental and Experimental Botany,* 33**,** 141-158.

OYANAGI, A., NAKAMOTO, T. & WADA, M. 1993b. Relationship between Root Growth Angle of Seedlings and Vertical Distribution of Roots in the Field in Wheat Cultivars. *Japanese journal of crop science,* 62**,** 565-570.

PALMGREN, M. G., EDENBRANDT, A. K., VEDEL, S. E., ANDERSEN, M. M., LANDES, X., ØSTERBERG, J. T., FALHOF, J., OLSEN, L. I., CHRISTENSEN, S. B., SANDØE, P., GAMBORG, C., KAPPEL, K., THORSEN, B. J. & PAGH, P. 2015. Are we ready for back-to-nature crop breeding? *Trends in Plant Science,* 20**,** 155-164.

PATERSON, A. H., BRUBAKER, C. L. & WENDEL, J. F. 1993. A rapid method for extraction of cotton (*Gossypium* spp.) genomic DNA suitable for RFLP or PCR analysis. *Plant Molecular Biology Reporter,* 11**,** 122-127.

PELLEGRINESCHI, A., NOGUERA, L. M., SKOVMAND, B., BRITO, R. M., VELAZQUEZ, L., SALGADO, M. M., HERNANDEZ, R., WARBURTON, M. & HOISINGTON, D. 2002. Identification of highly transformable wheat genotypes for mass production of fertile transgenic plants. *Genome,* 45**,** 421-430.

POSTMA, J. A., DATHE, A. & LYNCH, J. P. 2014. The Optimal Lateral Root Branching Density for Maize Depends on Nitrogen and Phosphorus Availability. *Plant Physiology,* 166**,** 590-602.

POUND, M. P., FRENCH, A. P., ATKINSON, J. A., WELLS, D. M., BENNETT, M. J. & PRIDMORE, T. 2013. RootNav: Navigating Images of Complex Root Architectures. *Plant Physiology,* 162**,** 1802-1814.

QIAO, L., ZHANG, W., LI, X., ZHANG, L., ZHANG, X., LI, X., GUO, H., REN, Y., ZHENG, J. & CHANG, Z. 2018. Characterization and Expression Patterns of Auxin Response Factors in Wheat. *Frontiers in Plant Science,* 9.

RAMÍREZ-GONZÁLEZ, R. H., BORRILL, P., LANG, D., HARRINGTON, S. A., BRINTON, J., VENTURINI, L., DAVEY, M., JACOBS, J., VAN EX, F., PASHA, A., KHEDIKAR, Y., ROBINSON, S. J., CORY, A. T., FLORIO, T., CONCIA, L., JUERY, C., SCHOONBEEK, H., STEUERNAGEL, B., XIANG, D., RIDOUT, C. J., CHALHOUB, B., MAYER, K. F. X., BENHAMED, M., LATRASSE, D., BENDAHMANE, A., CONSORTIUM, I. W. G. S., WULFF, B. B. H., APPELS, R., TIWARI, V., DATLA, R., CHOULET, F., POZNIAK, C. J., PROVART, N. J., SHARPE, A. G., PAUX, E., SPANNAGL, M., BRÄUTIGAM, A., UAUY, C., KOROL, A., SHARPE, A. G., JUHÁSZ, A., ROHDE, A., BELLEC, A., DISTELFELD, A., AKPINAR, B. A., KELLER, B., DARRIER, B., GILL, B., CHALHOUB, B., STEUERNAGEL, B., FEUILLET, C., CHAUDHARY, C., UAUY, C., POZNIAK, C., ORMANBEKOVA, D., XIANG, D., LATRASSE, D., SWARBRECK, D., BARABASCHI, D., RAATS, D., SERGEEVA, E., SALINA, E., PAUX, E., CATTONARO, F., CHOULET, F., KOBAYASHI, F., KEEBLE-GAGNERE, G., KAUR, G., MUEHLBAUER, G., KETTLEBOROUGH, G., YU, G., ŠIMKOVÁ, H., GUNDLACH, H., BERGES, H., RIMBERT, H., BUDAK, H., HANDA, H., SMALL, I., BARTOŠ, J., ROGERS, J., DOLEŽEL, J., KEILWAGEN, J., POLAND, J., MELONEK, J., JACOBS, J., WRIGHT, J.,

JONES, J. D. G., GUTIERREZ-GONZALEZ, J., EVERSOLE, K., NILSEN, K., MAYER, K. F. X., KANYUKA, K., SINGH, K., GAO, L., CONCIA, L., VENTURINI, L., CATTIVELLI, L., SPANNAGL, M., MASCHER, M., HAYDEN, M., et al. 2018. The transcriptional landscape of polyploid wheat. *Science,* 361**,** eaar6089.

RAN, F. A., HSU, P. D., WRIGHT, J., AGARWALA, V., SCOTT, D. A. & ZHANG, F. 2013. Genome engineering using the CRISPR-Cas9 system. *Nature Protocols,* 8**,** 2281-2308.

RASMUSSEN, R. 2001. Quantification on the LightCycler. *Rapid Cycle Real-Time PCR.* Springer.

RASOOL, F., UZAIR, M., ATTIA, K. A., ABUSHADY, A. M., REHMAN, O. U., FAROOQ, M. S., FIAZ, S., FAROOQ, U., SALEEM, B., TARIQ, Z., INAM, S., REHMAN, N., KIMIKO, I. & KHAN, M. R. 2023. Functional characterization of the IGT gene family in wheat reveals conservation and variation in root architecture under drought condition. *Plant Stress,* 10**,** 100217.

REYNOLDS, M., DRECCER, F. & TRETHOWAN, R. 2006. Drought-adaptive traits derived from wheat wild relatives and landraces. *Journal of Experimental Botany,* 58**,** 177-186.

RICH, S. M., CHRISTOPHER, J., RICHARDS, R. & WATT, M. 2020. Root phenotypes of young wheat plants grown in controlled environments show inconsistent correlation with mature root traits in the field. *Journal of Experimental Botany*.

RICH, S. M. & WATT, M. 2013. Soil conditions and cereal root system architecture: review and considerations for linking Darwin and Weaver. *Journal of Experimental Botany,* 64**,** 1193-1208.

RICHARD, C., HICKEY, L. T., FLETCHER, S., JENNINGS, R., CHENU, K. & CHRISTOPHER, J. T. 2015. High-throughput phenotyping of seminal root traits in wheat. *Plant Methods,* 11**,** 13.

ROOKE, L., BYRNE, D. & SALGUEIRO, S. 2000. Marker gene expression driven by the maize ubiquitin promoter in transgenic wheat. *Annals of Applied Biology,* 136**,** 167-172.

ROYCHOUDHRY, S., DEL BIANCO, M., KIEFFER, M. & KEPINSKI, S. 2013. Auxin Controls Gravitropic Setpoint Angle in Higher Plant Lateral Branches. *Current Biology,* 23**,** 1497-1504.

ROYCHOUDHRY, S., SAGEMAN-FURNAS, K., WOLVERTON, C., GRONES, P., TAN, S., MOLNÁR, G., DE ANGELIS, M., GOODMAN, H. L., CAPSTAFF, N., LLOYD, J. P. B., MULLEN, J., HANGARTER, R., FRIML, J. & KEPINSKI, S. 2023. Antigravitropic PIN polarization maintains non-vertical growth in lateral roots. *Nature Plants*.

SANCHEZ, D., SADOUN, S. B., MARY-HUARD, T., ALLIER, A., MOREAU, L. & CHARCOSSET, A. 2023. Improving the use of plant genetic resources to sustain breeding programs' efficiency. *Proceedings of the National Academy of Sciences,* 120**,** e2205780119.

SATO, K., ABE, F., MASCHER, M., HABERER, G., GUNDLACH, H., SPANNAGL, M., SHIRASAWA, K. & ISOBE, S. 2021. Chromosome-scale genome assembly of

the transformation-amenable common wheat cultivar 'Fielder'. *DNA Research,* 28.

SINGH, K., SINGH, J., JINDAL, S., SIDHU, G., DHALIWAL, A. & GILL, K. 2019. Structural and functional evolution of an auxin efflux carrier PIN1 and its functional characterization in common wheat. *Functional & Integrative Genomics,* 19**,** 29-41.

SINHA, S. K., RANI, M., KUMAR, A., KUMAR, S., VENKATESH, K. & MANDAL, P. K. 2018. Natural variation in root system architecture in diverse wheat genotypes grown under different nitrate conditions and root growth media. *Theoretical and Experimental Plant Physiology,* 30**,** 223-234.

SIVAMANI, E., LI, X., NALAPALLI, S., BARRON, Y., PRAIRIE, A., BRADLEY, D., DOYLE, M. & QUE, Q. 2015. Strategies to improve low copy transgenic events in Agrobacterium-mediated transformation of maize. *Transgenic Research,* 24**,** 1017-1027.

SMEDLEY, M. A., HAYTA, S., CLARKE, M. & HARWOOD, W. A. 2021. CRISPR-Cas9 Based Genome Editing in Wheat. *Current Protocols,* 1**,** e65.

SMITH, S. & DE SMET, I. 2012. Root system architecture: insights from Arabidopsis and cereal crops. *Philosophical Transactions of the Royal Society B: Biological Sciences,* 367**,** 1441-1452.

SONG, T., DAS, D., YANG, F., CHEN, M., TIAN, Y., CHENG, C., SUN, C., XU, W. & ZHANG, J. 2020. Genome-wide transcriptome analysis of roots in two rice varieties in response to alternate wetting and drying irrigation. *The Crop Journal,* 8**,** 586-601.

SU, S.-H., GIBBS, N. M., JANCEWICZ, A. L. & MASSON, P. H. 2017. Molecular Mechanisms of Root Gravitropism. *Current Biology,* 27**,** R964-R972.

SU, S.-H., KEITH, M. A. & MASSON, P. H. 2020. Gravity Signaling in Flowering Plant Roots. *Plants,* 9**,** 1290.

SZURMAN-ZUBRZYCKA, M., KUROWSKA, M., TILL, B. J. & SZAREJKO, I. 2023. Is it the end of TILLING era in plant science? *Frontiers in Plant Science,* 14.

TANIGUCHI, M., FURUTANI, M., NISHIMURA, T., NAKAMURA, M., FUSHITA, T., IIJIMA, K., BABA, K., TANAKA, H., TOYOTA, M., TASAKA, M. & MORITA, M. T. 2017. The Arabidopsis LAZY1 Family Plays a Key Role in Gravity Signaling within Statocytes and in Branch Angle Control of Roots and Shoots. *The Plant Cell,* 29**,** 1984-1999.

TARUI, Y. & IINO, M. 1997. Gravitropism of Oat and Wheat Coleoptiles: Dependence on the Stimulation Angle and Involvement of Autotropic Straightening. *Plant and Cell Physiology,* 38**,** 1346-1353.

TAYLOR, S. C., NADEAU, K., ABBASI, M., LACHANCE, C., NGUYEN, M. & FENRICH, J. 2019. The Ultimate qPCR Experiment: Producing Publication Quality, Reproducible Data the First Time. *Trends in Biotechnology,* 37**,** 761-774.

TIWARI, S., MUTHUSAMY, S. K., ROY, P. & DALAL, M. 2023. Genome wide analysis of BREVIS RADIX gene family from wheat (*Triticum aestivum*): A conserved

gene family differentially regulated by hormones and abiotic stresses. *International Journal of Biological Macromolecules,* 232**,** 123081.

TRACY, S. R., NAGEL, K. A., POSTMA, J. A., FASSBENDER, H., WASSON, A. & WATT, M. 2020. Crop Improvement from Phenotyping Roots: Highlights Reveal Expanding Opportunities. *Trends in Plant Science,* 25**,** 105-118.

TSIAFOULI, M. A., THÉBAULT, E., SGARDELIS, S. P., DE RUITER, P. C., VAN DER PUTTEN, W. H., BIRKHOFER, K., HEMERIK, L., DE VRIES, F. T., BARDGETT, R. D., BRADY, M. V., BJORNLUND, L., JØRGENSEN, H. B., CHRISTENSEN, S., HERTEFELDT, T. D., HOTES, S., GERA HOL, W. H., FROUZ, J., LIIRI, M., MORTIMER, S. R., SETÄLÄ, H., TZANOPOULOS, J., UTESENY, K., PIŽL, V., STARY, J., WOLTERS, V. & HEDLUND, K. 2015. Intensive agriculture reduces soil biodiversity across Europe. *Global Change Biology,* 21**,** 973-985.

TUBIELLO, F., ROSENZWEIG, C., CONCHEDDA, G., KARL, K., GÜTSCHOW, J., XUEYAO, P., OBLI-LARYEA, G., WANNER, N., QIU, S., BARROS, J., FLAMMINI, A., MENCOS-CONTRERAS, E., SOUZA, L., QUADRELLI, R., HEIÐARSDÓTTIR, H., BENOIT, P., HAYEK, M. & SANDALOW, D. 2021. Greenhouse gas emissions from food systems: Building the evidence base. *Environmental Research Letters,* 16**,** 65007.

UAUY, C., PARAISO, F., COLASUONNO, P., TRAN, R. K., TSAI, H., BERARDI, S., COMAI, L. & DUBCOVSKY, J. 2009. A modified TILLING approach to detect induced mutations in tetraploid and hexaploid wheat. *BMC Plant Biology,* 9**,** 115.

UGA, Y., EBANA, K., ABE, J., MORITA, S., OKUNO, K. & YANO, M. 2009. Variation in root morphology and anatomy among accessions of cultivated rice (*Oryza sativa* L.) with different genetic backgrounds. *Breeding Science,* 59**,** 87-93.

UGA, Y., OKUNO, K. & YANO, M. 2011. Dro1, a major QTL involved in deep rooting of rice under upland field conditions. *Journal of Experimental Botany,* 62**,** 2485-2494.

UGA, Y., SUGIMOTO, K., OGAWA, S., RANE, J., ISHITANI, M., HARA, N., KITOMI, Y., INUKAI, Y., ONO, K., KANNO, N., INOUE, H., TAKEHISA, H., MOTOYAMA, R., NAGAMURA, Y., WU, J., MATSUMOTO, T., TAKAI, T., OKUNO, K. & YANO, M. 2013. Control of root system architecture by *DEEPER ROOTING 1* increases rice yield under drought conditions. *Nature Genetics,* 45**,** 1097-1102.

ULMASOV, T., MURFETT, J., HAGEN, G. & GUILFOYLE, T. J. 1997. Aux/IAA proteins repress expression of reporter genes containing natural and highly active synthetic auxin response elements. *The Plant Cell,* 9**,** 1963-1971.

URFAN, M., SHARMA, S., HAKLA, H. R., RAJPUT, P., ANDOTRA, S., LEHANA, P. K., BHARDWAJ, R., KHAN, M. S., DAS, R., KUMAR, S. & PAL, S. 2022. Recent trends in root phenomics of plant systems with available methods - discrepancies and consonances. *Physiology and Molecular Biology of Plants,* 28**,** 1311-1321.

VAN DE WIEL, C. C. M., VAN DER LINDEN, C. G. & SCHOLTEN, O. E. 2016. Improving phosphorus use efficiency in agriculture: opportunities for breeding. *Euphytica,* 207**,** 1-22.

WAINES, J. G. & EHDAIE, B. 2007. Domestication and Crop Physiology: Roots of Green-Revolution Wheat. *Annals of Botany,* 100**,** 991-998.

WAITE, J. M., COLLUM, T. D. & DARDICK, C. 2020. AtDRO1 is nuclear localized in root tips under native conditions and impacts auxin localization. *Plant Molecular Biology,* 103**,** 197-210.

WAITE, J. M. & DARDICK, C. 2021. The roles of the IGT gene family in plant architecture: past, present, and future. *Current Opinion in Plant Biology,* 59**,** 101983.

WANG, H., HU, Z., HUANG, K., HAN, Y., ZHAO, A., HAN, H., SONG, L., FAN, C., LI, R., XIN, M., PENG, H., YAO, Y., SUN, Q. & NI, Z. 2018a. Three genomes differentially contribute to the seedling lateral root number in allohexaploid wheat: evidence from phenotype evolution and gene expression. *The Plant Journal,* 95**,** 976-987.

WANG, L., GUO, M., LI, Y., RUAN, W., MO, X., WU, Z., STURROCK, C. J., YU, H., LU, C., PENG, J. & MAO, C. 2017. LARGE ROOT ANGLE1, encoding OsPIN2, is involved in root system architecture in rice. *Journal of Experimental Botany,* 69**,** 385-397.

WANG, W., SIMMONDS, J., PAN, Q., DAVIDSON, D., HE, F., BATTAL, A., AKHUNOVA, A., TRICK, H. N., UAUY, C. & AKHUNOV, E. 2018b. Gene editing and mutagenesis reveal inter-cultivar differences and additivity in the contribution of *TaGW2* homoeologues to grain size and weight in wheat. *Theoretical and Applied Genetics,* 131**,** 2463-2475.

WASSON, A. P., REBETZKE, G. J., KIRKEGAARD, J. A., CHRISTOPHER, J., RICHARDS, R. A. & WATT, M. 2014. Soil coring at multiple field environments can directly quantify variation in deep root traits to select wheat genotypes for breeding. *Journal of Experimental Botany,* 65**,** 6231-6249.

WASSON, A. P., RICHARDS, R. A., CHATRATH, R., MISRA, S. C., PRASAD, S. V. S., REBETZKE, G. J., KIRKEGAARD, J. A., CHRISTOPHER, J. & WATT, M. 2012. Traits and selection strategies to improve root systems and water uptake in water-limited wheat crops. *Journal of Experimental Botany,* 63**,** 3485-3498.

WATSON, A., GHOSH, S., WILLIAMS, M. J., CUDDY, W. S., SIMMONDS, J., REY, M.-D., ASYRAF MD HATTA, M., HINCHLIFFE, A., STEED, A., REYNOLDS, D., ADAMSKI, N. M., BREAKSPEAR, A., KOROLEV, A., RAYNER, T., DIXON, L. E., RIAZ, A., MARTIN, W., RYAN, M., EDWARDS, D., BATLEY, J., RAMAN, H., CARTER, J., ROGERS, C., DOMONEY, C., MOORE, G., HARWOOD, W., NICHOLSON, P., DIETERS, M. J., DELACY, I. H., ZHOU, J., UAUY, C., BODEN, S. A., PARK, R. F., WULFF, B. B. H. & HICKEY, L. T. 2018. Speed breeding is a powerful tool to accelerate crop research and breeding. *Nature Plants,* 4**,** 23-29.

WENT, F. W. & THIMANN, K. V. 1937. *Phytohormones,* New York, Macmillian.

WILSON, A. K., PICKETT, F. B., TURNER, J. C. & ESTELLE, M. 1990. A dominant mutation inArabidopsis confers resistance to auxin, ethylene and abscisic acid. *Molecular and General Genetics MGG,* 222**,** 377-383.

WINFIELD, M. O., ALLEN, A. M., WILKINSON, P. A., BURRIDGE, A. J., BARKER, G. L. A., COGHILL, J., WATERFALL, C., WINGEN, L. U., GRIFFITHS, S. & EDWARDS, K. J. 2018. High-density genotyping of the A.E. Watkins Collection

of hexaploid landraces identifies a large molecular diversity compared to elite bread wheat. *Plant Biotechnology Journal,* 16**,** 165-175.

WINGEN, L. U., WEST, C., LEVERINGTON-WAITE, M., COLLIER, S., ORFORD, S., GORAM, R., YANG, C.-Y., KING, J., ALLEN, A. M., BURRIDGE, A., EDWARDS, K. J. & GRIFFITHS, S. 2017. Wheat Landrace Genome Diversity. *Genetics,* 205**,** 1657-1676.

WOJCIECHOWSKI, T., GOODING, M. J., RAMSAY, L. & GREGORY, P. J. 2009. The effects of dwarfing genes on seedling root growth of wheat. *Journal of Experimental Botany,* 60**,** 2565-2573.

WOLVERTON, C., PAYA, A. M. & TOSKA, J. 2011. Root cap angle and gravitropic response rate are uncoupled in the Arabidopsis *pgm-1* mutant. *Physiologia Plantarum,* 141**,** 373-382.

WU, D., DONG, J., YAO, Y., ZHAO, W. & GAO, X. 2015. Identification and evaluation of endogenous control genes for use in quantitative RT-PCR during wheat (*Triticum aestivum* L.) grain filling. *Genetics and Molecular Research,* 14**,** 10530-10542.

YANG, J., YUAN, Z., MENG, Q., HUANG, G., PÉRIN, C., BUREAU, C., MEUNIER, A.-C., INGOUFF, M., BENNETT, M. J., LIANG, W. & ZHANG, D. 2017. Dynamic Regulation of Auxin Response during Rice Development Revealed by Newly Established Hormone Biosensor Markers. *Frontiers in Plant Science,* 8**,** 256.

YANG, S., FRESNEDO-RAMÍREZ, J., WANG, M., COTE, L., SCHWEITZER, P., BARBA, P., TAKACS, E. M., CLARK, M., LUBY, J., MANNS, D. C., SACKS, G., MANSFIELD, A. K., LONDO, J., FENNELL, A., GADOURY, D., REISCH, B., CADLE-DAVIDSON, L. & SUN, Q. 2016. A next-generation marker genotyping platform (AmpSeq) in heterozygous crops: a case study for marker-assisted selection in grapevine. *Horticulture Research,* 3**,** 1-12.

YORK, L. M., SLACK, S., BENNETT, M. J. & JOHN, F. M. 2019. Wheat shovelomics I: A field phenotyping approach for characterising the structure and function of root systems in tillering species. *Biorxiv*.

YOSHIDA, S., FORNO, D. A., COCK, J. H. & GOMEZ, K., A 1976. *Laboratory manual for physiological studies of rice*, IRRI.

YOSHIHARA, T., MILLER, N. D., RABANAL, F. A., MYLES, H., KWAK, I.-Y., BROMAN, K. W., SADKHIN, B., BAXTER, I., DILKES, B. P., HUDSON, M. E. & SPALDING, E. P. 2022. Leveraging orthology within maize and Arabidopsis QTL to identify genes affecting natural variation in gravitropism. *Proceedings of the National Academy of Sciences,* 119**,** e2212199119.

YOSHIHARA, T. & SPALDING, E. P. 2017. LAZY Genes Mediate the Effects of Gravity on Auxin Gradients and Plant Architecture. *Plant Physiology,* 175**,** 959-969.

YOSHIHARA, T. & SPALDING, E. P. 2020. Switching the direction of stem gravitropism by altering two amino acids in AtLAZY1. *Plant Physiology,* 182**,** 1039-1051.

YOSHIHARA, T., SPALDING, E. P. & IINO, M. 2013. AtLAZY1 is a signaling component required for gravitropism of the *Arabidopsis thaliana* inflorescence. *The Plant Journal,* 74**,** 267-279.

YU, B., LIN, Z., LI, H., LI, X., LI, J., WANG, Y., ZHANG, X., ZHU, Z., ZHAI, W., WANG, X., XIE, D. & SUN, C. 2007. TAC1, a major quantitative trait locus controlling tiller angle in rice. *The Plant Journal,* 52**,** 891-898.

ZHANG, Y., XIAO, G., WANG, X., ZHANG, X. & FRIML, J. 2019. Evolution of fast root gravitropism in seed plants. *Nature Communications,* 10**,** 1-10.

ZHU, Z.-X., LIU, Y., LIU, S.-J., MAO, C.-Z., WU, Y.-R. & WU, P. 2012. A gain-of-function mutation in *OsIAA11* affects lateral root development in rice. *Molecular Plant,* 5**,** 154-161.